NUCLEAR MAGNETIC RESONANCE SPECTROSCOPIC STUDIES OF MOLECULAR INTERACTIONS WITH SPECIAL REFERENCE TO THEIR STEREO-SPECIFICITY

A Thesis presented to

The University of Aston in Birmingham

for the degree of

Doctor of Philosophy

by

R. R. YADAVA

The Chemistry Department

The University of Aston in Birmingham

August, 1972

SUMMARY

Molecular interactions between polar aliphatic molecules (solute) and aromatic solvent molecules have been studied widely by nuclear magnetic resonance spectroscopy. Most of the studies have been carried out using solutes containing a single or group of equivalent protons and because of the paucity of information they provide, many problems connected with the interactions specially their stereospecificity, remain unexplained. In an attempt to elucidate these problems solutes with several non-equivalent protons have been investigated during the work described herein. The complexes studied are those formed between vinyl solutes and benzene or non-polar alkyl substituted benzenes. The specific intention in this work was to determine the time-average structure of the complexes, the thermodynamic parameters pertaining to their formation, the nature of the interactions involved and the effect of substituents in the solute and solvent molecules.

The equilibrium quotients for the formation of each of the complexes and the additional shielding in the fully complexed state for the different non-equivalent protons in the solute have been determined from the dependence of the observed solvent-induced shift on the mole fraction of the aromatic solvent. Values of ΔG^{o}, ΔH^{o} and ΔS^{o} were determined from the equilibrium quotient values obtained at different temperatures.

The data accumulated are strongly indicative of the formation of weakly bound complexes. Significantly the thermodynamic parameters

are similar for the different non-equivalent protons in the same solute and suggest the formation of only one type, 1:1, of complex. Structures are deduced for these complexes in which the solute molecule tends to adopt a preferred time-average orientation relative to the solvent. The structures depend on the nature of the substituents in the interacting molecules and indicate the highly stereospecific nature of the interactions.

It is proposed that, both dipole-induced dipole interactions and steric factors govern the complex formation to a great extent.

ACKNOWLEDGEMENTS

I would like to express my sincere thanks to my supervisor, Dr. J. Homer, for his encouragement and assistance throughout the course of this work, in particular for the many helpful suggestions in the interpretation of the results.

My thanks are also due to Dr. M. C. Cooke, Dr. C. J. Jackson, D. L. Readhead, P. M. Whitney, P. Polanun and A. R. Dudley of the n.m.r. research group at the University of Aston for many helpful discussions and to E. J. Hartland for his technical assistance.

I am thankful to the n.m.r. research group led by Dr. L.F. Thomas at the University of Birmingham for making available a copy of the computer program LAOCOON 3 and helpful suggestions regarding its use.

I am also grateful to Professor W. G. S. Parker, Head of the Chemistry Department, for the provision of facilities for this research and to the Commonwealth Scholarships Commission in the United Kingdom for financing the work.

R. R. Yadava

CONTENTS

CHAPTER 1

Page

CHAPTER 2

Experimental Methods for the Observation of High Resolution Nuclear Magnetic Resonance

ILLUSTRATIONS

C H A P T E R 1

GENERAL AND THEORETICAL CONSIDERATIONS OF NUCLEAR MAGNETIC RESOMANCE SPECTROSCOPY

1.1. INTRODUCTION

In order to explain the presence of the hyperfine structure of atomic spectra, Pauli[1], in 1924, put forward the hypothesis that the nuclei of certain isotopes possess an intrinsic mechanical spin, i.e. they have an angular momentum (p). According to quantum mechanical laws, the angular momentum is quantized and its maximum measurable value for a nucleus is given by $\frac{h}{2\pi}$ .I, where h is Planck's constant and I is a characteristic property of each nuclear type referred to as nuclear spin or spin quantum number. I can have integral or half integral values depending on the particular nucleus. Since atomic nuclei are also associated with electric charge, mechanical spin gives rise to a magnetic moment, μ , the direction of which is coincident with the axis of spin. Such a spinning nucleus may be considered to have the properties of a tiny bar magnet. Using a molecular beam method, Stern and Gerlach[2] (1921) were able to show that the measurable values of an atomic magnetic moment are discrete. By directing a beam of hydrogen molecules through a steady magnetic field, Rabi et al [3] were successful in measuring the small magnetic moment of the hydrogen nucleus (proton). In the presence of an externally applied magnetic field, B_o, nuclear moments experience a torque and tend to adopt specific orientations with respect to the field direction. Each orientation corresponds to a characteristic energy, the number of allowed energy levels being limited to (2I + 1). It is possible to induce transitions between these nuclear energy levels by a second magnetic field B_1, derived from an alternating signal, usually in the radiofrequency region. The nuclei may absorb energy from the second field to give rise to what are called Nuclear Magnetic Resonance (NMR) Spectra.

The feasibility of the n.m.r. experiment was indicated by early developments in molecular beam technique . The latter was further developed

by subjecting the beam to an additional oscillating field[4] which could be swept through a range of frequencies. When the frequency of the oscillating field corresponded to $\frac{\mu B_o}{I.h}$, there was a sudden drop in the number of molecules reaching the detector, indicating an absorption of energy from the oscillating field. Though attempts[5,6] were made to observe nuclear magnetic resonance absorption earlier, it was not until late in 1945 that the first actual n.m.r. signals were observed by Purcell, Torrey and Pound[7], and by Bloch, Hansen and Packard[8] using respectively samples of paraffin wax and water. Since the initial discovery of n.m.r. phenomenon, advances in instrumental design and in the theory of nuclear magnectic resonance have so rapidly followed that this form of spectroscopy has become invaluable in the investigation of molecular structure and environmental effects [9-12].

While considering the theory of n.m.r. in the following sections, the properties of an isolated nucleus will first be considered and the basic equation for resonance will be derived. A classical treatment of resonance will yield the requirement of an additional rotating field B_1, and its direction of rotation will be obtained from quantum mechanical considerations. Assemblies of similar nuclei will then be considered in dealing with the nuclear energy level distribution, saturation and relaxation effects. Finally, nuclei in various molecular environments will be considered while dealing with the chemical shifts and chemical exchange phenomenon.

1.2 AN ISOLATED NUCLEUS IN A MAGNETIC FIELD

As a result of space quantization, a nucleus will have 2I + 1 distinct energy states and the corresponding components of angular momentum along any selected direction will have values I, (I-1), ...(-I+1),-I in terms of $h\left(=\frac{\hbar}{2\pi}\right)$ units. Since the magnetic moment and angular momentum are parallel vectors (Fig. 1.1), one may similarly define a

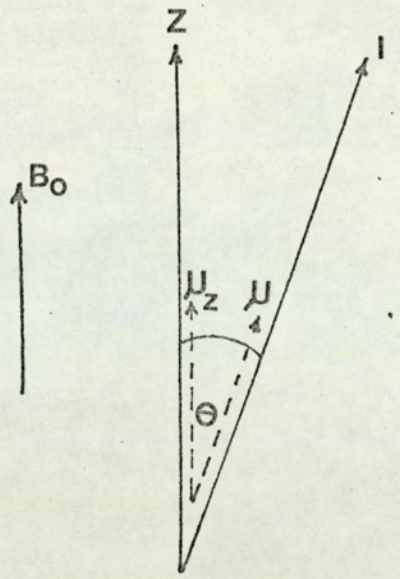

Fig.1.1 The relationship between the nuclear magnetic moment μ and the spin angular momentum I.

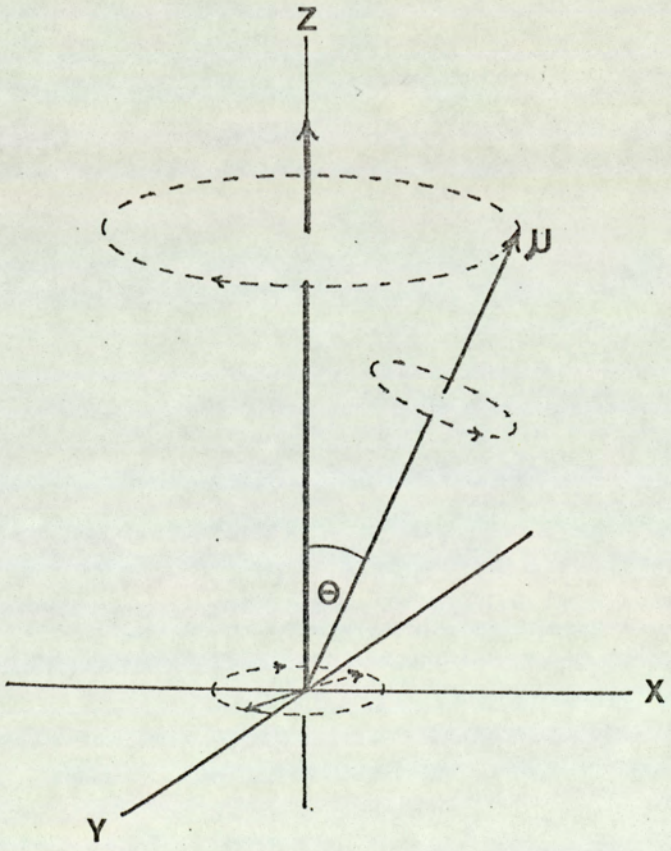

Fig. 1.2 Vectorial representation of the Classical Larmor Precession.

maximum measurable component of the magnetic moment, μ . The observable components of the magnetic moment in a selected direction are given by $\frac{m.\mu}{I}$, where m, the magnetic quantum number, may have the values

$$m = I, (I-1), (I-2), \ldots\ldots (-I+1), -I \qquad (1.1)$$

sometimes the magnetic moment is also expressed as:

$$\mu = \gamma (I\hbar) \qquad (1.2)$$

where $\gamma = \frac{\mu}{p}$ is a constant called the magnetogyric ratio , characteristic of the nucleus.

In the absence of an external magnetic field, the nuclear energy states are degenerate but as soon as an external field B_o is applied in Z direction, the energy E_z of a nucleus (relative to that in zero field) is given by:

$$E_z = -\mu_z B_o \qquad (1.3)$$

By substituting the allowed values of μ_z in eqn. (1.3) one finds that the allowed nuclear energy levels are:

$$-\mu B_o, \; -\frac{(I-1)}{I}\mu B_o, \ldots\ldots \frac{(I-1)}{I}\mu B_o, \mu B_o.$$

It is evident that the levels are equally spaced and the energy seperation between any two successive levels is $\frac{\mu B_o}{I}$. NMR spectra are obtained when transitions are induced between these energy levels by the absorption (or emission) of energy quanta. The selection rule governing nuclear transitions states that $m = \pm 1$, i.e. transitions are possible between successive levels only. The frequency of the radiation required to induce the transition can be calculated from the well known Bohr frequency condition and is given by:

$$\nu = \frac{\mu B_o}{Ih} \qquad (1.4)$$

or in terms of magnetogyric ratio γ , by

$$\nu = \frac{\gamma B_o}{2\pi} \qquad (1.5)$$

As the energy levels are equally spaced, there is a characteristic frequency of transition for a given value of B_o. For illustration, in the particular case of proton ($\mu = 1.41 \times 10^{-26}$ J/tesla) for $B_o = 1$ tesla, the appropriate frequency is 42.6 MHz, which lies in the radiofrequency region.

1.3 RESONANCE CRITERIA

To get an insight into the actual process of nuclear magnetic resonance, it is worthwhile building first a classical mechanical and subsequently a quantum mechanical picture of the phenomenon. The former explains the transition effects while the latter is helpful in understanding the steady state process.

1.3a Classical Treatment

If a spinning nucleus is placed in a magnetic field of strength B_o with its magnetic axis at some angle to the direction of the field, it will experience a torque tending to allign it parallel to the field. According to Newton's law of motion, the rate of change of angular momentum is equal to the torque, i.e.

$$\frac{dp}{dt} = L \qquad (1.6)$$

Since, according to the laws of magnetic theory[13]

$$L = \mu B_o \qquad (1.7)$$

equating the two values of the torque and replacing μ by $\gamma.p$, one gets:

$$\frac{dp}{dt} = \gamma . p . B_o \qquad (1.8)$$

The net result of placing the nuclear magnet in the external field B_o is that it starts precessing about the field axis with an angular velocity ω_o defined by:

$$\frac{dp}{dt} = p\omega_o$$

$$\text{i.e.} \quad \omega_o = \gamma B_o \qquad (1.9)$$

In terms of the precessional frequency, the same equation can be written as

$$\nu = \frac{\gamma B_o}{2\pi} \qquad (1.5)$$

The significant point that emerges out of the consideration so far is that the precession frequency, quite often known as the Larmor frequency, is independent of the inclination of the nuclear magnet to the field direction.

If a co-ordinate system rotating at the Larmor frequency ν , is set up and there is no other field acting on the nucleus, the magnetic moment vector μ would remain stationary in the reference frame. Let us consider now the effect of a second small rotating field B_1, acting on the precessing nucleus at right angles to the static field B_o (Fig.1.2). The precessing nucleus will experience another torque tending to tip its magnetic moment vector towards the plane perpendicular to the direction of the static field. So long as the direction of B_1 is moving in the rotating frame with a frequency not equal to the Larmor frequency ν , it will go out of phase after some time. The net effect will be a slight wobbling perturbation of the steady precessional motion. But if the direction of B_1 is rotating at the Larmor frequency, i.e. there is a resonance, the two motions synchronise. The torque B_1 will always be in the same direction throughout the rotation and the angle θ between the direction of μ and B_o will eventually change.

If the frequency of rotation of B_1 is swept through the Larmor frequency, the effect will be greatest at the Larmor frequency and it will show up as resonance phenomenon. Practically this effect can be observed by applying a linearly oscillating field since such a field can be regarded as superimposition of the two fields rotating in opposite directions. Only the component having the correct sense will synchronise with the precessing magnetic nuclei while the other component will have no effect.

1.3b Quantum Mechanical Treatment

For a nucleus of magnetic moment μ placed in a magnetic field B_o, the Hamiltonian is given by

$$\mathcal{H} = -\mu B_o \qquad (1.10)$$

On replacing μ by $\gamma\hbar I$ one gets

$$\mathcal{H} = -\gamma\hbar B_o I \qquad (1.11)$$

Corresponding stationary state functions are designated by m, the component of I in Z direction, and the energy levels of the system are given by

$$E = -\gamma\hbar m B_o \qquad (1.12)$$

It is necessary to introduce some form of perturbation in order to bring about a transition between the energy states. Application of an oscillating field serves the purpose for such a perturbation, the direction of the field being decided from the properties of the spin operators and the eigenfunctions appropriate to the particular nucleus in question.

For simplicity, henceforth, the arguments will be restricted to nuclei of spin $I = \frac{1}{2}$, for which there are only two possible energy levels given by $\pm\gamma\hbar B_o \times \frac{1}{2}$. Corresponding spin eigenfunctions are usually denoted by the symbols α and β. If I_x, I_y and I_z are defined as the x,y and z

components of the spin angular momentum operator, respectively, for such a nucleus, the respective probabilities of transition, when the nucleus is subjected to an oscillating field along the x and z – axes are given by [14]

$$W_x \propto (\alpha \,|I_x|\, \beta) = \tfrac{1}{2}\hbar \tag{1.13}$$

$$W_z \propto (\alpha \,|I_z|\, \beta) = 0 \tag{1.14}$$

which means that a parallel arrangement of steady and oscillating fields can not induce a transition between the energy levels while there is a finite probability of transition, if the oscillating field acts along x-axis. Similarly, it can be shown that there is a finite probability of transition when the oscillating field is applied along the y-axis.

Such a transition involves an energy change

$$\Delta E = \gamma \hbar B_o \tag{1.15}$$

For resonance, the frequency of the oscillating field must satisfy the relationship

$$\nu = \frac{\Delta E}{h} = \frac{\gamma B_o}{2\pi} \tag{1.16}$$

For a nucleus of spin I, pertrubed by an oscillating field of amplitude $2B_1$, the transition probability[14] between energy levels m and m^1 is given by

$$W^1 = \gamma^2 B_1^2 \cdot |\, \psi_m |\, Ix \,|\, \psi_m{}^1) \,|^2 \tag{1.17}$$

which is zero unless $m = m^1 \pm 1$, the selection rule for nuclear transitions.

1.4 THE POPULATION OF SPIN STATES

For a nucleus at resonance, the probabilities of stimulated absorption or emission of energy are equal since the effect of spontaneous emission

is negligible in the radiofrequency region[15]. Therefore, the observation of a nuclear magnetic resonance absorption signal will depend on the relative population of the two energy levels. If there are only two states with populations N_1 and N_2 and P is the probability of a transition occuring between them, the net absorption of energy is given by

$$P\ (N_1 - N_2) \tag{1.18}$$

For an assembly of nuclei in thermal equilibrium at temperature T, in the absence of the secondary field B_1, there is a Boltzmann distribution of nuclei between the various allowed energy states. For nuclei with spin I, there are 2I + 1 equally spaced levels seperated by an energy of $\frac{\mu B_o}{I}$ so that the probability of any nucleus occupying a particular level of magnetic quantum number m is given by

$$\frac{1}{2I+1} \quad \exp \quad \frac{m\mu B_o}{IkT} \tag{1.19}$$

which at room temperature and with B_o of the order of a tesla, approximately reduces to

$$\frac{1}{2I+1} \qquad 1 + \frac{m\mu B_o}{IkT} \tag{1.20}$$

For a nucleus of spin $I = \frac{1}{2}$, the probabilities of a nucleus being in the upper or lower energy states respectively are given by

$$\tfrac{1}{2}\left(1 - \frac{\mu B_o}{kT}\right) \tag{1.21}$$

and

$$\tfrac{1}{2}\left(1 + \frac{\mu B_o}{kT}\right) \tag{1.22}$$

i.e. there is a small excess population in the lower energy state . In fact, the observation of an n.m.r. signal depends on the maintenance of this excess population. It is also evident from the above relations that the excess population is directly proportional to the static field

B_o. Obviously the higher the field B_o, the higher the excess population in the lower energy state and hence the higher the sensitivity of the measurement.

1.5 SATURATION

Nuclear magnetic resonance spectroscopy differs from the optical spectroscopy [15,16] in that in the latter case the absorption of energy is followed by a very rapid return from the excited to the ground state, liberated energy being dissipated as heat. In n.m.r. spectroscopy, the continuous absorption of energy from the radiofrequency field will tend to reduce the excess population in the lower energy state, relative to that in the upper state, and hence reduce the net number of nuclei capable of absorbing energy. The magnitude of this effect will increase with the amplitude of the oscillating field and is referred to as saturation. In addition to reducing the overall absorption and consequently the signal intensity, saturation will distort the signal causing a broadening of the resonance line. Another experimental observation, which may result during saturation, is the appearance of multiple quantum transitions [17] which are forbidden by the first order selection rules.

1.6 RELAXTION PROCESSES

If a collection of nuclei of spin $I = \frac{1}{2}$ are irradiated, the rate of absorption is initially greater than the rate of emission, because of the slight excess of nuclei in the lower energy state. But the original excess steadily dwindles until the two states are equally populated. One may find that the absorption signal is strong when the radiofrequency radiation is first applied but that it gradually disappears. The situation is influenced by the existence of radiationless processes

which tend to restore the original distribution of energy levels. Such processes are generally referred to as relaxation processes of which there are two principal types.

1.6a Spin Lattice Relaxation

The magnetic nuclei are usually part of an assembly of molecules which constitute a sample under investigation and the entire molecular system is referred to as the lattice, irrespective of the physical state of the sample. For the moment, the attention will be confined to liquids and gases in which the atoms and molecules constituting the lattice will be undergoing random thermal motions. Since these atoms or molecules may contain magnetic nuclei and in any event will be magnetised, the molecular motions will result in fluctuating secondary magnetic fields. These magnetic fields can be regarded as being built up of a number of oscillating components so that there can be a component analogous to B_1 which will just match the precessional frequency of the magnetic nuclei. Since simple thermodynamics requires that the downward transition porbability should be greater than the upward transition probability, a nucleus in the excited state will relax to the lower state and the energy lost is given to the lattice as extra thermal energy.

Another feature of spin-lattice relaxation may now be considered. Initially, when an assembly of magnetic nuclei is not in a magnetic field, the two nuclear states are equally populated. When the sample is placed in the magnetic field it requires a certain time for the populations to reach their new equilibrium value. It is the spin-lattice relaxation process which is responsible for the initial production of the Boltzmann excess of nuclei in the lower state after the application of steady magnetic field.

If n_2 and n_1 are the number of nuclei per unit volume in the upper and lower states respectively, it is possible to evaluate the excess number of nuclei per unit volume, n, as a function of time.

$$n = n_1 - n_2 \tag{1.23}$$

It has been said earlier that the transition probabilities of absorption and emission are equal. This is no longer true in the presence of the spin-lattice relaxation process, for at equilibrium, the total number of upward transitions per unit time must be equal to the corresponding number of downward transitions.

Let W_1 and W_2 be respectively the probabilities per unit time for a given nucleus to make an upward or downward transition by interacting with molecular degrees of freedom. At equilibrium

$$n_1 W_1 = n_2 W_2 \tag{1.24}$$

i.e.

$$\frac{n_1}{n_2} = \frac{W_2}{W_1} \tag{1.25}$$

The Boltzmann distribution of nuclei between the two energy levels is given by

$$\frac{n_1}{n_2} = \exp\left(\frac{2\mu B_0}{kT}\right) \simeq 1 + \frac{2\mu B_0}{kT} \tag{1.26}$$

Provided that the interaction energy is small compared with the total energy of the system, i.e. the temperature is stationary, $\frac{W_2}{W_1}$ is independent of n_1 and n_2. Let

$$W_1 = W \exp\left(-\frac{\mu B_0}{kT}\right) \tag{1.27}$$

and

$$W_2 = W \exp\left(\frac{\mu B_0}{kT}\right) \tag{1.28}$$

where W is the mean of W_1 and W_2.

The rate of change of population is

$$\frac{dn_1}{dt} = -\frac{dn_2}{dt} = n_2W_2 - n_1W_1 \qquad (1.29)$$

which reduces to zero at equilibrium.

Since an upward transition decreases and downward transition increases the excess number of nuclei by 2

$$\frac{dn}{dt} = 2\,(n_2W_2 - n_1W_1) \qquad (1.30)$$

Expansion of the exponential in W_1 and W_2, by assuming that $\frac{\mu B_o}{kT} \ll 1$, gives

$$\frac{dn}{dt} = -2W\left[(n_1 - n_2) - (n_1 + n_2)\,\frac{\mu B_o}{kT}\right] \qquad (1.31)$$

If an equilibrium value of the excess number of nuclei in the lower energy state, n_{eq}, is defined by

$$n_{eq} = (n_1 + n_2)\,\frac{\mu B_o}{kT} \qquad (1.32)$$

it follows from eqns. (1.23) and (1.31) that

$$\frac{dn}{dt} = -2W\,(n - n_{eq}) \qquad (1.33)$$

i.e. the rate of approach to equilibrium is proportional to the departure from equilibrium.

On integration eqn. (1.33) leads to

$$n - n_{eq} = (n_o - n_{eq})\exp(-2Wt) \qquad (1.34)$$

where n_o is the initial value of n.

Let a time T_1 be defined as

$$T_1 = \frac{1}{2W} \qquad (1.35)$$

so that eqn. (1.34) can be written as

$$n - n_{eq} = (n_o - n_{eq}) \exp\left(-\frac{t}{T_1}\right) \qquad (1.36)$$

This time T_1 is a measure of the rate at which the spin system comes into thermal equilibrium with other degrees of freedom and is usually referred to as the spin-lattice relaxation time. Sometimes this has also been called the longitudinal relaxation time because it determines the approach to equilibrium of the component of macroscopic nuclear magnetic moment per unit volume lying parallel to B_o (see Sec.1.7).

Even if the excess population $n_1 - n_2$ is less than its equilibrium value, the relative populations in the two levels can still be described by the Boltzmann factor

$$\frac{n_1}{n_2} = \exp\left(\frac{2\mu B_o}{kT_s}\right) \simeq 1 + \frac{2\mu B_o}{kT_s} \qquad (1.37)$$

but now the room temperature T has to be replaced by a higher value T_s, referred to as the spin temperature.

1.6b Spin-Spin Relaxation

Each nuclear magnet is acted upon by not only the steady magnetic field B_o but also by a small local magnetic field B_{loc} produced by the neighbouring nuclear magnets. Since the neighbouring nuclear magnets are also themselves precessing about the direction of the magnetic field, the local field may be resolved into two components, oscillating (B_{osc}) and static (B_{stat}). The static component is parallel to the direction of the main field B_o. The other component is rotating at the precessional frequency in a plane perpendicular to the static field B_o. Thus a nucleus j producing a magnetic field oscillating at its Larmor frequency may induce a transition in nucleus K, in a manner similar to that induced by the applied oscillating field. The energy for this process comes from j and simultaneous re-orientation or flip-flop of both nuclei results. There is a simple exchange of spins and the total energy as well as the ratio of populations in different states remains constant throughout

the process. Only identitical nuclei are capable of undergoing such spin-exchange. Since the relative phases of the nuclei change in a time $(\Delta\nu)^{-1}$, a simple time interval will be required for spin exchange. This lifetime or phase memory time of a nuclear spin state has been termed the spin-spin relaxation time, T_2. Any resultant magnetic moment per unit volume at right angles to the steady field B_o is reduced to zero within this time and therefore, it is also referred to as the transverse relaxation time.

It has been pointed out earlier (see sec. 1.5) that the intensity of the irradiating radiofrequency field can affect the observed resonance signal by way of saturation. A quantitative treatment of the phenomenon will now be presented for an assembly of nuclei having spin $I = \frac{1}{2}$.

Before the radiofrequency field is applied, the rate of change of excess population per unit volume is given by

$$\frac{dn}{dt} = \frac{n_{eq} - n}{T_1} \tag{1.38}$$

where n_{eq} is the value of n when the spin system is in thermal equilibrium with the surroundings. When the radiofrequency field is applied, the amount of change in the excess population is 2nP, where P is the probability per unit time for a transition between the two energy levels under the influence of irradiation. Hence

$$\frac{dn}{dt} = \frac{n_{eq} - n}{T_1} - 2nP \tag{1.39}$$

The steady value of the excess number, n_s, is given by

$$\frac{n_s}{n_{eq}} = (1+2PT_1)^{-1} \tag{1.40}$$

A value for P can be obtained from standard radiation theory[18]. The probability of transition per unit time between two states having magnetic quantum numbers m and m^1 is

$$P_{m \to m^1} = \tfrac{1}{2} \gamma^2 B_1^2 \left| (m|I|m^1) \right|^2 \delta(\nu_{mm^1} - \bar{\nu}) \qquad (1.41)$$

where B_1 is the amplitude of the radiofrequency field rotating in the correct sense and in a plane at right angles to the main field B_o, and $(m|I|m^1)$ is the appropriate matrix element of the nuclear spin operator. $\delta(\nu_{mm^1} - \nu)$ is the Dirac function which is strictly zero at all values except for $\nu_{mm^1} = \nu$, thus giving rise to an infinitely sharp line. Since this is unreal, the function is replaced by a shape function $g(\nu)$ normalised as follows:

$$\int_o^\infty g(\nu) \cdot d\nu = 1 \qquad (1.42)$$

For $I = \frac{1}{2}$, eqn. (1.41) reduces to[10]

$$P = \tfrac{1}{4} \gamma^2 B_1^2 g(\nu) \qquad (1.43)$$

Therefore, $$\frac{n_s}{n_{eq}} = \left[1 + \tfrac{1}{2} \gamma^2 B_1^2 g(\nu) T_1\right]^{-1} \qquad (1.44)$$

The right hand side of eqn. (1.44) is usually denoted by Z and is referred to as the saturation factor. Saturation is greatest for the radiofrequency which gives the maximum value of shape function, which occurs for $2T_2$.

Therefore,

$$Z_o = \left[1 + \gamma^2 B_1^2 T_1 T_2\right]^{-1} \qquad (1.45)$$

where Z_o is the saturation factor for the maximum value of $g(\nu)$.

1.7 NUCLEAR MAGNETIC RESONANCE IN MACROSAMPLES

Bloch[19-21], using a series of phenomenological equations, has treated

the whole problem from a macroscopic point of view.

An assembly of nuclei in an applied magnetic field B_o have their various spin states occupied to different extents, which gives the sample a resultant magnetic moment. If M is the magnetic moment per unit volume of a substance under such circumstances, the susceptibility (χ_o) is given by the following relation

$$M = B_o \chi_o \tag{1.46}$$

The bulk magnetisation M is analogous to the nuclear magnetic moment μ, except in one respect that, in the absence of radiofrequency field, M has only a z component, whilst μ has (x,y and z) all the three components. The individual nuclei precess about the z axis and have random phases, hence x and y components average to zero in forming M.

The equation of motion for a single magnetic moment is

$$\frac{d\mu}{dt} = \gamma(\mu \times B) \tag{1.47}$$

Similarly, for an assembly of weakly interacting moments, contained in unit volume, the equation of motion is

$$\frac{dM}{dt} = \gamma(M \times B) \tag{1.48}$$

In the usual magnetic resonance experiment the three components of B are not all constant but have the values

$$B_x = B_1 \cos wt \tag{1.49}$$

$$B_y = -B_1 \sin wt \tag{1.50}$$

$$B_z = B_o \tag{1.51}$$

B_x and B_y together represent a radiofrequency field of amplitude B_1 rotating in a plane normal to the static field B_o. Assuming that

there are no other interactions involving the nuclei

$$\frac{dM_x}{dt} = \gamma (M_y B_o + M_z B_1 \sin\omega t) \qquad (1.52)$$

$$\frac{dM_y}{dt} = \gamma (-M_x B_o + M_z B_1 \cos\omega t) \qquad (1.53$$

$$\frac{dM_z}{dt} = \gamma (-M_x B_1 \sin\omega t - M_y B_1 \cos\omega t) \qquad (1.54)$$

The different relaxation processes must now also be taken into account. Prior to resonance, the spin system and the lattice are at thermal equilibrium and M_z is equal to the static magnetisation M_o. Once the resonance has occured, the spin system and the lattice are no longer at thermal equilibrium and M_z, instead of remaining constant, approaches M_o at a rate governed by the longitudinal relaxation time T_1. This rate is

$$\frac{dM_z}{dt} = \frac{M_o - M_z}{T_1} \qquad (1.55)$$

The individual nuclei will also be in phase after resonance, and M_x and M_y will have finite values, but due to the effect of spin-spin relaxation, the phase coherence will be lost and these components will decay to zero in time T_2. The rate of decay is given by

$$\frac{dM_x}{dt} = -\frac{M_x}{T_2} \qquad (1.56)$$

$$\frac{dM_y}{dt} = -\frac{M_y}{T_2} \qquad (1.57)$$

Combination of eqns. (1.52)-(1.54) with eqns. (1.55)-(1.57) leads to the Bloch equations which describe the actual behaviour of a macroscopic sample during an n.m.r. experiment (Fig. 1.3)

$$\frac{dM_x}{dt} = \gamma (M_y B_o + M_z B_1 \sin\omega t) - \frac{M_x}{T_2} \qquad (1.58)$$

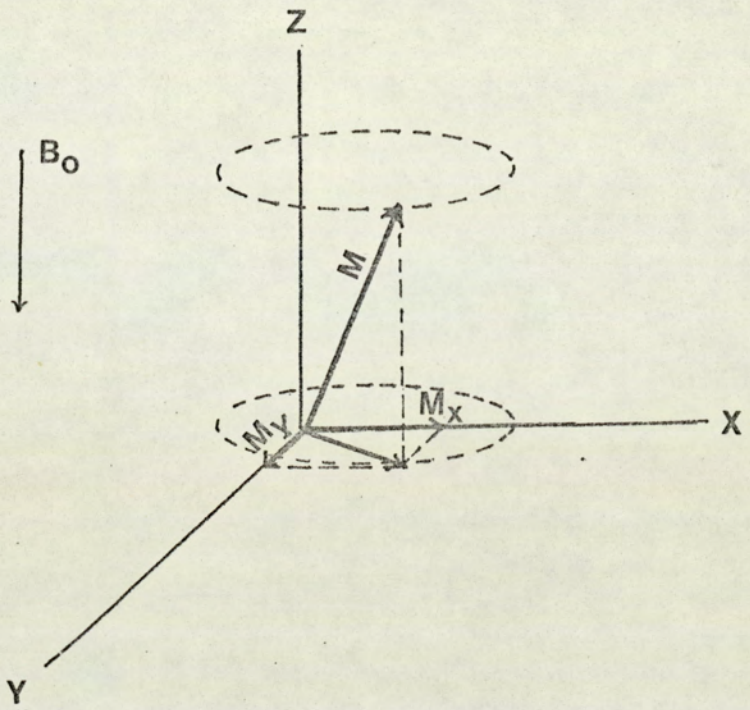

Fig 1.3 The Magnetisation vector M and its components in a fixed co-ordinate system.

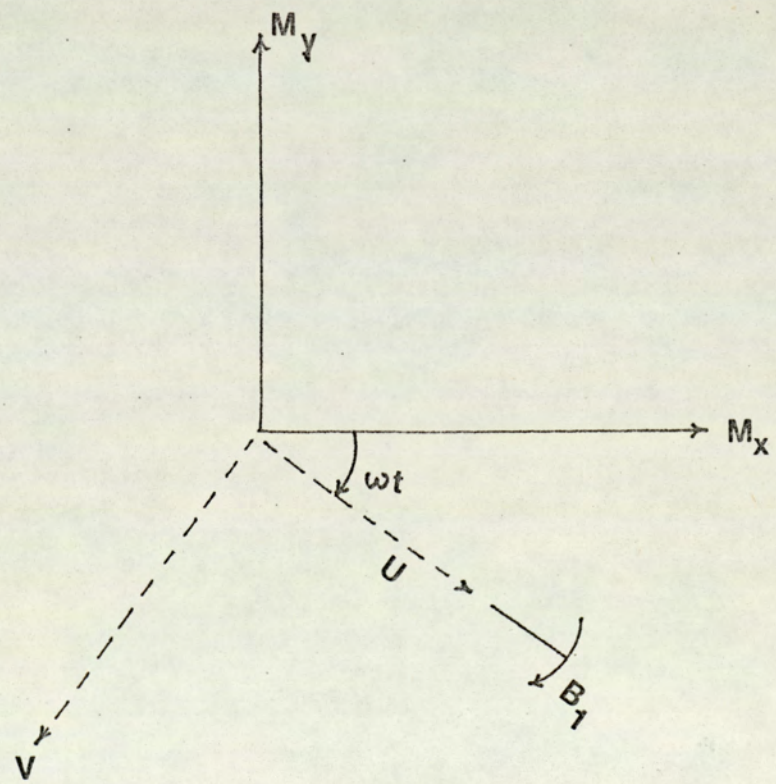

Fig. 1.4 Transverse components of the Magnetic moment referred to fixed axes (full lines) and axes rotating with the r.f. (dotted lines)

$$\frac{dM_y}{dt} = \gamma(-M_x B_o + M_z B_1 \cos\omega t) - \frac{M_y}{T_2} \tag{1.59}$$

$$\frac{dM_z}{dt} = \gamma(-M_x B_1 \sin\omega t - M_y B_1 \cos\omega t) + \left(\frac{M_o - M_z}{T_1}\right) \tag{1.60}$$

The Bloch equations take a simpler form if they are transferred to a set of axes rotating with the applied radiofrequency field. In this rotating frame (Fig.1.4) both B_o and B_1 are fixed while the new set of axes rotates with an angular velocity $-\omega$ about the z-axis. u and v are defined as the components of M along and perpendicular to the direction of B_1 respectively. They are often called the in-phase and out-of-phase components of M. The components are related as

$$M_x = u\cos\omega t - v\sin\omega t \tag{1.61}$$

$$M_y = -u\sin\omega t - v\cos\omega t \tag{1.62}$$

Substitution of (1.61) and (1.62) into the Bloch equations, noting that $\omega_o = \gamma B_o$, gives

$$\frac{du}{dt} + \frac{u}{T_2} + (\omega_o - \omega)v = o \tag{1.63}$$

$$\frac{dv}{dt} + \frac{v}{T_2} - (\omega_o - \omega)u + \gamma B_1 M_z = o \tag{1.64}$$

$$\frac{dM_z}{dt} + \frac{M_z - M_o}{T_1} - \gamma B_1 v = o \tag{1.65}$$

The solution of these equations is obtained under the steady state or slow passage conditions. Under these conditions, the absorption of radiofrequency energy is just balanced by the transfer of energy from the nuclei to the lattice so that $\frac{dM_z}{dt} = o$ Hence:

$$u = \frac{M_o \gamma B_1 T_2^2 (\omega_o - \omega)}{1 + T_2^2(\omega_o - \omega)^2 + \gamma^2 B_1^2 T_1 T_2} \tag{1.66}$$

$$v = \frac{M_o \gamma B_1 T_2}{1 + T_2^2(\omega_o - \omega)^2 + \gamma^2 B_1^2 T_1 T_2} \tag{1.67}$$

From eqn. (1.67) it is evident that when $\gamma^2 B_1^2 T_1 T_2 \ll 1$ the asbsorption or ' V-mode' signal should be proportional to $\frac{\gamma B_1 T_2}{1+T_2^2(\omega_0-\omega)^2}$. This describes a Lorentzian line[19-22] shape as shown in Fig. 1.5. At the centre when the resonance condition is just fulfilled, $(\omega_0-\omega) = 0$ and the signal height is proportional to $\gamma B_1 T_2$. Sometimes, it is preferable to use the dispersion or 'U-mode' signal as shown in Fig. 1.6.

The in-phase and out-of-phase magnetisations are also described in terms of the Bloch susceptibilities χ^1 and χ^{11}. The area under the absorption surve can be obtained by the inegration of the V term over all values of $(\omega_0-\omega)$. The result is directly proportional to χ_0 which is a direct function of the number of nuclei per unit volume. Hence the area under each resonance curve is a direct measure of the number of nuclei of a particular type undergoing resonance.

1.8 FACTORS AFFECTING THE LINE SHAPE

It has already been said that an n.m.r. absorption line is represented by a Lorentzion curve[19,22]. A quantum mechanical approach to the phenomenon predicts an infinitely sharp absorption line, however, for identical nuclei, absorption occurs over a small but finite frequency range due to several line broadening effects. The width of a line is defined as its width at half height expressed in terms of applied field or frequency. The various factors affecting the line shape will now be discussed.

1.8a Spin-Lattice Relaxation

The life time of a nucleus in a given state is limited by the spin-lattice relaxation mechanism and thus there is an uncertainity in the

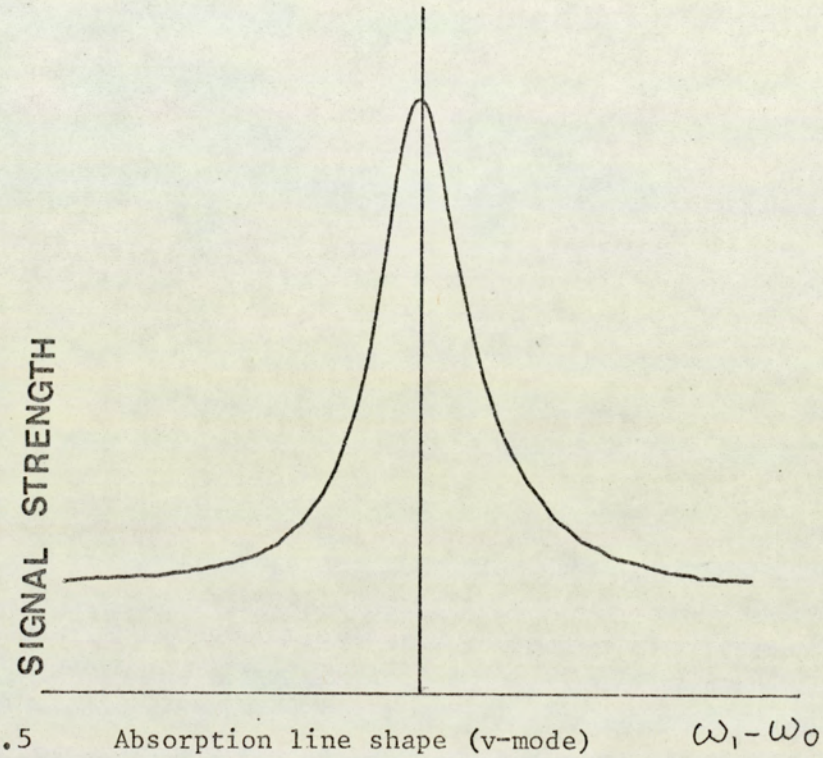

Fig. 1.5 Absorption line shape (v-mode) for n.m.r. resonance

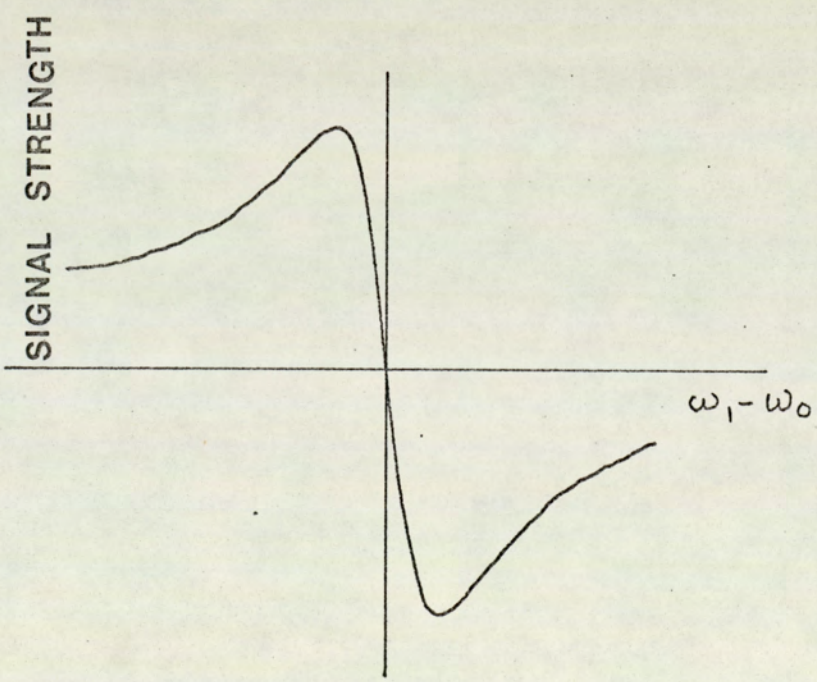

Fig. 1.6 Dispersion line shape (u-mode) for n.m.r. resonance

lifetime of that spin state which is of the order of $2T_1$. The order of the magnitude of broadening can be estimated from the uncertainity prinicple

$$\Delta E \cdot \Delta t \simeq \hbar \tag{1.68}$$

and since $$\Delta E = h\Delta\nu \tag{1.69}$$

it follows that

$$\Delta\nu = \frac{\hbar}{2T_1 h} \tag{1.70}$$

i.e. $$\Delta\nu = \frac{1}{4\pi T_1} \tag{1.71}$$

Eqn. (1.71) gives the uncertainity spread in the frequency of a given absorption line due to limitations placed on the nucleus by the spin-lattice relaxation mechanism.

1.8b Magnetic Dipolar Broadening

It has already been pointed out (see sec. 1.6b) that a magnetic nucleus experiences a small local magnetic field, B_{loc}, due to the neighbouring nuclear magnets, which can be resolved into static and oscillating components. The static field, which results in dipolar broadening, is given by

$$B_{stat} = \frac{\mu}{r^3}(1-3\cos^2\theta) \tag{1.72}$$

at a nucleus distance r away from the nucleus under consideration and lying on a line inclined at an angle θ to the magnetic dipolar axis. For solids the resultant local field can have any value between $\pm \frac{2\mu}{r^3}$, which is of the order of 10^{-3} tesla for protons. Magnetic resonance will thus occur over a range of frequencies and the line will be broadened[19]. In liquids and gases, where the molecules are undergoing rapid random motion, $\cos^2\theta$ averages to $\frac{1}{3}$ and $B_{stat} = 0$. The molecular motions necessary to produce such averaging are of shorter time than that required

to observe a nuclear resonance signal, and the effect of magnetic dipoles on line width in liquid and gaseous samples is negligible.

1.8c Spin-Spin Relaxation

The oscillating component of the local field due to the neighbouring nuclei brings about spin-spin relaxation. In a manner similar to that discussed in sec.1.8a, the spin-spin relaxation process introduces an uncertainty into the lifetime of any nuclear state and hence an uncertainty in the frequency at which resonance will occur. This leads to the observation of resonance over a small range of frequencies giving a broadened absorption signal.

1.8d. Electric Quadrupole Effects

Nuclei with spin number $I > \frac{1}{2}$ may possess a non-spherically symmetrical charge distribution and therefore a quadrupole moment Q. Nuclei do not have any electric dipole moment and so the energy of any nucleus is independent of its orientation in a uniform electric field. However, when an electric field gradient exists, the quadrupoles undergo precession and assume specific orientations in an inhomogeneous electric field. This displaces the nuclear magnetic levels. The interaction of nuclear quadrupoles with the fluctuating field gradient offers an additional method of relaxation. Consequently nuclei with quadrupole moments frequently exhibit very short spin-lattice relaxation times and the observed absorption lines are correspondingly broad.

1.8e. Other Factors Affecting The Line Shape

Inhomogeneity of the magnetic field B_o over the sample volume will cause line broadening due to resonance occuring not at a specific field strength, but over a range of field as different portions of the sample experience

the resonance condition at slightly different times. Rapid spinning of the sample partially overcomes this problem.

Certain transient effects are also responsible for the distortion of the signal shape. When the resonance line is swept through rapidly, it is followed by damped oscillations referred to as relaxation wiggles or ringing[23]. They originate from the inability of the nuclear magnetisation to follow the changing applied field B_o. After traversing the resonance condition, a magnetic moment persists in the plane at right angles to the main field for as long as a group of nuclei continue to precess in phase. Precession about B_o induces a signal at the precession frequency, the signal amplitude decaying at a rate governed by the phase memory time T_2. After passing through a true resonance condition, the precession frequency and the radiofrequency differ slightly, so that the two signals interfere with one another giving rise to a low frequency beat signal which decays exponentially with time[24].

1.9 CHEMICAL SHIFTS

So far in the discussion of n.m.r. it has been assumed that the resonance frequency of a nucleus is simply a function of the applied field and the megnetogyric ratio of the nucleus. However, it was discovered that the resonance frequency is, to a small degree, dependent upon the chemical environments of the nucleus. This phenomenon was observed first by Knight[25] for metals and metal salts, and later by Proctor and Yu[26] for ^{14}N compounds, and by Dickinson[27] for ^{19}F compounds. It has been discovered that this phenomenon is general for all magnetic nuclei and has been discussed in terms of 'The Chemical Shift'. The Chemical Shift is observed whenever two or more nuclei of the same isotopic species have different environments, a separate resonance usually being observed for each distinct group with an intensity proportional to the number of nuclei in that group.

The Chemical Shift is directly proportional to the strength of the applied field and arises from small intermolecular and intramolecular

contributions to the actual field experienced by a particular nucleus. If B_o is the applied field, the actual field B experienced by the nucleus is given by

$$B = B_o(1 - \sigma) \tag{1.73}$$

where σ is a dimensionless constant dependent on the chemical environment. The constant σ is called screening constant because the local field is usually slightly smaller than the applied field. The effect of screening constant will be to bring the Zeeman levels closer as illustrated below:

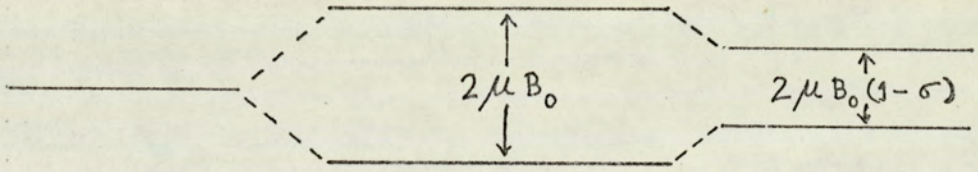

No field | Bare nucleus infield | Screened nucleus infield

As a result, the energy quantum required for a transition between the states is smaller and therefore the resonance will occur at a lower frequency. Alternatively, if the experiment is performed by varying the field B_o until resonance is obtained at a fixed frequency, the applied field will have to be of a value higher than that for an unscreened nucleus. If two isotopically similar nuclei in environments i and j have screening constants σ_i and σ_j respectively, for the same value of B_o the chemical shift δ_{ij} is given by

$$\delta_{ij} = \sigma_i - \sigma_j \tag{1.74}$$

The measurement of absolute chemical shift is not possible since this would require the comparison of resonance frequencies of the nuclear species in a particular environment with that of the same nucleus devoid

of all its electrons. Chemical shifts are therefore generally measured relative to a reference compound. For proton spectra, tetramethylsilane (TMS) is generally chosen as the reference compound since its resonance is a single sharp line occurring to highfield of most resonances of interest. On this basis, the chemical shift is measured in terms of a dimensionless number δ given by

$$\delta = \frac{(B_c - B_r)}{B_r} \quad (x10^6) \quad \text{ppm} \tag{1.75}$$

where B_c is the resonance field for the nucleus under observation and B_r is the resonance field for the reference compound. Since B is proportional to ν , eqn. (1.75) can be expressed as

$$\delta = \frac{(\nu_c - \nu_r)}{\text{Oscillator frequency}} \times 10^6 \tag{1.76}$$

where ν_c and ν_r are the frequencies corresponding to B_c and B_r in eqn. (1.75). As a convention, the nuclei which are less shielded than the reference are assigned negative chemical shifts.

For proton spectra, when using tetramethylsilane as an internal reference, a scale known as τ scale [28] is often used, such that the tetramethylsilane line at infinite dilution in carbontetrachloride is arbitrarily given the value $\tau = 10$. The τ value of any other resonance line is then given by

$$\tau = 10 + \delta \tag{1.77}$$

1.10 ORIGIN OF CHEMICAL SHIFT

Early attempts to account for the shielding of a nucleus were based on a theory developed by Lamb[29] who considered the magnetic shielding of a nucleus due to the induced electronic currents in a free atom with no orbital or spin angular momentum. When dealing with molecules this method becomes unsuitable and the first theoretical expression for the

screening of a nucleus in an isolated molecule was derived by Ramsey[30,31].

Even the Ramsey formula is not suitable for the calculation of screening constants in any but the smallest molecules. In order to deal with large molecules, it is convenient to break up the screening into several individual contributions, the sum of which will represent the total screening of the nucleus. Each of these contributions may be taken to have classical significance. This approach was first proposed by Saika and Slitcher[32] who divided the screening of a nucleus into three seperate atomic contributions. However, the shielding of any resonant nucleus A can be more completely and usefully divided into five contributions representing both intramolecular and intermolecular screening terms[10] given by

$$\sigma_A = \sigma_{dia}^{AA} + \sigma_{para}^{AA} + \sum_{B \neq A}' \sigma_{mag}^{AB} + \sigma_{del} + \sigma_{sol} \qquad (1.78)$$

That this division is reasonable can be deduced from the fact that for gases the screening constant σ may be expressed as a virial type expansion, i.e. an inverse power series[33] in the molar volume Vm

$$\sigma = \sigma_o + \frac{\sigma_1}{Vm} + \frac{\sigma_2}{Vm^2} + \ldots\ldots\ldots \qquad (1.79)$$

Here σ_o is the screening constant for an isolated unperturbed molecule, σ_1 is a correction for bimolecular interactions, and σ_2, σ_3 ..... are higher order corrections due to higher order collisions. Experimentally it has been shown that only the first two terms of (1.79) are important. σ_1 corresponds to the last term in eqn. (178). Higher order terms, σ_2, σ_3, ... are usually very small and can be neglected[34]. σ_o of eqn. (1.79) represents the four intramolecular terms of eqn. (1.78).

An effective difference in the magnitude of the different terms in eqn. (1.78) for two nuclei contributes to the chemical shift between them.

Each of these terms will be discussed in turn.

1.10.a The Diamagnetic Term σ_{dia}

If an atom with a spherically symmetrical electron distribution is placed in a uniform magnetic field, the field causes the electrons to undergo a circulatory motion about the nucleus. The direction of Larmor precession is such that it produces a secondary magnetic field which, in the region of nucleus, is opposed to the applied field. The nucleus experiences the effect of both the applied and the induced field and the resultant field is therefore less than the applied field. The strength of the induced field is proportional to the strength of the applied field. Pople[35,36] for mathematical convenience, has separated the induced electronic circulations in molecules into three components. The first component, local diamagnetic currents, correspond to the atomic case discussed above. The electronic distribution about the nucleus is considered to be spherically symmetrical since the effects of departure from such symmetry are allowed for later by the consideration of two other types of sirculations, local paramagnetic circulations and inter-atomic circulations. Local diamagnetic currents, therefore, provide a source of positive shielding, i.e. they reduce the total field experienced by the nucleus. The only way in which molecular environments can affect the local diamagnetic shielding is by an alteration of the electron density around the nucleus concerned.

1.10b. The Paramagnetic Term σ_{para}

The paramagnetic term arises because the magnetically induced motions of the electrons are restricted in certain directions. Mathematically, the paramagnetic shielding term corresponds to a mixing, under the influence of the applied field, of the ground state electronic configuration with

low lying excited states of correct symmetry[37,38].

1.10c. Interatomic Shielding σ_{mag}

This term may make a positive or negative contribution to screening and is thought to arise principally from the neighbour anisotropy effect[39]. Atoms or groups which comprise the molecule may have anisotropic susceptibility. Thus when the molecule is placed in a strong magnetic field, the magnetisations in the direction of the principal axes of bonds can be different so that an effective magnetic moment is induced. The secondary fields produced at a nucleus by these induced dipoles are responsible for the neighbour anisotropy effect. The magnitude of σ_{mag} depends on the nature of the atom or group in which the secondary field originates and the molecular geometry.

1.10d. Delocalised Electron Shielding σ_{del}

Certain structures permit the circulation of electrons over a number of atomic centres and when this can occur, an additional shielding mechanism is available. Diamagnetic currents of this type are more readily developed in large closed loops such as the conjugated π- orbitals of benzene[40] which in essence behaves as a molecular solenoid. The induced field at the aromatic protons is parallel to the main field and hence these protons are deshielded by the ring current. The protons situated on or near the six-fold axis of benzene ring experience the diamagnetic part of the induced field and are therefore shielded due to this effect.

1.10e. Intermolecular Screening Effect σ_{sol}

In recent years [41,42], the study of intermolecular screening effect has received considerable attention and many authors have used the term 'Solvent Effects' for such screening. The term σ_{sol} accounts for the

direct or reaction effect of the solvent molecule(s) on the molecules whose screening is being considered. σ_{sol} can itself be considered to arise from several intermolecular effects[43], and may be expressed as

$$\sigma_{sol} = \sigma_b + \sigma_a + \sigma_w + \sigma_E + \sigma_c \qquad (1.80)$$

where σ_b is the screening contribution arising from the medium bulk susceptibility, σ_a that arising from the magnetic anisotropy of the medium, σ_w that due to the van der Waals or dispersion forces between the solute and solvent molecules, and σ_E that mainly produced by the electric field induced in the medium by a polar solute. σ_c is the contribution to the chemical shift change brought about by the 'Specific interaction' between solvent and solute molecules. A difference in any of the terms in eqn. (1.80) for the two nuclei can effect the σ_{sol} screening contributions. These differences may be appreciable for two nuclei in different intermolecular environments, and are thus particularly important when using an external reference for the measurement of chemical shifts. In this particular procedure, the reference liquid is sealed in a small thin capillary tube which is then put in the sample to be measured. Some of these effects may be largely eliminated by the use of an internal reference where the reference is present in the sample itself. In the investigations reported here in this work, an internal reference has been used. The various solvent screening terms will be considered now though there are as yet no really good theories for any of them except σ_b.

1.10f. Bulk Magnetic Susceptibility Term σ_b

An expression for σ_b can be derived in a manner similar to that for electric polarization effects. The total volume of a sample may be divided into two regions by defining a sphere around any molecule within the sample, large enough to be of macroscopic dimensions and small compared with the size of the sample. In the presence of the applied field B_o, the medium will be polarized and the field experienced by a nucleus at the centre of the sphere will be a sum of three parts:

(i) the external field;

(ii) the field due to the induced magnetisation in the region between the small sphere and the sample boundary;

(iii) the field due to the induced magnetisation in the inner sphere.

The bulk susceptibility arises from (ii). The effective field at a nucleus in a medium of susceptibility χ_v is given by[44]

$$B_{eff} = B_o \left[1 + \left(\frac{4\pi}{3} - \alpha\right)\chi_v\right] \qquad (1.81)$$

where α is a shape factor which is $\frac{4\pi}{3}$ for a sphere and 2π for a cylinder of length large compared to its radius. Since high resolution measurements are usually made in cylindrical tubes, the medium susceptibility contribution to shielding constant, when B_o is transverse to the tube, is $\frac{2\pi}{3}\chi_v$,

i.e.

$$\sigma_{obs} = \sigma_{mol} + \frac{2\pi}{3}\chi_v \qquad (1.82)$$

The observed chemical shift δ_{obs} and the chemical shift corrected for the difference in susceptibility are thus related by

$$\delta^{corr}_{A-B} = \delta^{obs}_{A-B} + \frac{2\pi}{3}(\chi_B - \chi_A) \qquad (1.83)$$

This equation relates to perfect cylinders and a general expression for arbitrarily shaped vessels has also been obtained by Frost and Hall[45].

If an internal reference compound is used, χ_A and χ_B will be equal and no correction is needed. In the investigations reported here, an internal reference has been employed and therefore, σ_b can be neglected.

1.10g. <u>The Anisotropy Term</u> σ_a

The field experienced by the individual molecules in the sample is

significantly affected in the presence of solvent molecules exhibiting anisotropy in their magnetic susceptibility. This term becomes predominant when a solute molecule takes up a preferred orientation with respect to the solvent molecule due to stereospecific interactions.

The anisotropy is most clearly seen in the large differential shift often found between solutes in aromatic and non-aromatic solvents. Qualitatively these shifts may be explained in terms of large diamagnetic anisotropy of an aromatic molecule which arises from the circulation of aromatic π-electrons (ring current effect)[40]. The distribution of solvent molecules surrounding a solute molecule may be non-random at small distances because of the latter's presence and this may result in a time averaged non-zero susceptibility tensor, which leads to screening at the nucleus of the solute molecule[46]. Possible causes of this non-randomness include electric dipolar interactions[47-52], size and shape of the solute[53-55], and the steric crowding in condensed aromatics[56]. When polar solutes are present specific collision complexes of finite lifetime may be formed due to particularly strong attractive forces, and in these cases only that part of the screening attributable to non-random orientations may be considered to constitue σ_a, since anisotropy screening is present in addition to any screening due to complex formation[57].

Buckingham et al[43] have shown that the anisotropic shielding of spherical molecules by disc shaped and rod shaped molecules may be calculated using eqns. (1.84) and (1.85) respectively

$$\sigma_{a(disc)} \simeq -\frac{2n\Delta\chi}{3R^3} \qquad (1.84)$$

$$\sigma_{a(rod)} \simeq \frac{n\Delta\chi}{3R^3} \qquad (1.85)$$

where $\Delta\chi$ is the difference in magnetic susceptibilities parallel and perpendicular to the symmetry axis of the magnetically anisotropic

molecule, R is the distance from the centre of the anisotropic molecule to the centre of the resonating nucleus, and n the number of molecules in the effective range of R. Eqns. (1.84) and (1.85) result from the limiting conditions for eqn. (1.86) which was also deduced by Buckingham et al. and is effectively equivalent to more explicit expression given by Stephen[58].

$$\sigma_a = \tfrac{1}{3} n R^{-3} \Delta\chi (1-3\cos^2\theta) \qquad (1.86)$$

where θ is the angle between the axis of the solvent molecule and the line joinging the centre of the solvent and the nucleus under consideration. It must be said at this stage that all these expressions are dependent on McConnell's equation [39] which specifically applies to intramolecular situations.

Abraham[59] has suggested eqn. (1.87) as a less qualitative and more generally applicable expression than (1.84) and (1.85)

$$\sigma_a = -10^{30} \cdot \tfrac{2}{3} \Delta\chi \frac{\gamma - h}{(\gamma+2h)(\gamma^2 + h^2)^{3/2}} \qquad (1.87)$$

This was derived by considering the anisotropic molecules to be a cylinder of effective radius $\gamma(A^o)$ and height $2h(A^o)$ with different magnetic susceptibilities $\chi_{\parallel}$ and $\chi_{\perp}$ along and perpendicular to the cylinder-axis. Eqn. (1.87) does, however, only provide an estimate of the shielding contribution from a single anisotropic molecule. Homer et al[60] have extended eqn. (1.87) to give good results.

Becconsall[61-63] has recently calculated the screening effect of benzene on a number of approximately spherical molecules of different size. These calculations are based on a model in which only the solvent molecules within a shell, effectively containing the solute, contribute to the solvent anisotropy, the remaining solvent molecules in the bulk being ineffective. But this model also does not give very reasonable results.

1.10h. Van der Waal or Dispersion Screening σ_W

The dispersion screening term, σ_W, arises from time-variant electric dipoles present in all molecules which produce electric fields temporarily polarising adjacent molecules[64] and thereby altering the screening of nuclei in these molecules. Howard, Linder and Emerson[65] proposed a procedure for calculating the value of σ_W, by treating the solute as being surrounded by a continuous dielectric medium. But Lumbroso et al[66] consider that this does not give good agreement with experimentally determined values and subsequent improvements in the theory by de Montgolfier[67] lead to little better agreement with experiment. Treating the solute surrounded by a discrete number of solvent molecules, Rummens et al.[68] have presented both a binary 'collision gas' model and a 'cage' model of estimating σ_W. However, this gives reasonable answers for small molecules only. In general, calculated values of σ_W are very small but Raynes et al.[69] have apparently measured real dispersion screenings which are large. Homer and Huck[70] have calculated the magnitude of σ_W in nitroform-aromatic-cyclohexane system. It has been shown that the difference between the calculated screening of the solute and the reference, in the concentration range from almost pure cyclohexane to pure aromatic, never exceeds about 0.002 ppm and was considered to be negligible compared to the experimental accuracy. For analogous systems investigated in this work, the σ_W contribution will be considered negligible.

1.10i. Reaction Field Screening σ_E

An electric field E acting along the axis of an X-H bond will draw electrons away from the proton, thus making it less shielded. The magnitude of the reduction in shielding is given by[10]

$$\sigma_E = 2 \times 10^{-5} - 2 \times 10^{-2}E - 10^{-18}E^2 \qquad (1.88)$$

If E is an intramolecular field arising due to the presence of a polar group in the molecule itself, σ_E is finite, but in the absence of preferred molecular orientations E averages to zero at any particular nucleus in liquid or gas samples. However, a polar molecule in solution polarises the surrounding medium and the nuclei in the molecule experience a reaction field whose value is dependent on the random motion of the molecule. The most significant reaction field normally encountered for solutions of polar molecules has been defined in two ways. Firstly, Buckingham[71] followed the approach of Onsagar to define E in the form of eqn. (1.89)

$$E = \frac{2(\epsilon_2 - 1)(n_1^2 - 1)\mu_1}{3(2\epsilon_2 + n_1^2)\alpha_1} \qquad (1.89)$$

where ϵ_2 is the medium dielectric constant, and μ_1, n_1 and α_1 are the dipole moment, refractive index and polarizability of the solute respectively. The solute is considered as a sphere having a point electric dipole acting at its centre with μ the gas phase value. Diehl and Freeman[72] have accounted for the shape of the solute molecule in eqn. (1.90) by considering the dipole to act from the centre of a non-spherical cavity with semi-axes a,b and c.

$$E = \frac{\mu}{abc}\, 3\, \xi_a \left[1 + (n^2 - 1)\, \xi_a\right] \left[\frac{(\epsilon - 1)}{\epsilon + (n^2\, \xi_a)/(1 - \xi_a)}\right] \qquad (1.90)$$

where ξ_a is a shape factor for the solute. Homer[73] has shown that in order to predict the difference in shielding in a particular solute due to reaction fields set up in different solvents, it is adequate to consider the solute as spherical. Huck[74] has shown that for three component systems, similar to those reported in the present investigation, the shieldings of the solute due to aromatic and cyclohexane differ only slightly and no correction to observed shifts is necessary.

Whilst only the so-called reaction field constant has been discussed it

is obvious that any electric fields of an intermolecular origin that perturb the solute will contribute to σ_E.

1.10j. The Specific Association Term σ_c

The term σ_c has been applied to the effect on chemical shifts of any specific solute-solvent interactions in solution; in this usage, shifts due to anisotropy effects associated with specific interactions are sometimes included in the σ_a term. However, in this investigation σ_c shall be taken to represent the effect of solvent anisotropy in a geometrically specific solute-solvent orientation which has been brought about by the formation of a collision complex.

Collision complexes between aromatic hydrocarbons (solvent) and other aliphatic as well as aromatic compounds (solute) are well known. In most of the cases, complex formation has been studied by measuring the proton shifts of solutes containing either a single or a group of equivalent hydrogen atoms. Such studies can not provide enough information to establish the stereospecific nature of the complex. However, by using molecules with more than one non-equivalent hydrogen atoms as solute, one can derive valuable information regarding the currently contentious stereospecific nature of the complex. If the collisions are not completely random and the solute, on the average, has got a tendency to adopt a preferred orientation with respect to the solvent molecules, the different non-equivalent protons in the solute molecule are expected to suffer unequal solvent induced shifts, as a result of complex formation. The present investigation has been taken up especially with this end in view. Vinyl derivatives, $CH_2 = CHX$, provide a good example of a solute with three non-equivalent protons and complex formation between several of these with benzene has been studied at several temperatures. Solute molecules with different values of dipole moment have been selected so that some information regarding the nature of the complex can be obtained. The studies have also been repeated with alkyl substituted

benzenes as solvent with a view to study the effect of such substitution in the benzene ring on complex formation.

1.11 SPIN-SPIN COUPLING

Nuclear magnetic resonance signals arising from a set of identical nuclei, when examined[75] under high resolution conditions, were found to consist of a group of lines rather than a single line. A further significant fact about the spectra was that the separation between the components of the multiplet, measured on frequency scale, was independent of the applied field B_o, instead of being proportional to it as would be the case if the different signals arose from different sheilding constants. In the simplest case the spacings between these multiplet lines are equal and the magnitude of this splitting is known as the coupling or spin-spin interaction constant, represented by the symbol J.

To discuss spin-spin coupling fully, it is necessary to take into account all possible magnetic interactions[76]. There are a number of them which result in the observed multiplicity, but not all of them are equally important. The interactions may be grouped as follows. Firstly, there are various electronic orbital-orbital, orbital-spin, spin-spin, and spin-external field interactions. Secondly, there is the nuclear-electronic-electronic-nuclear interaction.

It was proposed by Gutowsky, McCall and Slichter[77] and also by Hahn and Maxwell[78] that the multiplets arise from an interaction between neighbouring nuclear spins which is proportional to their scalar product $I(1) \cdot I(2)$, where $I(1)$ and $I(2)$ are nuclear spin vectors. Unlike the direct interaction of the magnetic dipoles, an energy of this sort is not averaged to zero by the molecular motions. Ramsey and Purcell[79] interpreted this effect as arising from an indirect coupling mechanism via the bonding electrons in the molecule. A nuclear spin tends to

orient the spins of the nearby electrons and consequently spins of the other nuclei. Ramsey has given a general expression for spin-spin splitting but it is difficult to evaluate even in simple cases. Approximate calculations, however, show that this electron spin mechanism is the most important contribution although in general all magnetic interactions could play some part.

Spin-spin interactions exhibit the following important features which help in distinguishing them from the chemical shifts:

(i) When nuclei are equally screened and are magnetically equivalent no coupling is observed between them. Nuclei are said to be magnetically equivalent when they have the same Chemical Shifts and couple equally to all other resonant nuclei in the molecule.

(ii) The coupling is independent of the strength of the applied field.

(iii) In general, the magnitude of coupling constant decreases as the number of bonds separating the interacting nuclei increases.

(iv) The magnitude of the coupling constant between two nuclei generally increases with the atomic number of both the nuclei.

(v) Spin-spin coupling effects are mutual, i.e. the splitting observed in one band is identical to the splitting in the band of interacting nuclei.

When the chemical shift difference between the interacting nuclei is large compared with the coupling constant and the spectra conform to what is called first order conditions, the following two more regularities are observed:

(vi) The multiplicity of the band arising from a group of equivalent nuclei is determined by the neighbouring groups of equivalent nuclei. A neighbouring group of equivalent nuclei causes a multiplicity which is given by the formula $(2nI+1)$ where n is the number of equivalent nuclei of spin I in that group. If there are more than two interacting groups, the multiplicity of one,

A, is given by $(2n_B I_B + 1)(2n_c I_c + 1)$ .....

(vii) The intensities of the nultiplets are symmetric about the centre of the band and when the multiplicity is produced by a group of equivalent nuclei with $I = \frac{1}{2}$, the relative intensities are given by the coefficients of the terms in the expansion of $(Y + 1)^n$.

When the magnitudes of chemical shifts are comparable with the corresponding coupling constants, the spectrum does not obey the rules of multiplicity and relative intensities given above for the case of first order spectra and a rather complex pattern is obtained which requires a detailed analysis. Such spectra are said to be of second order.

The convention adopted for the classification of spectra is to use the symbols A,B,C, ...X,Y,Z, to characterize the individual nuclei within a nuclear spin system. The letters close together in the aplhabet e.g. A,B,C .... generally represent magnetically non-equivalent nuclei of the same species having small relative chemical shifts of the same order of magnitude as the coupling constants between them. X,Y and Z are used to represent a similar set of nuclei, not necessarily of the same species as the first set, but having a large chemical shift from the first set. Magnetically equivalent nuclei are described by the same symbol, their number being indicated by a subscript e.g. A_2. Nuclei which show chemical shift equivalence but are not magnetically equivalent, are referred to by the same letter but are distinguished from each other by means of primes e.g. AA'. Since the investigations carried out in this work are concerned with ABC spectra, the procedure for the analysis of this class will be considered in detail in Chapter 3 of this work.

1.12 CHEMICAL EXCHANGE PHENOMENON

In oder to get a high resotution n.m.r. spectrum, the spin-lattice relaxation time T_1 has to be longer than 0.1 second. This long time scale

inherent in the method allows many phenomena occuring in shorter times to affect the resonance signal. Defining τ_A and τ_B as the first order lifetimes of a magnetic nucleus X in two molecular environments A and B, the probability of X in A moving to B is $\frac{1}{\tau_A}$ and vice versa; and $\omega_A - \omega_B$ is the chemical shift difference of X in the two environments, measured in rad. sec.$^{-1}$. When no exchange is taking place $\tau_A = \tau_B = \infty$, and two distinct signals will be observed with a chemical shift of $\omega_A - \omega_B$. So long as the chemical shift difference between the two sites is sufficiently large, two distinct signals will be there, even if the rate of exchange in reasonably slow ($\tau_A \gg (\omega_A - \omega_B) \ll \tau_B$) and the separation will be $\omega_A - \omega_B$, but both lines will be broadened due to exchange. As the rate of exchange increases, these lines eventually coalesce and a new signal is obtained at some intermediate frequency, ω, such that

$$\omega = P_A \cdot \omega_A + P_B \cdot \omega_B \qquad (1.91)$$

where

$$P_A = \frac{\tau_A}{\tau_A + \tau_B} \qquad (1.92)$$

and

$$P_B = \frac{\tau_B}{\tau_A + \tau_B} \qquad (1.93)$$

i.e. P_A and P_B are the fractions of time spent by X in environments A and B respectively. For similar reasons, if an atom is removed from an environment in a time short compared with the reciprocal of the spin coupling constant, spin coupling features are also affected.

Many phenomena in solution can be studied by making use of the chemical exchange effect; one that has received considerable attention recently is the study of molecular interactions in solution. Investigations of this type form the basis of the work described in this thesis. If complexes formed between polar solutes and aromatic solvents are considered, these can be investigated by studying the dependence of the observed solute time-average chemical shift on sample composition.

CHAPTER 2

EXPERIMENTAL METHODS FOR THE OBSERVATION OF HIGH RESOLUTION NUCLEAR MAGNETIC RESONANCE

2.1 INTRODUCTION

From the consideration of the general theory of n.m.r. in the previous chapter, it clearly emerges that any apparatus assembly for the observation of an n.m.r. signal should consist essentially of the following parts:

(i) a magnet capable of producing a very strong homogenous field;

(ii) a means of continuously varying the magnetic field and/or frequency over a small range;

(iii) a 'probe' which is essentially a sample holder, supporting the irradiation and detection coils, and having provision for spinning the sample;

(iv) a radiofrequency oscillator;

(v) a radiofrequency receiver;

(vi) presentation facilities utilizing an oscilloscope and/or recorder.

The basic requirements for the individual components of a high resolution nuclear magnetic resonance spectrometer will now be briefly discussed, followed by a consideration of two commercial spectrometers, the Perkin-Elmer R10 and HA 100D Varian NMR spectrometers used in these investigations.

2.2. THE MAGNET

Both permanent and electromagnets have been used to obtain nuclear magnetic resonance spectra. The essential feature of the magnet is that it should possess a region between the pole faces in which the magnetic field is homogeneous to a high order (1 in 10^9). Because of larger chemical shifts and increased signal intensity at higher field,

strength, it is desirable that the strength of the field should be as high as is practically possible.

The upper limit of the field strength obtainable from conventional magnets for n.m.r. purposes is about 2.5 tesla. This limit arises out of homogeneity considerations over a volume of 0.1 cm^3. To obtain the desired degree of homogeneity in a pole gap of 12-20 mm, necessary to accomodate the radiofrequency probe and the sample, an elaborate magnet system is required. The pole pieces should be of 150-300 mm in diameter, so that the central portion of the field can have a 'flat' contour and suffer as little as possible from 'edge effects', i.e. bending of the lines of magnetic force near the edge of the pole pieces. The pole faces should be parallel, almost optically flat[80], and free from machining marks. The pole cap material must be metallurgically uniform and are usually chromium-plated to reduce the effects of corrosion. Both permanent and electromagnets are capable of an intrinsic homogeneity of 1 part in 10^6, which may be further improved with Golay Shim Coils to 1 part in 10^8. These coils, situated in pairs on the pole faces of the magnet, are arranged such that a stabilized direct current when passed through them may be adjusted to produce field gradients in specific directions. These gradients are helpful in counteracting the inhomogeneities of the intrinsic magnetic field. Electromagnets sometimes require careful 'cycling' in order to obtain the degree of homogeneity required for n.m.r. experiments. The homogeneity of the field may be further improved by spinning the sample.

For accurate measurement of the chemical shifts, it is necessary that the field should be stable. Permanent magnets are generally enclosed in a thermostated enclosure to reduce the field-drift to a minimum. Ambient field disturbances can be minimised by mu-metal screening or field sensing devices. In spectrometers using electromagnets additional

stability is obtained by field/frequency lock systems (see sec.2.7.b).

High resolution n.m.r. spectrometers incorporating either a permanent magnet or electromagnet employ flux-stabilizing coils[81]. These coils are used to detect changes in the total flux across the gap and the voltage induced in them is applied to a galvanometer which acts as a source of integrated correction signal which is passed through a pair of compensating coils. The flux produced by these cancels the original change of flux and restores the galvanometer deflection to zero.

The advantage of an electromagnet is that it is possible to pre-set the field strength at anywhere from zero to its maximum value. This is useful in that the instrument can be used for the examination of more than one isotope without changing the radiofrequency oscillator. A more important advantage derives from the possibility of measuring the spectrum of the same isotope at different field strengths. This feature is extremely helpful in the interpretation of complex spectra since it differentiates between the field-dependent chemical shifts and the field invariant spin-spin couplings. The operation and control of the instruments which utilize permanent magnets is much simpler. Provided the magnet is adequately thermostated, a homogeneous field is always present and few adjustments are necessary. The homogeneity of field attainable by either type of magnet is nevertheless comparable. However, since the facility for wide variations in the field strength (apart from that necessary for scanning the spectrum) is not available, the permanent magnets lack in flexibility of operation but this is compensated to some extent by the good stability of an efficiently thermostated permanent magnet.

Superconducting magnets, in which a field of the required homogeneity

may be produced at strengths up to 5 tesla, are now being employed[82] in n.m.r. spectrometers. Such solenoids require elaborate control systems to maintain the temperature of the conducting wire in the region of $10^{o}K$, this usually being achieved with liquid helium.

2.3 MAGNETIC FIELD SWEEP

The condition for the observation of an n.m.r. signal from any nucleus is that the eqn. (2.1) must be satisfied.

$$\nu_o = \frac{\gamma B_o}{2\pi} \qquad (2.1)$$

It follows, therefore, that the precessing magnetic nuclei can be brought into resonance with the rotating magnetic field by suitable variation of the frequency of either the former or the latter. A change in the precessional frequency can be affected by varying the strength of the applied field (B_o) while a rotating magnetic field B_1 of a different frequency can be obtained by varying the frequency of the Y. f. oscillator. The early difficulties of providing a suitably stable and linear frequency sweep led to the use of magnetic field sweep.

Two types of magnetic field sweeps, a recurrent sweep and a slow sweep, are available with most of the spectrometers. In the former case, the output of a saw-tooth generator is amplified and fed to a pair of Helmholtz coils which flank the sample with their axes parallel to the direction of the static field. Each coil has the same number of turns and the separation between the coils is equal to their radius. This liner sweep is utilized while searching for the resonance field condition of a nucleus or when making spectrometric adjustments.

A slow sweep unit is provided for recording the signal under slow passage conditions so that the line distortion is minimum. The slow sweep may be achieved by the introduction of an error signal to the flux stabilizer, which then falsely corrects the applied field. Hence a change in the magnetic field is brought about by a steady increase in the current through the correction coils. The rate of variation of the small applied field is governed by the magnitude of the dc voltage. A simpler means of field sweep can be derived from a motor driven potentiometer linked to a recorder to produce a permanent record of the spectrum.

Sometimes it is necessary to apply permanent but relatively small field shifts. In permanent magnets this is achieved by an additional pair of coils which carry current to produce pre-calibrated field shifts. In electromagnets, the flux-stabilizer is used to vary the field by the introduction of a false error signal.

2.4 RADIOFREQUENCY OSCILLATOR

It has already been said (see sec. 1.3) that in order to induce a nuclear energy transition, it is necessary to provide a rotating electromagnetic field B_1, the magnetic component of which moves in a plane perpendicular to the direction of the static field B_o. It has been a convenient practice to use a linearly oscillating field which also serves the purpose (see sec. 1.3.a).

The practical limitations placed on the field obtainable from conventional magnets require the use of a maximum radiofrequency of 100 MHz for the observation of ^1H spectra. Similar to the main magnetic field, the radiofrequency oscillators also require a stability of 1 part in $10^8 - 10^9$ per minute. Such signals are usually obtained by the proper selection and multiplication of harmonics from a carefully thermostated

quartz crystal oscillator. The radiofrequency power delivered to the probe is kept at a constant level by incorporating an automatic gain control amplifier as the final stage of the radiofrequency unit, prior to its output being fed to the probe via an attenuator system. Frequency sweeps can be performed by utilizing the side bands produced by moldulation of the carrier with an a.c. signal of linearly varying low frequency.

2.5 FUNCTIONS OF THE DETECTION SYSTEM

The passage of radiofrequency radiation through the magnetised sample is associated with two phenomena, namely absorption and dispersion. The line shapes associated with the absorption and dispersion modes are shown in Figs. 1.5 and 1.6. Although the resonance frequency can be determined by observing either of the two modes, absorption or dispersion, the former is usually preferred in practice as it is easy to interpret. Basically the function of the detector is two fold, firstly to separate the absorption signal from the dispersion signal and secondly to separate the absorption signal from that supplied by the r.f. oscillator. The second function is necessary because,although the amplitude of the applied r.f. signal remains constant, it is very much larger than the amplitude of the absorption signal.

The sample holder, or probe, is the assembly which carries the air turbine for sample spinning, the receiver coils, the linear sweep coils and the pre-amplifier. Usually two type of probes, single coil and the double coil, are employed. The two type of probes and the corresponding principles of detection are sufficiently different and will be discussed separately while dealing with the commercial spectrometers which use them.

2.6 THE PERKIN-ELMER R10 HIGH RESOLUTION NMR SPECTROMETER

2.6.a The Magnet

The Perkin-Elmer R10 spectrometer employs a permanent magnet capable of producing a field of strength 1.4092 tesla. The pole pieces are approximately 125 mm in diameter and seperated by an air-gap of about 25 mm. The magnet assembly is housed in an aluminium box lined with thick layers of expanded polystyrene containing temperature sensing devices and heating elements. This enables the magnet to be thermostated and maintained at a temperature of 306.6$\pm$ 0.001^{o}K. This high degree of temperature stabilization overcomes the problem of field drift to a large extent. The probe assembly is held between the pole pieces by a rigid aluminium bar. The sample coil is wound on a hollow glass former in which the sample tube is spun by means of a small air turbine. The spectrometer employs the single coil method of detection and uses a twin-T bridge for the purpose. The bridge circuitory is housed in a mu-metal box attached directly to the probe unit.

In the first successful n.m.r. experiment, Purcell, Torrey and Pound[7] used the single coil method of detection. It involes the measurement of the effect of absorption and/or dispersion signals at the transmitter coil itself. This is accomplished by the use of a radiofrequency bridge functioning much the same way as a Wheatstone bridge. The Twin-T bridge has been found most satisfactory in high resolution spectrometers in that it gives a good stability of bridge balance. Such stability is necessary if a mixture of u and v mode signals is to be avoided. Bridge systems typically used consist of two similar circuits, one circuit containing the sample coil and the other containing a dummy coil. The bridge network balances out the transmitter signal and allows the absorption or dispersion signal to pass as an out-of-balance e.m.f. across the bridge which, after amplification and rectification, can be displayed on the

oscilloscope or recorded. The r.f. bridge is so designed that both the phase as well as the amplitude of the out-of-balance transmitter signal can be controlled. The unwanted dispersion signal can be suppressed by taking advantage of the fact that the dispersion and absorption signals differ in phase by $\frac{\pi}{2}$. Even if the transmitter signal is not completely balanced, the contribution of dispersion mode to the signal going to the amplifier is negligible. Fig. 2.1 represents vectorially the absorption (V-mode) signal, dispersion (U-mode) signal, out-of-balance transmitter signal (V-mode leakage) and the signal which is fed to the amplifier. So long as the vector sum of the absorption and out-of-balance transmitter signals is large in comparison to the dispersion signal, the angle ϕ will be small. Since the contribution of U-mode is proportional to sin ϕ , it will make a negligible contribution to the signal being fed to the amplifier.

The field sweep is provided by a saw-tooth wave form applied to sweep coils on the pole pieces; this voltage is also arranged to produce the time base for an oscilloscope. Alternatively, the field sweep may be derived from the recorder and synchronised with the rotation of the recorder drum.

An ambient field conpensator unit fitted to the spectrometer detects very small changes in the horizontal component of earth's magnetic field and feeds a compensating current to a pair of detection coils fitted around the pole pieces of the magnet. Thus disturbances originating more than 5m away can be eliminated. An additional pair of coils allows computer controlled field shifts to be made, when necessary.

2.6.b. Detection of the NMR Signal

The arrangement of electronic components of the R10 spectrometer is

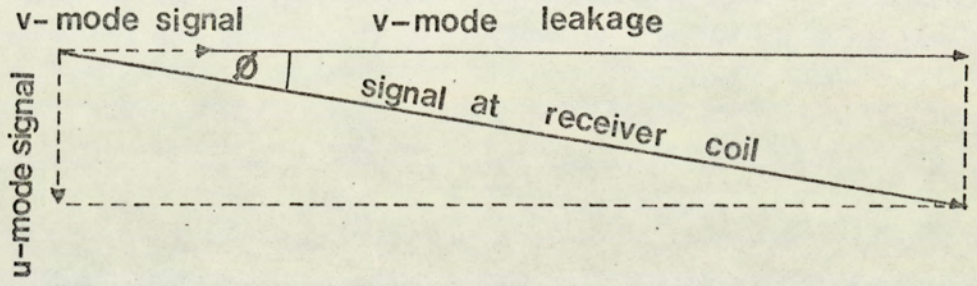

Fig. 2.1 Suppression of the u-mode component of the magnetisation vector by adding in-phase leakage to the v-mode component.

shown in Fig.2.2. The r.f. signal for ^{1}H n.m.r. is obtained from an accurately thermostated 5MHz quartz crystal oscillator. The second harmonic (15MHz) of the crystel frequency is selected and further multiplied fourfold to give 60MHz. A 60.004MHz signal is obtained after mixing the 60MHz signal with a 4KHz signal obtained indirectly from a crystal-controlled calibrating oscillator, the original carrier and the unwanted side-band being suppressed.

The single side-band signal (60.004MHz) is fed via an automatic gain control amplifier and a variable attenuator to the input of the Twin-T bridge network. The bridge circuit can be adjusted to an exact null by means of amplitude and phase controls. At resonance, the inductance of the sample coil changes and the bridge circuit is no longer balanced. Any out-of-balance of the bridge, with phase and amplitude characteristics, caused by the nuclear absorption is fed at 60.004MHz into r.f. amplifier where it is amplified. The original 60.000MHz frequency is also fed to the amplifier at a low level (the "homodyne signal") and mixes with the 60.004MHz n.m.r. signal from the bridge and after amplification, the mixed signals pass through a diode detector whose output is the beating 4KHz signal. After further amplification, this signal is fed to a phase detector which is also supplied with the 4KHz reference signal, derived from that supplying the single side band unit. The reference phase is adjusted manually to obtain the desired mode of presentation; usually the the absorption mode is selected. These two signals are mixed to give zero output until a resonance is encountered, when a dc signal appears across the detector output. The output of the phase detector can be supplied to an oscilloscope or recorder. A series of condensers in RS circuit can be selected to cut down the response time of the circuit and enhances the signal-to-noise ratio.

The output from the phase detector is usually superimposed upon a small

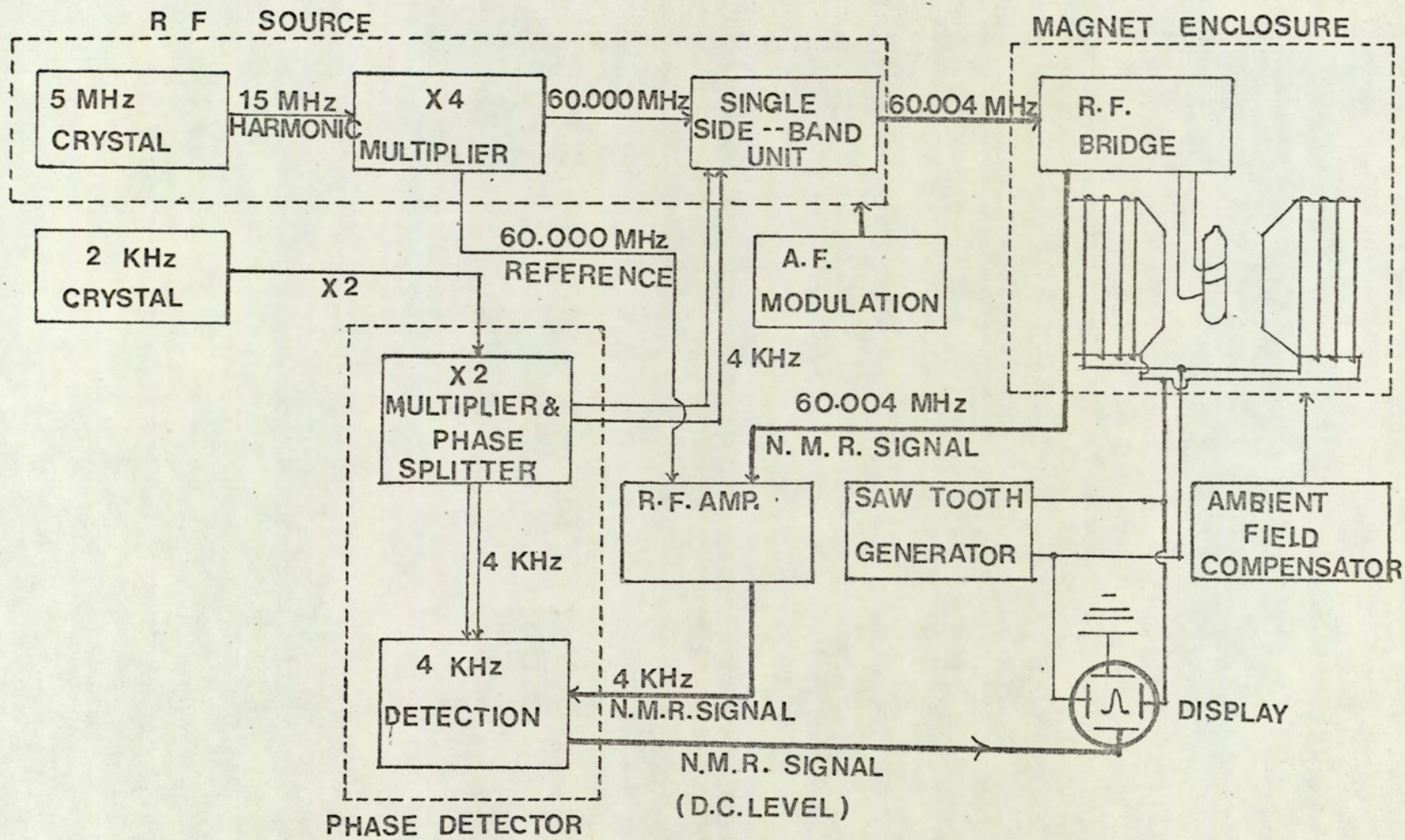

Fig. 2.2 Schematic diagram of the Perkin-Elmer R10 N.M.R. Spectrometer

standing dc component which may arise from the imperfect balance of the r.f. bridge and slight assymmetry of the phase detector itself. This component can be backed-off by an equal dc voltage of opposite sign. This provides a satisfactory condition for the determination of peak areas with a built-in integrator.. By passing the n.m.r. signal through a circuit containing a dc amplifier connected across a condenser, an integral of the absorption spectrum can be obtained. The area under the absorption signal in a spectrum is proportional to the number of nuclei which give rise to the signal.

2.6.c Calibration of the Spectra

The recorder on the R10 spectrometer utilizes pre-calibrated charts which align themselves in the same relative position on the recorder drum. The rotation of the drum is linked to the magnetic field sweep With the help of field shift controls, fairly accurate shift measurements can be made for routine work. Line frequencies can be measured with a greater precision by audiofrequency side band modulation technique for which there is a provision on the R10 spectrometer. By such independent calibration any drift in the field is largely accounted for. An inverted replica of the modulcation signal, displaced by the modulation frequency is produced on either side of the fundamental. By suitable variation of the modulcation frequency, a series of inverted signals of accurately known frequencies is produced on the spectrum. The relative frequencies of the unknown lines are deduced by interpolation. For the investigations reported later the calibration side bands of the strong reference peak of cyclohexane were used. The audiofrequency signals were obtained from a Muirhead-Wigan D890A oscillator

and the frequencies produced were checked with a Venner 3336 frequency counter.

2.6.d The Perkin-Elmer Variable Temperature Assembly

As it has already been said, the Perkin-Elmer R10 spectrometer employs a carefully thermostated magnet operating at 306.6°K and normally the sample is also supposed to be at the same temperature. However, sometimes it is desirable to study the effect of temperature changes on n.m.r. spectra, for which purpose a variable temperature probe accessory is available for R10 spectrometer. Using this sample temperatures can be maintained anywhere in the range 133.2°K to 513.2°K.

The variable temperature probe consists of an inner assembly within which the sample tube can be spun. The inner assembly is contained in a Dewar vessel which is itself surrounded by a jacket through which water, thermostatically controlled at the magnet temperature, is circulated. Due to this elaborate arrangement, the variations in the sample temperature are prevented from being transmitted to the magnet, and thus prevent changes in the field. The sample is heated by a circulation of hot air and radiation from a copper tube. Both the circulating air and the copper tube are heated electrically. Temperatures bellow 306.6°K are obtained by appropriate mixing of heated air and nitrogen vapour from a supply of liquid nitrogen. There is a platinum resistance thermometer within 5mm of the r.f. coil. This thermometer monitors the sample temperature and any changes in the dialled temperature are automatically corrected for. For accurate

temperature measurement, a calibrated thermocouple is fitted to the probe, the e.m.f. produced being measured by means of a potentiometer.

2.7 THE HA 100D VARIAN NMR SPECTROMETER

2.7.a The Electromagnet

A 305 mm electromagnet furnishes the magnetic field for the HA 100D Varian spectrometer. The magnet is designed for optimum field homogeneity at a field intensity of 2.349 tesla, and is equipped with a manually operated field trimmer whichcompensates for gradual changes in field homogeneity along the y-axis. The magnet has two water-cooled low impedance coils connected in series and mounted in a trunnion-supported yoke. The pole cap covers, which also contain the homogeneity coils, and yoke insulating jacket, insulate the pole and yoke from the effect of ambient air temperature changes.

Heat is dissipated by the magnet and the magnet temperature is controlled automatically by passing de-ionized water through the magnet cooling system. This stabilization of the magnet temperature helps in maintaining the high resolution of the magnetic field.

A regulated magnet power supply unit furnishes dc power to the magnet. The magnet current is adjustable from zero to a maximum value for various magnetic field requirements. Solid state amplifier and passgate circuits regulate the current against $\pm$ 10% voltage variations.

2.7.b. The Field-Frequency Lock System

The HA 100D Varian spectrometer uses a field-frequency lock system which will now be described. Field-frequency control is a system whereby the radiofrequency source and the magnetic field strength at the sample are held in constant proportion. In an internal lock system, a reference material is added to all the samples to be studied so that the analytical sample and the reference sample are subjected to the same applied field. By modulation of the carrier, n.m.r. experiments are conducted simultaneously. The lock sample is nominally fixed at resonance in the dispersion mode and an error signal is derived from this to drive the servoloop for field-frequency stabilization. A second experiment enables the remainder of the spectrum to be detected.

All R.F. signals used are derived by magnetic field modulation, at audiofrequencies, of the carrier and may be separated from one another in synchronous (sometimes called phase-sensitive) detectors referenced to the relevant modulation frequency. The mode of signal, absorption or dispersion, can be set by the audiofrequency reference phase applied to the synchronous detector. An equivalent situation occurs if, instead of field modulation, the r.f. oscillator is frequency modulated. Nuclear magnetic responses will be observable whenever one of the instrumental frequencies coincides with the nuclear precession frequency. The modulation side-band is adjusted to be on resonance for the internal reference compound, with the modulation index set to avoid saturation. The reference phase of the control channel synchronous detector is set for pure dispersion mode, a shape that is well suited for use as an error signal to pull the

magnetic field back into resonance, should either the field of the frequency tend to drift. The error signal may be monitored on an oscilloscope and performs the correction through the high gain flux-stabilizer.

In the frequency mode, the control channel operates at fixed B_o and a constant modulation frequency while the analytical channel modulation frequency is swept in a linear fashion through the desired region of the spectrum, the frequency control being mechanically linked to the horizontal motion of the recorder arm. Since the movement of the recorder arm from left to right corresponds to decreasing modulation frequency, frequency sweep spectra are obtained by using the high frequency set of modulation side-bands to excite the resonance, so that the lines in the spectrum appear in the conventional order as if the magnetic field has been swept from low to high field at fixed frequency.

In the field sweep mode, the analytical channel operates at a constant modulation frequency derived from the mannual oscillator while the control channel modulation frequency is swept linearly from say 3500 Hz to 2500 Hz on the widest sweep. The low frequency set of modulation side bands are used. When the recorder arm is stationary, the n.m.r. signal from the reference dispersion mode line is near zero volts. As soon as the recorder arm is moved, the r.f. field used to excite the internal reference line is swept and the reference line tends to move off resonance, thus generating a finite dc error signal that drives the main magnetic field in a linear fashion so as to hold the reference signal at resonance. In this mode, the modulation index of the analytical channel is kept constant throughout the sweep; this

is harder to realise in frequency sweep mode.

On each of the five possible sweep widths, when the recorder arm reaches the indicator mark on the right-hand side of the chart, the sweep oscillator is at 2500 Hz. If the manual oscillator is also at 2500 Hz, then the locked signal coincides with the indicator mark. However, it may often be required to examine an expanded part of the spectrum, far removed from the locked signal. This may be accomplished by off-setting the manual oscillator above or below 2500 Hz thus displacing the locked signal down the chart to the left or off the chart to the right of the indicator mark.

While transferring from field sweep to frequency sweep mode, the functions of the two r.f. modulation controls are interchanged and their settings have to be modified to avoid saturation of the locked signal.

2.7.c The Probe

The probe contains sweep coils, a transmitter coil, a receiver coil, and the set of paddles for adjusting the leakage between the transmitter and receiver coils. The receiver coil is wound on an insert and has its magnetic axis parallel to the longitudinal axis of the sample. The transmitter coil is wound in two sections that surround the receiver coil at right angles to its axis. A Faraday shield, located between the coils, reduces the electrostatic coupling to a minimum. The sweep coils are located in annular slots on the sides of the probe, with their magnetic axis parallel to the transverse axis of the probe. The probe itself is milled from a single aluminium

forging to produce maximum dimensional stability.

2.7.d The Detection System

The HA 100D spectrometer employs a double coil, or crossed coil as it is called, method of detection. It was first used by Bloch, Hansen and Packard[8] and is sometimes called the nuclear induction method. In this method, a separate receiver coil is wound around the sample with its axis perpendicular to both the axis of the transmitter coil and the direction of the main field Bo. In this arrangement, the receiver picks up the signal resulting from the absorption of energy by the nuclei present in the sample. If the two coils have their axes at right angles to each other, they will not be coupled and therefore, the transmitter is separated from the absorption and dispersion signals. Any departure from orthogonality between the coils will cause a coupling between the two coils and hence the induction of a leakage voltage in the receiver coil. In fact, a small amount of leakage from the transmitter coil, in-phase with the absorption signal, is desirable in order to suppress the dispersion signal. The amount of leakage is controlled by 'paddles' which are semi-circular metal sheets mounted at the end of the transmitter coil. These paddles can modify the lines of force due to the field and therefore provide variable degree of inductive and capacitative coupling between the two coils.

The HA 100D spectrometer is operated in two modes, the HR mode and the HA mode. The two modes of operation will now be briefly dealt with.

2.7.e. HR Mode of Operation

In the HR mode, the r.f. unit (Fig. 2.3) alone, without proton stabilization unit, is used. The r.f. unit contains a highly stable fixed-frequency transmitter and a high gain superheterodyne receiver. The r.f. level at the probe, from the transmitter section, is controlled by a push-button switch attenuator and isolated by a buffer amplifier to eliminate any frequency shift with load variations. The n.m.r. signal from the low noise preamplifier in the probe assembly is fed to the first of the two stages of the r.f. amplification. The r.f. signal is then mixed with the local oscillator frequency (95 MHz) in the mixer D resulting in a 5 MHz signal being passed to the first of the two stages of IF amplification. Receiver gain is accomplished by varying bias in the two IF stages with the receiver gain control. Mixer B mixes the transmitter frequency from the 100 MHz oscillator with the local oscillator frequency (95 MHz) to produce a 5MHz reference signal which is subsequently fed to IF amplifier C. The IF amplifier output is applied to a diode detector circuit which includes the detector level meter and to a phase detector circuit. The phase detector circuit mixes the reference output from the IF amplifier C and 5MHz n.m.r. signal from IF amplifier A to produce a phase detected dc output. The frequency response switch enables diode detection or phase detection. The recorder level control provides attenuation of the output signal.

In the HR mode of operation, a 2.5 KHz modulator, forming a part of the integrator-decoupler unit, energizes the probe ac sweep coils to modulate the magnetic field in the region of the sample. This accessory

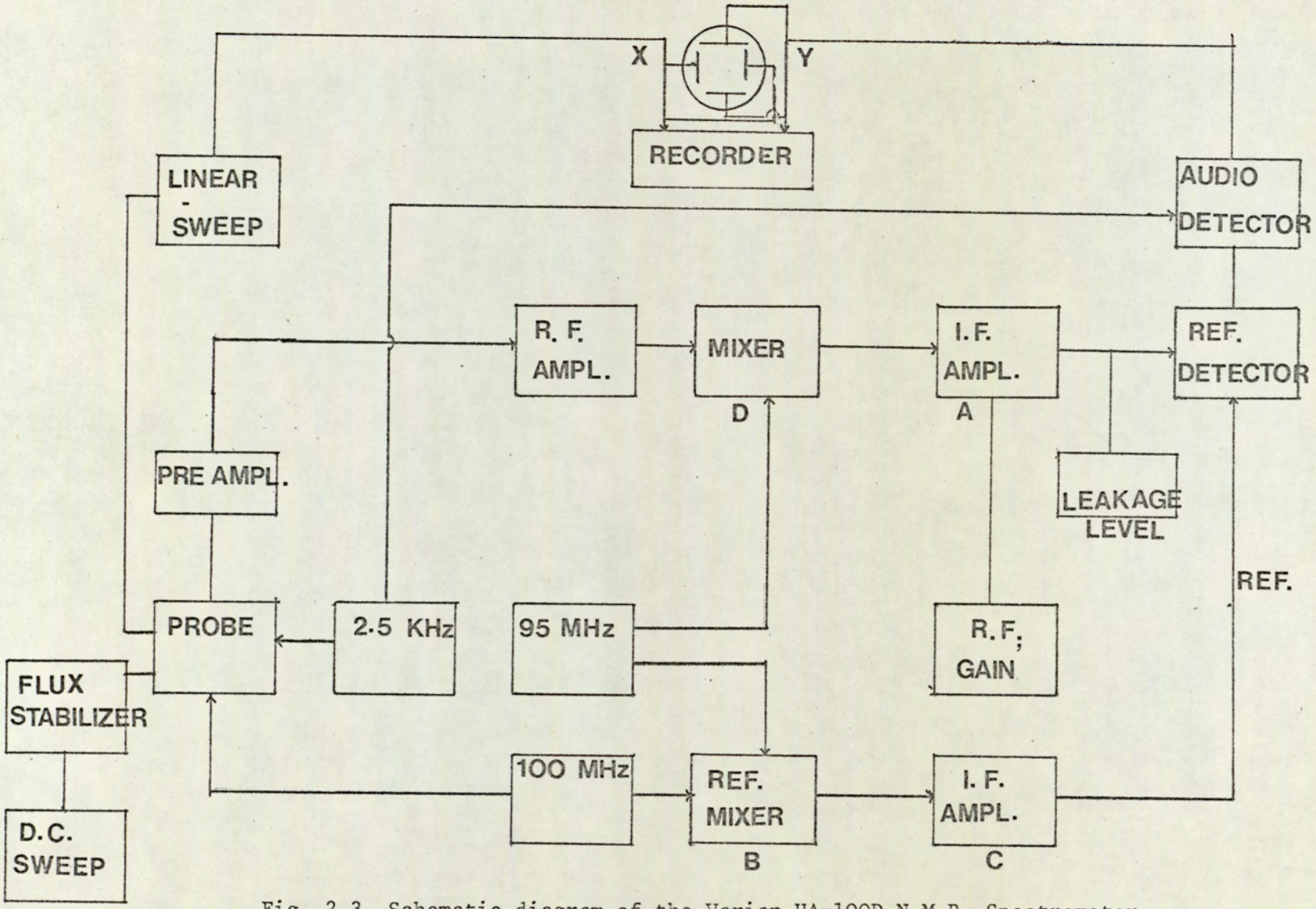

Fig. 2.3 Schematic diagram of the Varian HA-100D N.M.R. Spectrometer (HR mode of operation)

stabilizes the base line of the spectrum output by means of field modulation and phase sensitive detection.

2.7.f. HA Mode of Operation

In the HA mode of operation, the interal reference proton stabilization unit (Fig.2.4) provides n.m.r. stabilization by furnishing audiogain and phase detection in both signal and control channels, between the r.f. unit (Fig.2.3), the recorder and the magnet stabilization circuits. The proton stabilization unit consists of a transmitting section and a receiver section contained on printed circuit cards.

The transmitting section contains two audiofrequency oscillators; a sweep frequency oscillator and a manual frequency oscillator. The output frequencies from the oscillators are added, amplified and filtered, then applied to the ac sweep coils of the probe. In this mode the signals going out of the probe are the carrier and the carrier wave modulated by the beat frequencies from the two oscillators, the sweep frequency oscillator and the manual frequency oscillator.

The receiver section processes the audiosignal from the r.f. unit phase detector. The signals are the nuclear side band resonances produced by the modulation of the field through the ac sweep coils by the sweep and manual oscillators.

The receiver section has two channels: (1) the control channel which provides audiogain, phase detection and filtering for the control resonance, and (2) the analytical channel which provides audiogain and

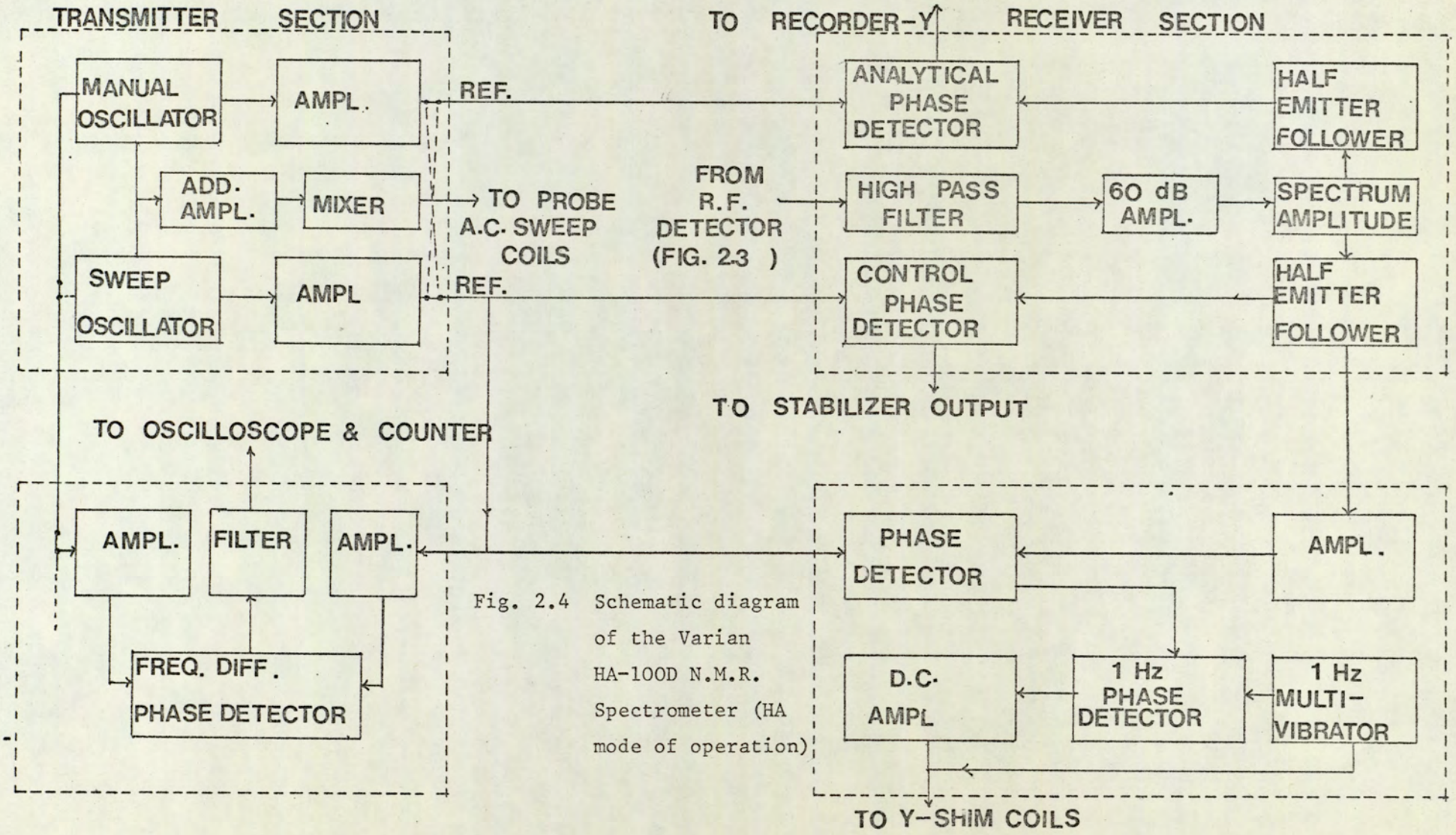

Fig. 2.4 Schematic diagram of the Varian HA-100D N.M.R. Spectrometer (HA mode of operation)

phase detection for the analytical sample resonance.

Input signals to the receiver are applied to a 60 dB amplifier and high pass filter circuit which reduces the spinner noise and amplifies the detected control and analytical sideband resonances. The spectrum amplitude controls the signal level in the amplifier.

Two separate emitter follower circuits provide impedance matching to the control amplifier and phase detector in the control channel, and also to the audioamplifier and phase detector in the analytical channel. The control signal is applied to the control amplifier and phase detector through a Field-Frequency switch. The reference frequency for phase detection is supplied by either the manual or sweep oscillator. The detected coherrent side band is coupled through the Lock On switch to the stabilization filter circuit card. The stabilization filter provides low pass filtering for the dc control signal which is applied to the flux-stabilizer to complete the control loop.

The analytical channel output from the emitter follower is applied to the audio amplifier and phase detector. The reference frequency for phase detection is obtained either from the sweep oscillator or the manual oscillator. The detected coherent side band is coupled to the integrator/decoupler where it is amplified and/or integrated and then applied to the recorder circuits.

Depending on the mode of operation, either the manual oscillator or the sweep oscillator output is applied as reference voltage to the frequency difference phase detector. The reference voltage is amplified

and shaped into a square wave then applied to the switching circuit. The switching circuit compares the phase of the two discrete signals to produce a differential frequency, which is coupled through a low-pass filter for application to a counter or an oscilloscope.

2.7.g. The Autoshim Homogeneity Control

The autoshim control maintains optimum homogeneity of the magnetic field by automatic adjustment of the y-axis shim coil current in response to an amplitude change in the control signal. Manual adjustment of the y-axis homogeneity controls is eliminated for each sample that is run.

A 1Hz square wave, generated in the autoshim control circuits, modulates the y-axis shim coil current. The shim coil field in turn modulates the n.m.r. signal. When the shim current is not at optimum value, the modulation of the n.m.r. signal is detectable as the square wave sweeps the current beyond the optimum value. The signal modulation is phase detected to obtain a dc voltage which is then fed back to the shim coils to maintain the current at optimum value.

2.7.h The Slow Sweep

The flux stabilizer unit produces slow to extremely slow sweep rates. Changes in the buck out coil induce a current in the pick up coil. The field control system will then adjust to a rate of current change in the buck out coil which equalizes voltage at two appropriate points in the circuit. This action provides a changing field or sweep.

2.7.i. The Recorder

The HA 100D spectrometer employs a flatbed recorder for a graphic record of the spectra on a calibrated chart. The pen records across the chart at selected sweep rates. Frequencies of the observed signal and the locked signal are obtained using a Varian 4315A frequency counter by putting the signal monitor to sweep or Man. OSc. Frequency and thus effectively counting the two audio-modulation frequencies.

2.7.j. The XL-100 Variable Temperature Accessory

The accessory automatically controls sample temperatures in the range 153.2° to 473.2°K. The main components of the accessory are the variable temperature controller, a heat senser assembly, a liquid nitrogen container, arrangements for conducting nitrogen gas through the system and a heat exchanger. The controller contains a bridge circuit which includes the temperature controls, the senser and an amplifier that supplies a constant value of current to the heater while the bridge is balanced. As the heated gas flows past the senser, the temperature sensitive element presents a value of the resistance that maintains the bridge in balance. A change in the temperature control settings or in the senser resistance unbalances the bridge resulting in a change of heater current. The nitrogen gas temperature is increased or decreased accordingly and effects a corresponding change in senser resistance. The bridge balance is regained and the heater current again assumes a steady value.

The controller circuit maintains $\pm 1^{\circ}$K, for 5mm samples, maximum

temperature variation at the senser and regulates the temperature at the sample within $\pm 2^{\circ}K$ of the values nominally dialled.

CHAPTER 3

THE ANALYSIS OF SECOND ORDER SPECTRA

ABC SPIN SYSTEMS

3.1 INTRODUCTION

Some simple features of n.m.r. spectra caused by spin-spin interaction between differently shielded nuclei have been described earlier (see sec.1.11). The spectral regularities described are observed only when the magnitude of chemical shift between the interacting nuclei is far greater than the value of coupling constant berween them. Such spectra are referred to as the first order spectra and it is possible to obtain chemical shifts and coupling constants directly from such a spectrum (Fig.3.1). However, when the magnitudes of the two parameters, i.e. chemical shifts and coupling constants, are comparable, the simple rules of spectral analysis are no longer valid. Under such circumstances, the chemical shifts and spin-spin couplings give rise to a complex pattern of lines, usually referred to as second order spectra, which often have few features of regularity. The components of the multiplets are usually of unequal intensity and the chemical shift difference can no longer be obtained by assuming that the true resonance frequency for a particular nucleus is at the centre of its multiplet absorption (Fig.3.2). The individual multiplets may even merge. Chemical shift differences and the spin-spin coupling constants can only be obtained (by calculation) from such a spectrum by subjecting it to a full quantum mechanical analysis. One has to evaluate the nuclear energy levels and stationary state wave-functions for the system in the absence of r.f. field. The next step is to calculate the energies and probabilities (intensities) of the transitions that may be observed when such a system is subject to a r.f. field. By assigning each line to a definite transition, a theoretical spectrum is constructed which is fitted

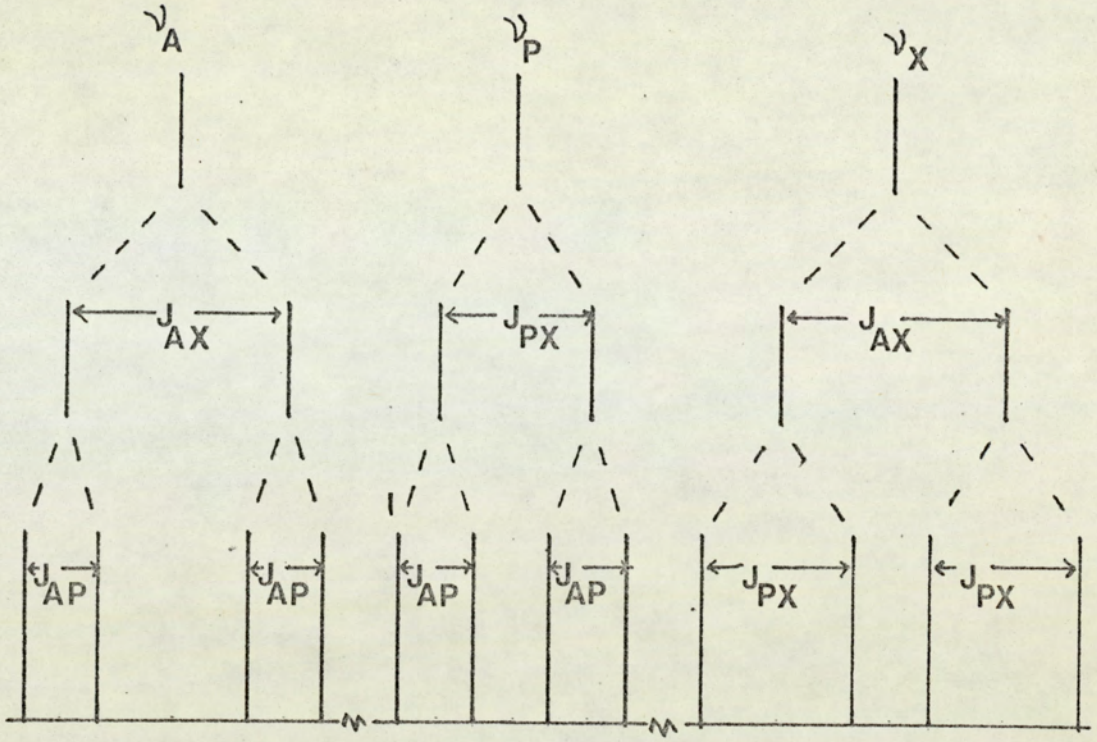

Fig. 3.1 Typical first order n.m.r. spectrum for a three-spin ($I = \frac{1}{2}$), APX system.

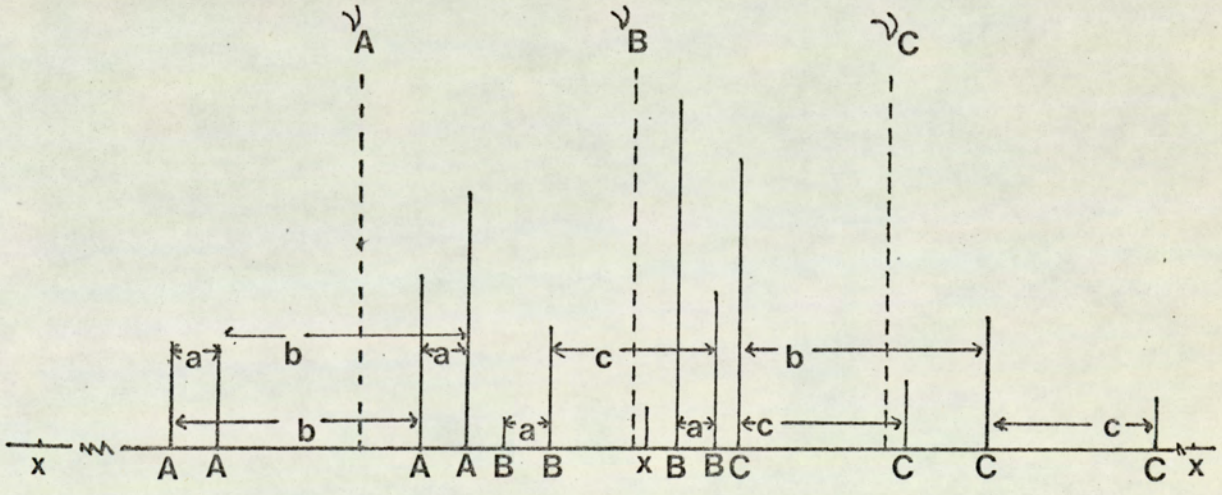

Fig. 3.2 Typical second order n.m.r. spectrum for a three-spin ($I = \frac{1}{2}$), ABC system.

to the observed spectrum, and from which values of chemical shifts and coupling constants are obtainable.

The basic theoretical steps required for the analysis of such spectra were developed by Gutowsky, McCall and Slichter,[83] Hahn and Maxwell[84], McConnell, McLean and Reilly[85], Wilson[86], Anderson[87], and Banerjee et al[88]. Since then many detailed accounts of spectral analysis have become available.[9,10,89-91]

Since the compounds that have been studied during the course of the present investigation give rise to the second order spectra, the procedure for the analysis of such spectra will be dealt with in detail in the following sections.

3.2 QUANTUM-MECHANICAL CONSIDERATIONS IN GENERAL

Experiments aimed at obtaining values of the chemical shifts and spin-spin coupling constants are performed in the presence of a r.f. field, B_1, of intensity small enough to avoid saturation. Under such circumstances B_1 does not change the energies of the stationary states of the system and the energy levels can be found by solving the time-independent Schrödinger equation

$$\mathcal{H}\varphi = E\varphi \qquad (3.1)$$

in which $\mathcal{H}$ is the Hamiltonian operator and φ is the stationary state wave function. The actual form of the Hamiltonian operator and the stationary state wave functions will be elucidated.

3.2.a. Form of the Hamiltonian

The complete Hamiltonian is a sum of two terms given by:

$$\mathcal{H} = \mathcal{H}^{(0)} + \mathcal{H}^{(1)} \tag{3.2}$$

where $\mathcal{H}^{(0)}$ describes the interaction of the nuclear magnetic moments with B_o and $\mathcal{H}^{(1)}$ is the spin coupling interaction.

The energy of a nucleus in a strong magnetic field B acting in the negative Z direction is given by $\gamma \hbar B I_z$ ergs or $\frac{\gamma B I_z}{2\pi}$ Hz where the terms carry their usual meaning. For a set of nuclei with magnetogyric ratios γ_i acted upon by fields B_i, the Hamiltonian will be

$$\mathcal{H}^{(0)} = \frac{1}{2\pi} \sum_i \gamma_i B_i I_{z(i)} \tag{3.3}$$

Because of local screening B_i will differ from B_o and is given by $B_i = B_o(1 - \sigma_i)$. For convenience in theoretical discussions, further calculations will be carried out under the assumption that B_o is held constant. Although in practice it is otherwise but the arguments will not be affected.

Since $\nu_i = \frac{\gamma_i B_i}{2\pi}$ $\mathcal{H}^{(0)}$ can also be expressed as

$$\mathcal{H}^{(0)} = \sum_i \nu_i I_{z(i)} \tag{3.4}$$

and $$\mathcal{H}^{(0)} = \sum_i \nu_o(1 - \sigma_i) I_{z(i)} \tag{3.5}$$

The part of the complete Hamiltonian due to indirect spin coupling is represented in terms of the scalar products of the spin vectors of the magnetic nuclei

$$\mathcal{H}^{(1)} = \sum_{i<j} J_{ij} I_{(i)} I_{(j)} \qquad (3.6)$$

3.2.b. Basic Functions

The wave functions of the Hamiltonian given by eqn. (3.2) can be expressed as a linear combination of a closed set of functions ψ; the simplest set of such functions are the basic product functions. A basic product function is the eigen function of a Hermitian operator F_z, the total spin component in the z direction, which commutes with $\mathcal{H}$.

For simplicity further arguments will be concerned with nuclei of spin $I = \frac{1}{2}$ only. If the system contains p such nuclei, the total number of possible states is 2^p and the basic product functions for any state will have the form

$$\psi_n = \alpha \cdot \beta \cdot \alpha \text{ ------} \qquad (3.7)$$

where the γ th symbol on the right hand side of the eqn. (3.7) applies to the γ th nucleus. As usual, α and β are single nucleus wave functions corresponding to the states $I_z = +\frac{1}{2}$ and $I_z = -\frac{1}{2}$ respectively.

3.2.c. Symmetry Properties

The quantum-mechanical problem is greatly simplified if the molecule has symmetry properties because then the basic product functions can be expressed in irreducible forms which are easier to handle.

The possible symmetry elements that allow the system to be transformed

to arrangements indistinguishible from the original, by an exchange of position between identical nuclei, are:

σ	reflection at a plane
i	inversion about a centre of symmetry
$(C_p)^n$	rotation by an angle $n.\frac{2\pi}{p}$ about a p-fold axis
S_p	rotation by an angle $\frac{2\pi}{p}$ about a p.fold axis followed by reflection about a plane perpendicular to the axis.
I	mathematical necessity requires that the operation of essentially leaving the system alone be performed.

If all the points in a nuclear arrangement are left unchanged by a possible combination of symmetry operations, then this combination is called a point group. The definition can be illustrated by taking the example of point group C_{2v} . To be described by this point group, the molecule must have a two-fold symmetry axis, C_2 and 2 planes of symmetry, σ_v and σ_v' through this axis. Formaldehyde is an example of a molecule belonging to this point group. The molecule has got a 2-fold symmetry axis $C_{2(z)}$ along the c = o bond, and two planes of symmetry, xz and yz, the latter being the plane of the molecule itself (Fig. 3.3) Having established the appropriate point group for a molecule, the basic product functions can be reformulated. For example, for a set of two equivalent nuclei, the basic product functions are $\alpha\alpha$, $\alpha\beta$, $\beta\alpha$ and $\beta\beta$ and the irreducible representations are:

$$\alpha\alpha \ , \ \frac{1}{\sqrt{2}}(\alpha\beta+\beta\alpha), \ \frac{1}{\sqrt{2}}(\alpha\beta-\beta\alpha) \text{ and}$$

The normalisation factor $\frac{1}{\sqrt{2}}$ is obtained by taking the square root of the inverse of the sum of squares of the coefficients, i.e. $\frac{1}{\sqrt{1^2+1^2}}$

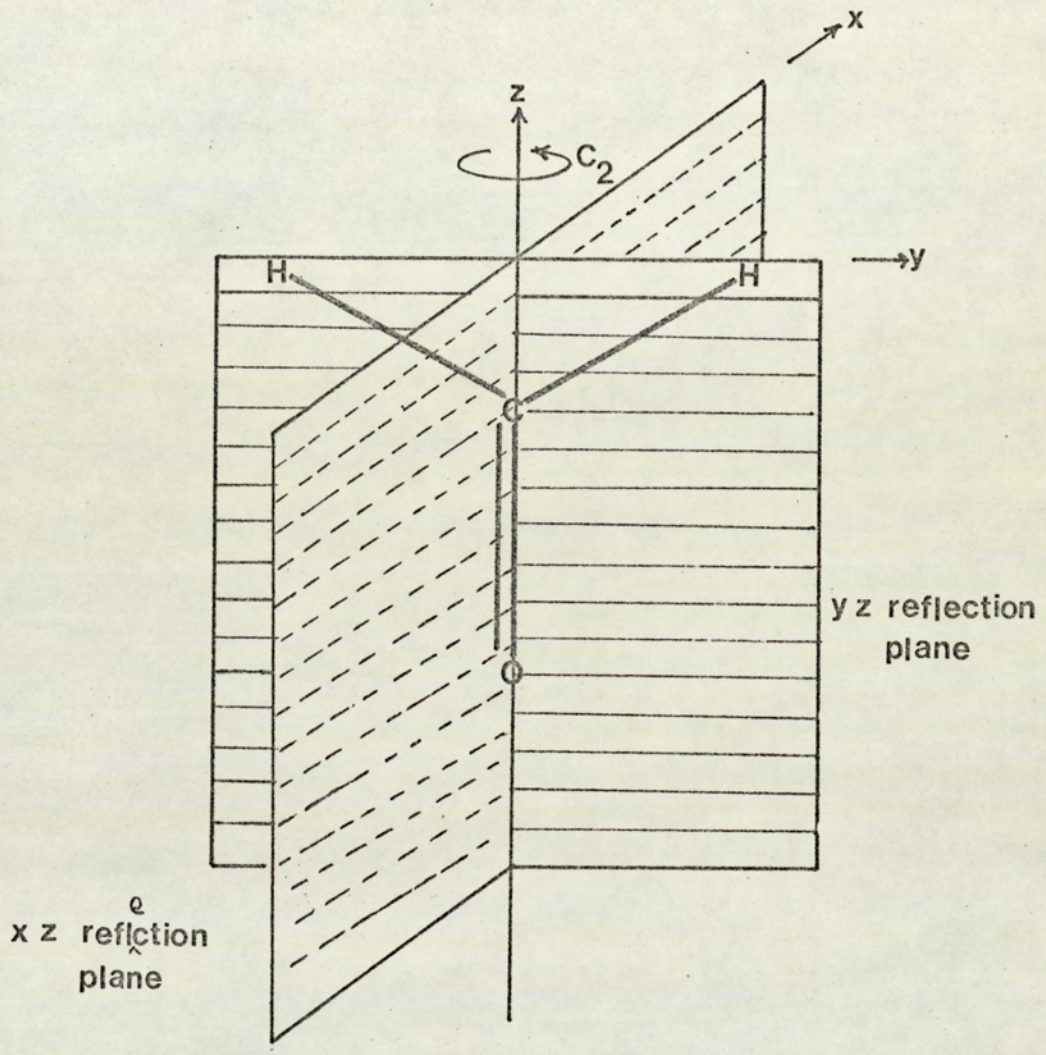

Fig. 3.3 Symmetry properties for the formaldehyde molecule (group C_{2v})

C_{2v}	I	$C_{2(z)}$	$\sigma_{v(xz)}$	$\sigma_{v(yz)}$
A_1	+1	+1	+1	+1
A_2	+1	+1	−1	−1
B_1	+1	−1	+1	−1
B_2	+1	−1	−1	+1

3.2.d. The Secular Equation

If the nuclei were independent, the basic product functions would themselves have been the stationary state wave functions in the presence of the external magnetic field. However, the spin-spin interaction causes mixing between different product functions. In view of this, the Hamiltonian $\mathcal{H}^{(0)}$ will have only diagonal matrix elements with respect to the function ψ_n, where as $\mathcal{H}^{(1)}$ may also have off-diagonal elements. Since the various basic product functions ψ_n, are orthonormal to each other, the correct stationary state wave functions are obtained as the linear combination of these product functions which diagonalise the matrix of the complete Hamiltonian. The energies of the different states are obtained as solutions of the secular equation

$$\left| \mathcal{H}_{mn} - E\,\delta_{mn} \right| = 0 \qquad (3.8)$$

where $\delta_{mn} = 1$ if $m = n$ and is zero otherwise. This secular equation is of order 2^p but it can usually be factorised into a number of equations of lower order, in view of the fact that no mixing occurs between functions with different values of F_z given by

$$F_z = \sum_i I_{z(i)} \qquad (3.9)$$

As a consequence of this, the off-diagnonal elements of the Hamiltonian matrix between basic product functions and the determinant representing the eqn. (3.8) factorises into (p+1) separate determinants of smaller order representing (p+1) equations coresponding to all values of F_z. Further factorisation of the secular equation is possible if nuclei of different species or nuclei of the same species with

chemical shifts large compared with spin coupling constants are present, because, to a high approximation, no mixing occurs between functions which differ in values of the total spin components $F_2(X), F_2(Y)$ ... This arises because mixing is negligible if the difference between diagonal matrix elements of $\mathcal{H}$ is large compared with the corresponding off-diagonal elements. In the case of symmetrical molecules, no mixing occurs between functions of different symmetries.

3.2.e. The Matrix Elements

The next step is to find out the matrix elements of the total Hamiltonian. As already stated $\mathcal{H}(0)$ has got only diagonal elements which are given by

$$(\psi_m \left| \mathcal{H}^{(0)} \right| \psi_m) = \sum_i \nu_i \left[I_{z(i)} \right]_m \qquad (3.10)$$

where $I_{z(i)\ m}$ is $+\frac{1}{2}$ if nucleus i has spin α in ψ_m and $-\frac{1}{2}$ if it has β spin.

The diagonal elements of the spin coupling Hamiltonian, $\mathcal{H}^{(1)}$, are given by

$$(\psi_m \left| \mathcal{H}^{(1)} \right| \psi_m) = \tfrac{1}{4} \sum_{i<j} \mathcal{E} J_{ij} T_{ij} \qquad (3.11)$$

where T_{ij} = +1 or −1 depending on whether the spins i and j are parallel or anti-parallel.

If the wave functions are combination terms such as

$$\psi_m = \frac{1}{\sqrt{2}} \alpha (\alpha\beta + \beta\alpha) \alpha \qquad (3.12)$$

the diagonal elements are evaluated as follows:

$$(\Psi_m \left| \mathcal{H}^{(1)} \right| \Psi_m)$$

$$= \left(\frac{1}{\sqrt{2}} \alpha (\alpha\beta + \beta\alpha) \alpha \left| \mathcal{H}^{(1)} \right| \frac{1}{\sqrt{2}} \alpha (\alpha\beta + \beta\alpha) \alpha \right)$$

$$= \left(\frac{1}{\sqrt{2}} \alpha\alpha\beta\alpha \left| \mathcal{H}^{(1)} \right| \frac{1}{\sqrt{2}} \alpha\alpha\beta\alpha \right) + \left(\frac{1}{\sqrt{2}} \alpha\alpha\beta\alpha \left| \mathcal{H}^{(1)} \right| \frac{1}{\sqrt{2}} \alpha\beta\alpha\alpha \right)$$

$$+ \left(\frac{1}{\sqrt{2}} \alpha\beta\alpha\alpha \left| \mathcal{H}^{(1)} \right| \frac{1}{\sqrt{2}} \alpha\alpha\beta\alpha \right) + \left(\frac{1}{\sqrt{2}} \alpha\beta\alpha\alpha \left| \mathcal{H}^{(1)} \right| \frac{1}{\sqrt{2}} \alpha\beta\alpha\alpha \right) \quad (3.13)$$

giving terms in which the two wave functions are equivalent and non-equivalent, the latter being governed by the off-diagonal equations.

$\mathcal{H}^{(1)}$ will also have off-diagonal elements which are given by:

$$(\Psi_m \left| \mathcal{H}^{(1)} \right| \Psi_n) = \tfrac{1}{2} U J_{ij} \quad (m \neq n) \quad (3.14)$$

where U - 1 if Ψ_m differs from Ψ_n by one spin interchange between i and j only and is zero otherwise. e.g.

$$\left(\frac{1}{\sqrt{2}} \alpha (\alpha\beta + \beta\alpha) \alpha \left| \mathcal{H}^{(1)} \right| \beta\alpha\alpha\alpha \right) = \tfrac{1}{2} \cdot \frac{1}{\sqrt{2}} (J_{12} + J_{13}) \quad (3.15)$$

where J_{12} and J_{13} are the coupling constants between the first and the second, and first and the third nucleus respectively. It should be noted that the matrix representing the Hamiltonian is symmetrical about the leading diagonal, i.e.

$$\mathcal{H}_{mn} = \mathcal{H}_{nm} \quad (3.16)$$

3.2.f Stationary State Functions and the Eigenvectors

The energies can be calculated by diagonalisation of the sub-matrices of the total Hamiltonian. For the calculation of the line intensities,

it is necessary to evaluate the stationary state functions representing the new states resulting from the mixing due to spin-spin interaction. Such functions can be obtained as a linear combination of basic product functions and are given by:

$$\varphi_q = \sum_m a_{qm} \psi_m \qquad q = 1,2,....$$

For example, if a state called 2 mixes with levels 3 and 4, (see table 3.2)

$$\varphi_2 = a_{22} \psi_2 + a_{23} \psi_3 + a_{24} \psi_4 \tag{3.18}$$

in which q = 2 and m = 2,3 and 4.

The relative values of coefficients (eigenvectors) are obtained from the consideration that they satisfy a set of linear equations

$$\sum_n \mathcal{H}_{mn} a_{qn} = E_q a_{qm} \tag{3.19}$$

In the case of mixing just considered the eqn. (3.19) will take the form

$$\mathcal{H}_{22} a_{22} + \mathcal{H}_{23} a_{23} + \mathcal{H}_{24} a_{24} = E_2 a_{22} \tag{3.20}$$

(q = 2, m = 2, n = 2,3 and 4)

$$\mathcal{H}_{32} a_{22} + \mathcal{H}_{33} a_{23} + \mathcal{H}_{34} a_{24} = E_2 a_{23} \tag{3.21}$$

(q = 2, m = 3, n = 2,3,4)

$$\mathcal{H}_{42} a_{22} + \mathcal{H}_{43} a_{23} + \mathcal{H}_{44} a_{24} = E_2 a_{24} \tag{3.22}$$

(q = 2, m = 4, n = 2,3,4)

From expressions like this only the ratios $a_{22} : a_{23}$ ..... are obtained. Absolute values of the coefficients are fixed by the condition that the wave function (3.17) should be normalised, i.e.

$$\sum a^{*}_{qm} \cdot a_{qm} = 1 \qquad (3.23)$$

Applying the eqn. (3.23) to the coefficients occurring in eqns. (3.20) - (3.22), one gets

$$a_{22}^{2} + a_{23}^{2} + a_{24}^{2} = 1 \qquad (3.24)$$

similarly

$$a_{32}^{2} + a_{33}^{2} + a_{34}^{2} = 1 \qquad (3.25)$$

and

$$a_{42}^{2} + a_{43}^{2} + a_{44}^{2} = 1 \qquad (3.26)$$

3.2.g. Transition Probabilities

Eqns. (3.19) - (3.26) allow the evaluation of a_{22}, a_{23} and a_{24} etc. and thus the final stationary state wave functions. Once the complete set of stationary state wave functions for $\mathcal{H}$ has been obtained, the transition probabilities and therefore, the line intensities can be calculated. The intensity of the signal arising from the transition $q \rightarrow q'$ is proportional to $(\varphi_q \mid M_x \mid \varphi_{q'})^2$ where $M_x \propto \sum_i I_{x(i)}$

Since the operator $I_{x(i)}$ will have a matrix element between two basic product functions which differ only in the spin of nucleus i, the total matrix element in $(\varphi_q \mid M_x \mid \varphi_q)^2$ will have values of the total spin component F_z differing by ± 1. This fact leads to the important selection rule that the transitions are restricted to

$$F_z = \pm 1 \qquad (3.27)$$

For syminetrical molecules transitions can occur only between functions of the same symmetry. For a set of nuclei of different species or of

the same species but having large chemical shifts compared with the coupling constants between them, only transitions between functions which differ by ± 1 in one of $F_2(X)$, $F_2(Y)$ .... are allowed.

The calculation of intensities can be carried out in terms of single functions of the type $(\psi_p | M_x | \psi_q)$ which are zero unless ψ_q and ψ_p differ only in the spin of one nucleus in which case it is equal to 1.

e.g. if $$\varphi_p = a_{mm} \psi_m + a_{mn} \psi_n \qquad (3.28)$$

and $$\varphi_q = a_{nm} \psi_m + a_{nn} \psi_n \qquad (3.29)$$

the relative intensity of transition between the levels is proportional to

$$\Big| (a_{mm} \psi_m | M_x | a_{nm} \psi_m) + (a_{mm} \psi_m | M_x | a_{nn} \psi_n) + (a_{mn} \psi_n | M_x | a_{nm} \psi_m) + (a_{mn} \psi_n | M_x | a_{nn} \psi_n) \Big|^2$$

The procedure can be further illustrated by calculating the relative intensity for one of the transitions, say between levels 2 and 5 (transition no. 4 in table 3.3) for ABC systems.

The corresponding stationary state functions (see table 3.2), obtained from the basic product functions (see table 3.1), are:

$$\varphi_2 = a_{22} \psi_2 + a_{23} \cdot \psi_3 + a_{24} \psi_4 \qquad (3.30)$$

$$\varphi_5 = a_{55} \psi_5 + a_{56} \psi_6 + a_{57} \psi_7 \qquad (3.31)$$

The appropriate intensity is

$$\Big| \varphi_2 | M_x | \varphi_5 \Big|^2$$

$$= \Big| (a_{22} \psi_2 + a_{23} \psi_3 + a_{24} \psi_4) | M_x | (a_{55} \psi_5 + a_{56} \psi_6 + a_{57} \psi_7) \Big|^2$$

$$= \Big| (a_{22}\,\Psi_2 \,|M_x|\, a_{55}\,\Psi_5) + (a_{22}\,\Psi_2|M_x|\,a_{56}\,\Psi_6) + (a_{22}\,\Psi_2|M_x|\,a_{57}\,\Psi_7)$$
$$+ (a_{23}\,\Psi_3|M_x|\,a_{55}\,\Psi_5) + (a_{23}\,\Psi_3|M_x|\,a_{56}\,\Psi_6) + (a_{23}\,\Psi_3|M_x|\,a_{57}\,\Psi_7)$$
$$+(a_{24}\,\Psi_4|M_x|\,a_{55}\,\Psi_5) + (a_{24}\,\Psi_4|M_x|\,a_{56}\,\Psi_6) + (a_{24}\Psi_4|M_x|\,a_{57}\,\Psi_7)\Big|^2 \qquad (3.32)$$

substituting the values of Ψ_i from table 3.1, eqn. 3.32 reduces to the form

$$\left|\varphi_2 \,|M_x|\, \varphi_5\right|^2$$
$$= \Big| (a_{22}\alpha\alpha\beta\,|M_x|\,a_{55}\alpha\beta\beta) + (a_{22}\alpha\alpha\beta\,|M_x|\,a_{56}\beta\alpha\beta) + (a_{22}\alpha\alpha\beta\,|M_x|\,a_{57}\beta\beta\alpha)$$
$$+ (a_{23}\alpha\beta\alpha\,|M_x|\,a_{55}\alpha\beta\beta) + (a_{23}\alpha\beta\alpha\,|M_x|\,a_{56}\beta\alpha\beta) + (a_{23}\alpha\beta\alpha\,|M_x|\,a_{57}\beta\beta\alpha)$$
$$+ (a_{24}\beta\alpha\alpha\,|M_x|\,a_{55}\alpha\beta\beta) + (a_{24}\beta\alpha\alpha\,|M_x|\,a_{56}\beta\alpha\beta) + (a_{24}\beta\alpha\alpha|M_x|\,a_{57}\beta\beta\alpha)\Big|^2 \qquad (3.33)$$

Applying the condition that $(\Psi_p \,|M_x|\, \Psi_q)$ is zero unless Ψ_p and Ψ_q differ in the spin of only one nucleus i in which case it is equal to 1, eqn. (3.33) simplifies to

$$\left|\varphi_2 \,|M_x|\, \varphi_5\right|^2$$
$$= \left[a_{22}\,(a_{55} + a_{56}) + a_{23}\,(a_{55} + a_{57}) + a_{24}\,(a_{56} + a_{57})\right]^2 \qquad (3.34)$$

3.3 THE ABC SPIN SYSTEM

A molecule containing three magnetically non-equivalent nuclei of the same species such that the chemical shifts between pairs of nuclei are of the same order of magnitude as the corresponding coupling constants (both expressed in the same unit), constitutes an ABC system (see sec. 1.11). Since the investigations reported herein are based on the study of vinyl compounds, CH_2 = CHX, which exhibit typical ABC n.m.r. spectra, the analysis of this class will be considered in detail.

3.3.a. Quantum Mechanical Considerations

The total number of energy states for an ABC system is $2^3 = 8$. There are no symmetry considerations to be taken into account for an ABC system and the basic product functions are themselves used as a basis for the wave functions of the system. Table 3.1 gives the basic product functions, ψ_i, and the diagonal matrix elements, $\mathcal{H}_{nn}$, of the Hamiltonian for ABC systems, in terms of the three absorption frequencies ν_A, ν_B and ν_C, and the spin coupling constants J_{AB}, J_{AC} and J_{BC}.

The non-zero off-diagonal elements have been calculated by eqn. (3.14) and are as follows:

Table 3.1

Basic Product Functions and the Diagonal Matric Eelements for the ABC system

n	ψ_n	Total spin F_z	Diagonal Matrix Elements
1	$\alpha\alpha\alpha$	$+\frac{3}{2}$	$\frac{1}{2}(\nu_A+\nu_B+\nu_C)+\frac{1}{4}(J_{AB}+J_{AC}+J_{BC})$
2	$\alpha\alpha\beta$	$+\frac{1}{2}$	$\frac{1}{2}(\nu_A+\nu_B-\nu_C)+\frac{1}{4}(J_{AB}-J_{AC}-J_{BC})$
3	$\alpha\beta\alpha$	$+\frac{1}{2}$	$\frac{1}{2}(\nu_A-\nu_B+\nu_C)+\frac{1}{4}(-J_{AB}+J_{AC}-J_{BC})$
4	$\beta\alpha\alpha$	$+\frac{1}{2}$	$\frac{1}{2}(-\nu_A+\nu_B+\nu_C)+\frac{1}{4}(-J_{AB}-J_{AC}+J_{BC})$
5	$\alpha\beta\beta$	$-\frac{1}{2}$	$\frac{1}{2}(\nu_A-\nu_B-\nu_C)+\frac{1}{4}(-J_{AB}-J_{AC}+J_{BC})$
6	$\beta\alpha\beta$	$-\frac{1}{2}$	$\frac{1}{2}(-\nu_A+\nu_B-\nu_C)+\frac{1}{4}(-J_{AB}+J_{AC}-J_{BC})$
7	$\beta\beta\alpha$	$-\frac{1}{2}$	$\frac{1}{2}(-\nu_A-\nu_B+\nu_C)+\frac{1}{4}(J_{AB}-J_{AC}-J_{BC})$
8	$\beta\beta\beta$	$-\frac{3}{2}$	$\frac{1}{2}(-\nu_A-\nu_B-\nu_C)+\frac{1}{4}(J_{AB}+J_{AC}+J_{BC})$

$$H_{23} = H_{67} = \tfrac{1}{2}J_{BC} \qquad (3.35)$$

$$H_{24} = H_{57} = \tfrac{1}{2}J_{AC} \qquad (3.36)$$

$$H_{34} = H_{56} = \tfrac{1}{2}J_{AB} \qquad (3.37)$$

The matrix representing the Hamiltonian can be factorised into two 1 x 1 and two 3 x 3 sub-matrices. Each of the four sub-matrices corresponds to one of the four different values of total spin component

$$F_z = \frac{3}{2}, \frac{1}{2}, -\frac{1}{2} \text{ and } -\frac{3}{2}$$

Analytical diagonalisation of the Hamiltonian leads to eight energy levels or eigenvalues, E_1 to E_8 each corresponding to an eigenfunction, φ_1 to φ_8. The values of eigenfunctions have been calculated by eqn. (3.17) and are listed in the table 3.2.

Table 3.2

Eigenfunctions (φ_n) and Eigenvalues (E_n) for the ABC system

E_n	φ_n
E_1	$\alpha\alpha\alpha$
E_2	$a_{22}(\alpha\alpha\beta) + a_{23}(\alpha\beta\alpha) + a_{24}(\beta\alpha\alpha)$
E_3	$a_{32}(\alpha\alpha\beta) + a_{33}(\alpha\beta\alpha) + a_{34}(\beta\alpha\alpha)$
E_4	$a_{42}(\alpha\alpha\beta) + a_{43}(\alpha\beta\alpha) + a_{44}(\beta\alpha\alpha)$
E_5	$a_{55}(\alpha\beta\beta) + a_{56}(\beta\alpha\beta) + a_{57}(\beta\beta\alpha)$
E_6	$a_{65}(\alpha\beta\beta) + a_{66}(\beta\alpha\beta) + a_{67}(\beta\beta\alpha)$
E_7	$a_{75}(\alpha\beta\beta) + a_{76}(\beta\alpha\beta) + a_{77}(\beta\beta\alpha)$
E_8	$\beta\beta\beta$

As it is evident from table 3,2, basic product functions themselves are stationary state functions for the states 1 and 8 as there is no mixing

of these levels with any other level. In view of the selection rule that transitions are allowed between the eigenvalues in which the change of total spin ΔF_z is ± 1, there are 15 possible transitions for an ABC system. The 15 transitions and the corresponding transition probabilities, which determine the relative intensities of the corresponding lines, are given in table 3.3. The lines are labelled as A,B or C transitions when the change of spin giving rise to the line is, in the unperturbed state, solely resident in the A,B or C nucleus respectively, or as combination lines when all the three nuclei change their spins simultaneously.

For a simple 3 spin system, APX, where the chemical shifts between pairs of nuclei are far larger than the corresponding coupling constants, the complete spectrum consists of three symmetrical quartets, one for each resonating nucleus. All lines of the same quartet are of equal intensity and the separation between different pair of lines is equal to the different coupling constants (Fig.3.1). The combination lines have got zero intensity and are not observed. But in a true ABC spectrum the observed separations between pair of lines in groups A,B and C now differ from the actual coupling constant. Nevertheless, the observed splittings are still repeated four times in the complete spectrum, in a manner similar to the first order spectra, and the sum of observed common spacings is equal to the sum of actual coupling constants. The four lines corresponding to the four transitions of a nucleus are no longer of equal intensity due to spin interaction (Fig.3.2). Three new combination lines appear such that any pair of them is symmetrically situated about the centre of one of the quartets. Combination lines share intensity with the fundamental lines. The

TABLE 3.3

The allowed transitions for an ABC system

Transition Number	Transition Energy	Transition Probability	Nucleus
1	E_1-E_2	$(a_{22}+a_{23}+a_{24})^2$	C
2	E_1-E_3	$(a_{32}+a_{33}+a_{34})^2$	B
3	E_1-E_4	$(a_{42}+a_{43}+a_{44})^2$	A
4	E_2-E_5	$\left[a_{22}(a_{55}+a_{56})+a_{23}(a_{55}+a_{57})+a_{24}(9_{56}+a_{57})\right]^2$	B
5	E_2-E_6	$\left[a_{22}(a_{65}+a_{66})+a_{23}(a_{65}+a_{67})+a_{24}(a_{66}+a_{67})\right]^2$	A
6	E_2-E_7	$\left[a_{22}(a_{75}+a_{76})+a_{23}(a_{75}+a_{77})+a_{24}(a_{76}+a_{77})\right]^2$	Comb.
7	E_3-E_5	$\left[a_{32}(a_{55}+a_{56})+a_{33}(a_{55}+a_{57})+a_{34}(a_{56}+a_{57})\right]^2$	C
8	E_3-E_6	$\left[a_{32}(a_{65}+a_{66})+a_{33}(a_{65}+a_{67})+a_{34}(a_{66}+a_{67})\right]^2$	Comb.
9	E_3-E_7	$\left[a_{32}(a_{75}+a_{76})+a_{33}(a_{75}+a_{77})+a_{34}(a_{76}+a_{77})\right]^2$	A
10	E_4-E_5	$\left[a_{42}(a_{55}+a_{56})+a_{43}(a_{55}+a_{57})+a_{44}(a_{56}+a_{57})\right]^2$	Comb.
11	E_4-E_6	$\left[a_{42}(a_{65}+a_{66})+a_{43}(a_{65}+a_{67})+a_{44}(a_{66}+a_{67})\right]^2$	C
12	E_4-E_7	$\left[a_{42}(a_{75}+a_{76})+a_{43}(a_{75}+a_{77})+a_{44}(a_{76}+a_{77})\right]^2$	B
13	E_5-E_8	$(a_{55}+a_{56}+a_{57})^2$	A
14	E_6-E_8	$(a_{65}+a_{66}+a_{67})^2$	B
15	E_7-E_8	$(a_{75}+a_{76}+a_{77})^2$	C

intensities of different lines in an ABC spectrum are interrelated by certain rules:[92,93]

(i) A combination line shares intensity with a line such that the two transitions giving rise to the lines have one energy level in common and the other levels are neighbouring ones associated with the same block of overall Hamiltonian, e.g. line no. 6 in table 3.3 will share intensity with lines no. 4,5,9 and 12.

(ii) $I_{1i} = 3 \qquad (i = 2,3 \text{ and } 4)$ (3.38)

$I_{ij} = 6 \qquad (j = 5,6 \text{ and } 7)$ (3.39)

$I_{j8} = 3$ (3.40)

where I denotes the intensity of a line resulting from a transition between levels indicated by the subscripts and the total intensity of the spectrum is normalised to 12, e.g. sum of intensities of lines numbered 1,2 and 3 in table 3.3 which originate due to transitions between levels 1-2, 1-3 and 1-4 respectively will be equal to 3. The above points are illustrated by the data given in table 3.4. In further discussions, throughout this investigation, the following convention will be observed in labelling the three vinyl protons.

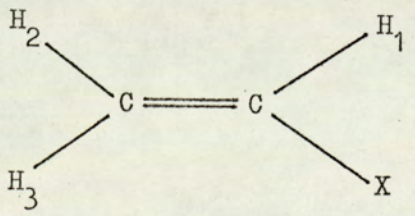

3.3.b. Iterative Methods for Analysing ABC Spectra-LAOCOON3

The analysis of an ABC spectrum becomes difficult due to the fact that

TABLE 3.4[a b]

Acylonitrile Spectrum

ν_1 = -203.671

ν_2 = -220.060

ν_3 = -238.782

Molecular Parameters (Hz):

J_{12} = 11.685

J_{13} = 17.954

J_{23} = 1.021

Transition Number	Experimental Frequency	Calculated Frequency	Intensity	Error
6	-	-263.268	0.020	-
13	-250.800	-250.815	0.535	0.015
5	-247.800	-247.765	0.534	-0.035
9	-234.420	-234.420	1.038	0.000
3	-231.350	-231.370	1.663	0.020
14	-	-228.930	0.145	-
4	-225.840	-225.880	0.767	0.040
8	-	-218.917	0.214	-
12	-217.730	-217.715	2.262	-0.015
2	-214.690	-214.665	1.015	-0.025
15	-213.410	-213.427	2.321	0.017
11	-202.210	-202.212	0.397	0.002
7	-197.090	-197.032	0.763	-0.058
1	-185.780	-185.817	0.321	0.037

a. The spectrum was recorded from a 4 mole% solution of acrylonitrile in benzene (66 mole%) and cyclohexane, the frequencies being measure against internal cyclohexane reference at 60.004MHz and 306.6°K.

b. Number of figures in the data are given for the sake of completeness and do not represent the limit of accuracy in the experimental measurements.

even after the factorisation of the Hamiltonian matrix, one is dealing with 3 x 3 sub-matrices and the corresponding secular equations are cubic. The roots and the three eigenvectors of the equation can not be expressed in simple algebric form. However, one can usually obtain reasonably good values by iterative methods. In an iterative method, one guesses trial values for chemical shifts and coupling constants and performs a numerical diagonalisation of the Hamiltonian matrix. The result is compared with the experimental spectrum, improved trial values of the parameters are chosen, and the whole process is repeated until one converges on constant values. Iterative methods have been applied by Swalen and Reilly[94], by Hoffman[95], and by Arata, Shimizu and Fujiwara[96]. S. Castellano and A. A. Bothner-By[97] have devised a method of analysing n.m.r. spectra by least squares. Their method is very closely related to that of Hoffman[95]. The authors have put the entire method of analysis on a FORTRAN computer program LAOCOON 2. Since a later version of this program, LAOCOON 3, has been used for spectral analysis in most of the cases reported here in this work, this method of iterative analysis will be considered in detail.

In any such iterative procedure of spectral analysis, the best values of the parameters are those which make the sum of squared residuals of transition frequencies a minimum. Thus, for each parameter p_j, the condition is that

$$\left(\partial/\partial p_j\right)\sum_{i=1}^{l}\left(\nu_{obs}-\nu_{calc}\right)_i^2 = -2\sum_{i=1}^{l}\left(\nu_{obs}-\nu_{calc}\right)_i\left(\partial\nu_{calc}/\partial p_j\right)_i = 0 \qquad (3.41)$$

where l is the number of transition frequencies observed and $\left(\nu_{obs}-\nu_{calc}\right)_i$ is the difference between the observed and calculated frequencies for the i th line. If, for small changes in the parameter

p_j, linear changes in the transition frequencies $\Delta \nu_i$ are assumed, one may write:

$$\Delta \nu_i = \frac{\partial \nu_i}{\partial p_j} \cdot \Delta p_j \qquad (3.42)$$

The changes in the parameters for a coincidance between the calculated and observed lines has to be calculated by equations of the type

$$\sum_j \left(\frac{\partial \nu_i}{\partial p_j}\right) \Delta p_j = \left(\nu_{obs} - \nu_{calc} \right)_i \qquad (3.43)$$

These equations of condition may be qritten in matrix form as

$$D \Delta = N \qquad (3.44)$$

where D is the matrix of partial differentials, Δ is the vector of corrections to the parameters, and N is the vector of residuals in the frequencies. Standard least square procedure is to form the system of normal equations.

$$DTD \Delta = DTN \qquad (3.45)$$

where DTD is a real symmetrix matrix with a non-vanishing determinant. Solution of eqn. (3.41) reduces to zero only when DTN = 0, which means that eqn. (3.41) is satisfied for all parameters. The convergence is thus to the desired least - square fit. For all those cases when $\Delta \neq 0$, parameters are adjusted such that they give a least-squares solution if the transition frequencies were linearly dependent on the parameters. Thus the method gains over the other iterative methods in the respect that it is strongly convergent.

The partial differentials $\frac{\partial \nu_i}{\partial p_j}$ can be expressed as:

$$\frac{\partial \nu_i}{\partial p_j} = \frac{\partial \lambda_m}{\partial p_j} - \frac{\partial \lambda_n}{\partial p_j} \qquad (3.46)$$

λ_m and λ_n being the eigenvalues connected by the transition. The differentials of the eigenvalues are the diagonal elements of $U^{-1}\left(\partial \mathcal{H}/\partial p_j\right) U$, where U and U^{-1} represent the eigenvector matrix and its transpose. Since the differential of $\mathcal{H}$ in the basic representation is trivial, the evaluation of $\frac{\partial \lambda_m}{\partial p_j}$ requires only a knowledge of the eigenvectors. The errors associated with the correction to the parameter, Δp_j, and hence with the parameter when $\Delta = 0$, are given by:

$$\sigma_j = \left[m_j N.N \ \det (DTD) \ (l - x) \right]^{\frac{1}{2}} \qquad (3.47)$$

where σ_j is the standard deviation of the parameter j, m_j is the minor of the coefficients $(DTD)_{jj}$ in the matrix of coefficients of the normal equation, N.N is the sume of squares of the residuals, l is the number of equations of condition, and x is the number of independent parameters. However, due to certain advantages, the errors are computed after transforming to a set of new variables which are the linear combinations of the parameters which cause the matrix of normal equations to appear in diagonal form. Under such circumstances eqn. (3.47) reduces to the form

$$\sigma_q = \left[N.N \ d_{qq} \ (l - x) \right]^{\frac{1}{2}} \qquad (3.48)$$

where d_{qq} is the qth diagonal element of the diagonalised normal equation matrix, σ_q is the standard deviation of the qth linear combination of parameters obtained from the basic set of parameters and the qth eigenvector.

The actual computer program for this method consists of two parts. In the first part, a set of trial values for the parameters is read in and the resulting spectrum is computed. Eigenvectors are stored on a magnetic tape for use in the second part of the program. The output for the first part of the program consists of all input data, origin number, frequencies and intensities of all the transitions with intensity greater than a selected minimum. There is also produced a second table with the calculated lines given in order of increasing frequency within a pre-selected frequency range which facilitates the comparison of theoretical spectrum with an observed spectrum.

The second half of the program is used for the least-squares adjustment and error calculation. The second half accepts as input (1) the maximum number of iteration cycles to be performed; (2) the origin number and the experimentally observed frequency for each transition assigned; (3) the subscripts identifying the parameters. Then the second part of the program performs least-squares iteration as stated earlier. In each cycle, the new eigenvectors are stored and are used in crudely diagonalising the adjusted Hamiltonian for succeeding cycle. Iteration stops when the meximum specified number of iterations has been performed or the error in line fitting decreases insignificantly ($<1\%$) or increases due to round off error. The matrix of the normal equations is then diagonalised and error vectors and the corresponding standard deviations are calculated. Finally, from the last set of eigenvalues and eigenvectors, the best calculated spectrum is computed. In the output, all input data, best values of parameters, the error vectors and the probable errors, and the two tabulations of calculated spectrum are reproduced. In each tabulation, the frequency of each calculated line is also accompanied by the observed frequency

of the corresponding line as well as the error in fitting. A revised version of the program was operated on the KDF9 computer, situated at Birmingham University, through Cotan - 3 Culham-on-line system. A shorter version of the program which can be operated on computers of comparatively small size has also since been written[98].

It has been pointed out[99,100] that the parameters obtained after such iterative analysis may not be correct or unique. Depending on the particular set of trial parameters originally chosen, in some cases, two or more entirely different set of parameters consistent with the experimental spectrum, within the experimental error limits, may be obtained or convergence may never be achieved. In order to make sure that no such ambiguity exists with the results reported in this investigation, analyses were repeated with more than one set of trial parameters sufficiently different as compared to possible experimental errors. In each case, the iterations converged to the same solution (tables 3.5 - 3.7) except in the case of some vinyl bromide spectra recorded in the presence of high concentration of benzene. Figs. 3.4 and 3.5 represent an experimental spectrum and the corresponding theoretical spectrum. Even in the case of vinyl bromide spectra, so long as they were recorded in the presence of cyclohexane, p-xylene or low concentration of benzene, there was no ambiguity. This shows that p-xylene is a better solvent for simplifying the analysis of vinyl bromide spectra rather than benzene as suggested earlier[101]. In fact the ambiguity arises when the intensity of combination lines becomes comparable to those of the fundamental lines[92]. In such a spectrum one can interchange assignments of the combination lines and the fundamental lines without disturbing the

TABLE 3.5.a.*

Results of LAOCOON 3 analysis for acrylonitrile sprectrum

Input parameters (Hz):	ν_1	= -203.600	J_{12}	=	11.600
	ν_2	= -220.100	J_{13}	=	18.000
	ν_3	= -238.800	J_{23}	=	1.100
Interation 0	RMS Error = 0.059				
Iteration 1	RMS Error = 0.029				
Iteration 2	RMS Error = 0.029				
Best Values (Hz):	ν_1	= -203.671	J_{12}	=	11.685
	ν_2	= -220.060	J_{13}	=	17.954
	ν_3	= -238.782	J_{23}	=	1.021

TABLE 3.5.b*

Results of LAOCOON 3 analysis for the same spectrum of acryloritrile, iterated with an alternative set of trial parameters.

Input parameters (Hz):	ν_1	= -204.000	J_{12}	=	11.800
	ν_2	= -219.000	J_{13}	=	17.800
	ν_3	= -239.500	J_{23}	=	0.800
Iteration 0	RMS Error = 0.622				
Iteration 1	RMS Error = 0.034				
Iteration 2	RMS Error = 0.029				
Iteration 3	RMS Error = 0.029				
Best Values (Hz):	ν_1	= -203.671	J_{12}	=	11.685
	ν_2	= -220.060	J_{13}	=	17.954
	ν_3	= -238.782	J_{23}	=	1.021

* The sprectrum was measured from a 4 mole % solution of acrylonitrile in benzene (66 mole%) at 60.004MHz against internal cyclohexane reference.

TABLE 3.6.a.*

Results of LAOCOON 3 analysis for vinylmethyl ketone spectrum

Input parameters(Hz):	ν_1	= -277.400	J_{12}	=	10.800
	ν_2	= -229.000	J_{13}	=	17.800
	ν_3	= -255.000	J_{23}	=	1.000
Iteration 0	RMS	Error = 0.131			
Iteration 1	RMS	Error = 0.013			
Iteration 2	RMS	Error = 0.013			
Best Values (Hz):	ν_1	= -277.586	J_{12}	=	10.697
	ν_2	= -229.113	J_{13}	=	17.774
	ν_3	= -225.064	J_{23}	=	0.979

TABLE 3.6.b.*

Results of LAOCOON 3 analysis for the same spectrum of vinyl methyl ketone, with an alternative set of trial parameters

Input parameters (Hz):	ν_1	= -276.000	J_{12}	=	10.000
	ν_2	= -230.000	J_{13}	=	18.500
	ν_3	= -254.000	J_{23}	=	0.800
Iteration 0	RMS	Error = 1.286			
Iteration 1	RMS	Error = 0.015			
Iteration 2	RMS	Error = 0.013			
Iteration 3	RMS	Error = 0.013			
Best values (Hz):	ν_1	= -277.586	J_{12}	=	10.697
	ν_2	= -229.113	J_{13}	=	17.774
	ν_3	= -255.064	J_{23}	=	0.979

* The spectrum was recorded from a 4 mole% solution of vinyl methyl ketone in benzene (95 mole%) at 60.004 MHz against internal cyclohexane reference.

TABLE 3.7.a.*

Results of LAOCOON 3 analysis for vinyl bromide spectrum

Input parameters (Hz):		ν_1	= -276.700	J_{12}	= 7.100
		ν_2	= -245.200	J_{13}	= 15.000
		ν_3	= -246.700	J_{23}	= -1.600
Iteration	0	RMS	Error = 0.265		
Iteration	1	RMS	Error = 0.017		
Iteration	2	RMS	Error = 0.017		
Best values (Hz):		ν_1	= -277.106	J_{12}	= 7.223
		ν_2	= -245.380	J_{13}	= 15.017
		ν_3	= -246.548	J_{23}	= -1.690

TABLE 3.7.b.*

Results of LAOCOON 3 analysis for the same spectrum of vinyl bromide, with an alternative set of trial parameters.

Input parameters (Hz):		ν_1	= -276.000	J_{12}	= 7.000
		ν_2	= -244.500	J_{13}	= 14.500
		ν_3	= -247.500	J_{23}	= -1.400
Iteration	0	RMS	Error = 0.964		
Iteration	1	RMS	Error = 0.098		
Iteration	2	RMS	Error = 0.017		
Iteration	3	RMS	Error = 0.017		
Best values)Hz):		ν_1	= -277.106	J_{12}	= 7.223
		ν_2	= -245.380	J_{13}	= 15.017
		ν_3	= -246.548	J_{23}	= -1.690

* The sprectrum was recorded from a 4 mole% solution of vinyl bromide in p-xylene (75 mole%) at 60.004 MHz against internal cyclohexane reference.

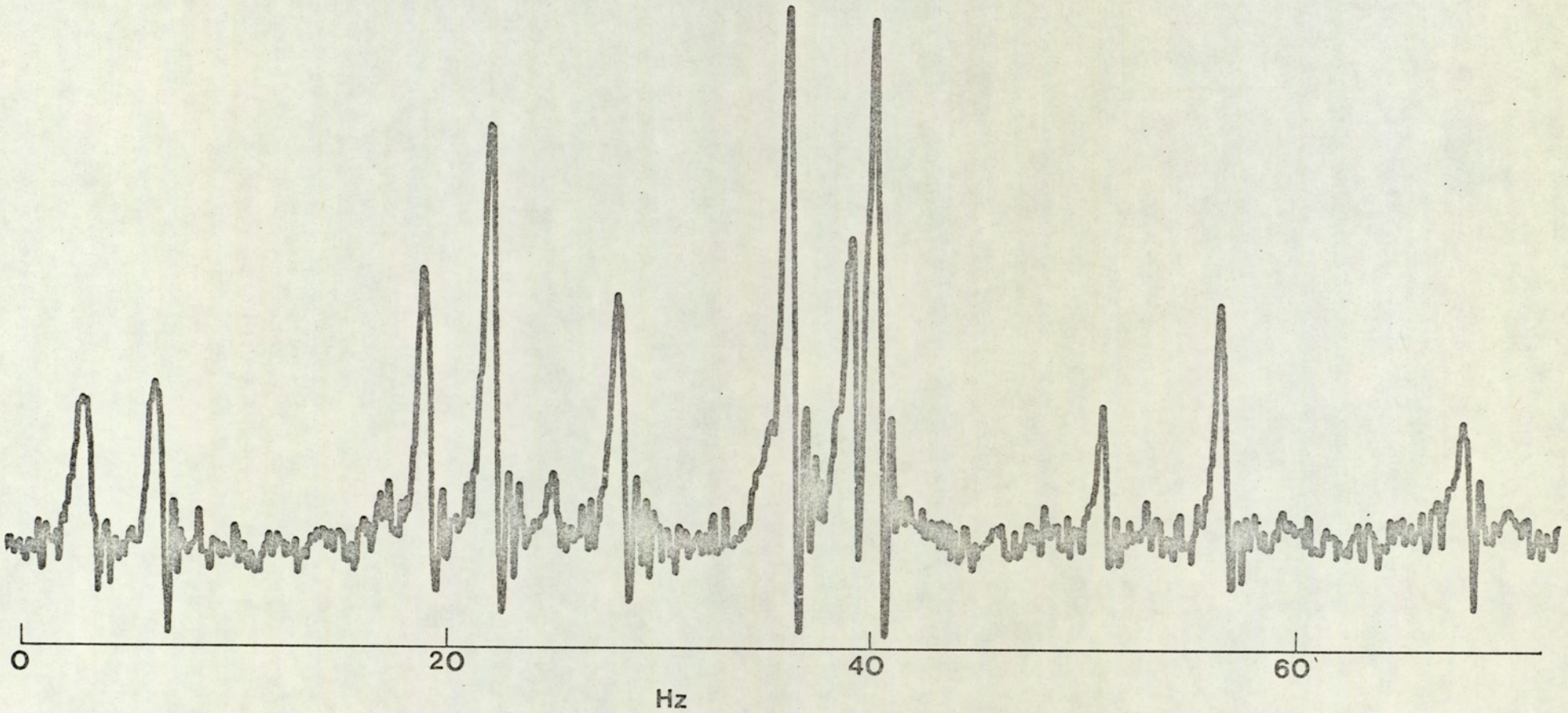

Fig. 3.4 60.004MHz observed n.m.r. spectrum for acrylonitrile (table 3.4)

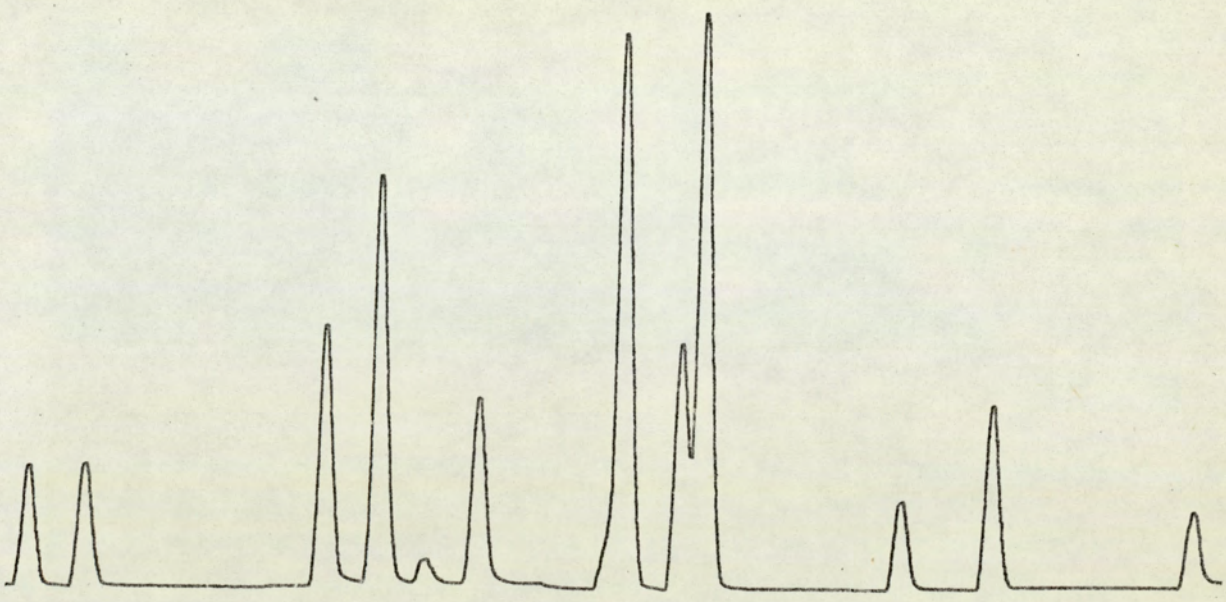

Fig. 3.5 Theoretical n.m.r. spectrum for acrylonitrile simulted from the parameters (table 3.4) obtained after the LAOCOON3 analysis of the observed spectrum (Fig.3.4)

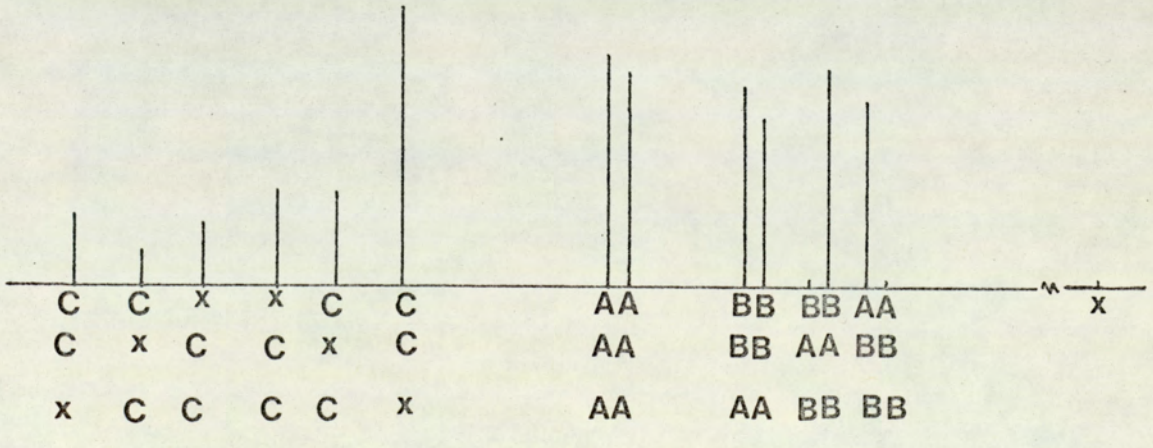

Fig. 3.6 Three alternative groupings for an ABC spectrum

regular substractive features. Fig. 3.6 illustrates such a situation for a vinyl bromide spectrum. The symmetrical location of the combination lines (marked X in Fig.3.6) with respect to the C group allows an interchange in the trial assignments of fundamental and combination lines to be made within the group while still retaining the three constant separations throughout the spectrum by re-assigning A and B group lines. The three possible assignments are shown in the figure. One actually comes across such a situation for vinyl bromide spectra recorded in presence of high concentration of benzene where LAOCOON 3 fails to converge to a solution (table 3.8). In other cases where combination lines are weak in intensity, there is no such ambiguity in assignment. The accuracy of the results is further confirmed from the fact that the values for the parameters obtained by LAOCOON 3 analyses during the present investigation are very close to the values (table 3.9) obtained by other workers[102-106] using methods viz. ^{13}C sattellite spectral analysis and tickling experiment etc., which are not subject to any ambiguity. Representative sets were analysed by the trace-invariance method and solutions identical to those given by LAOCOON 3 analysis were obtained.

3.3.c. The Trace Invariance Method

The cases where LAOCOON 3 analysis failed to converge to a satisfactory solution were analysed by an elaborate method devised by Castellano and Waugh[99], which gives all possible sets of parameters consistent with the observed spectrum. The method is based on the property of trace invariance of each sub-matrix and intensity sum rules.

TABLE 3.8

Results of LAOCOON 3 analysis for a spectrum of vinyl bromide (4 mole%) in benzene (95 mole%)

Input parameters (Hz): $\nu_1 = -271.000$ $J_{12} = 7.200$

$\nu_2 = -237.300$ $J_{13} = 15.000$

$\nu_3 = -243.600$ $J_{23} = -1.600$

Iteration 0 RMS Error = 2.765

Iteration 1 RMS Error = 7.933

TABLE 3.9

Values of coupling constants (Hz) for vinyl compounds obtained after analysing the spectra by different methods.

Compound	Reference	Method	J_{12}	J_{13}	J_{23}
Acrylonitrile	102	^{13}C spectral studies	11.75	17.92	0.91
	103	tickling experiment	11.75	17.86	0.87
	this work	LAOCOON 3	11.68	17.95	1.02
	this work	trace invariance	11.68	17.95	1.02
Vinyl bromide	106	^{13}C sprectal studies	7.25	15.11	-1.62
	this work	LAOCOON 3	7.22	15.02	-1.69
	this work	trace invariance	7.22	15.02	-1.69
Vinyl methyl	104/105	trace invariance	10.77	17.83	1.10
ketone	104	trace invariance	10.96	17.58	1.11
	this work	LAOCOON 3	10.70	17.77	0.98

As it has already been said, the 15 allowed transition frequencies for ABC spin systems obey certain simple regularities, resembling those found when the influence of spin coupling can be treated by first order. Keeping the regularities in mind, the 15 allowed ABC transitions can be classified as:

$$\begin{array}{lll} A_1 & B_1 & C_1 \\ A_2 & B_2 & C_2 \\ A_3 & B_3 & C_3 \\ A_4 & B_4 & C_4 \\ A_x & B_x & C_x \end{array} \qquad (3.49)$$

where A_i, B_i and C_i are the fundamental frequencies associated with nuclei A,B and C respectively, and A_x, B_x and C_x are the three combination transitions. Such frequency tables are usually called groupings. The three groups, A,B, and C, each form a quartet having spacings common with other quartets (Fig.3.2). Designating a as the spacing common to groups A and B, b as common to A and C, and c as common to B and C, the following relationships can be noticed:

$$\begin{aligned} A_1 - A_3 = A_2 - A_4 &= B_1 - B_3 = B_2 - B_4 = a \\ A_1 - A_2 = A_3 - A_4 &= C_1 - C_3 = C_2 - C_4 = b \\ B_1 - B_2 = B_3 - B_4 &= C_1 - C_2 = C_3 - C_4 = c \end{aligned} \qquad (3.50)$$

Further, designating W_a, W_b and W_c as the mean frequencies of groups A,B and C respectively, and with

$$W_a + W_b + W_c = 0 \qquad (3.51)$$

it is found that

$$\begin{aligned} A_1 + A_4 &= A_2 + A_3 = -A_x = 2W_a \\ B_1 + B_4 &= B_2 + B_3 = -B_x = 2W_b \\ C_1 + C_4 &= C_2 + C_3 = -C_x = 2W_c \end{aligned} \qquad (3.52)$$

It has been pointed out by Castellano and Waugh that there are 15 such possible groupings in all, leading eventually to 10 independent sets of eigenvalues.

Using the constans a,b,c,W_c, W_b and W_c defined by (3.50) - (3.52), the 10 sets of eigenvalues can be constructed in the following way[107]:

$$E_1 = \tfrac{1}{4}(a + b + c)$$

$$E_2 = -W_c + \tfrac{1}{4}(a - b - c)$$

$$E_3 = -W_b + \tfrac{1}{4}(-a + b - c)$$

$$E_4 = -W_a + \tfrac{1}{4}(-a - b + c)$$

$$E_5 = W_c + \tfrac{1}{4}(a - b - c)$$

$$E_6 = W_b + \tfrac{1}{4}(-a + b - c)$$

$$E_7 = W_a + \tfrac{1}{4}(-a - b + c)$$

$$E_8 = \tfrac{1}{4}(a + b + c) \qquad (1)$$

In (1) replacing a by -a (2)

In (1) replacing b by -b (3)

In (1) replacing c by -c (4)

In (1) replacing b by $W_b - W_a - \frac{1}{2}(b+c)$

c by $W_b - W_a + \frac{1}{2}(b + c)$

W_a by $\frac{1}{2}\left[-W_c + \frac{1}{2}(b - c)\right]$

W_b by $\frac{1}{2}\left[-W_c - \frac{1}{2}(b - c)\right]$ (5)

In (5) replacing a by -a (6)

In (1) replacing a by $W_c - W_a - \frac{1}{2}(a + c)$

c by $W_c - W_a + \frac{1}{2}(a + c)$

W_a by $\frac{1}{2}\left[-W_b + \frac{1}{2}(a - c)\right]$

W_b by $\frac{1}{2}\left[-W_b - \frac{1}{2}(a - c)\right]$ (7)

In (7) replacing b by -b (8)

In (1) replacing a by $W_c - W_b - \frac{1}{2}(a + b)$

b by $W_c - W_b + \frac{1}{2}(a + b)$

W_b by $\frac{1}{2}\left[-W_a + \frac{1}{2}(a - b)\right]$

$$W_c \text{ by } \tfrac{1}{2}\left[-W_c - \tfrac{1}{2}(a - b)\right] \qquad (9)$$

In (9) replacing c by -c (10)

The same sets of eigenvalues are always generated irrespective of the choice of the original grouping.

In applying the foregoing rules to actual spectral analysis, one begins by examining the spectrum for the repeated spacings required by (3.50). When these have been found, the lines are arranged in a grouping using the criteria (3.50). At this stage the averaged experimental frequencies are adjusted by small amounts to make the frequency table (3.49) agree exactly with spacing rules (3.50). Any missing lines are also assigned to make the frequency table internally consistent. The sum of all the fundamental lines is calculated and a new origin is chosen so as to make the sum equal to zero and therefore also satisfy the condition (3.51). Any missing combination lines can also be filled in the table using (3.52). Now the 10 sets of eigenvalues and the various sets of chemical shifts and coupling constants associated with them can be obtained. At one stage during the calculation, a quartic equation results for each of the 10 independent eigenvalue sets. In view of this, it would appear that 40 sets of chemical shifts and coupling constants are in general consistent with a three-spin system. However, it turns out that a number of these sets contain some complex parameters and are therefore spurious. The existance of complex solutions to the analysis problem explains the fact why, sometimes in attempting to perform a LAOCOON 3 analysis starting from an arbitrary set of trial parameters, convergence is not achieved at all. By applying intensity sum rules (see sec. 3.3.a.) some

sets of eigenvalues can be eliminated at very early stage of the calculation. The various sets of real chemical shifts and coupling constants associated with the remaining sets of eigenvalues are often very different. Cavanaugh [107] has put the whole procedure of this analysis of general three-spin systems on a computer program. The input for the FORTRAN program consists of the common spacings between the quartets, the mean frequencies of the groups A,B and C, measured intensities of the 15 transitions, and the frequency of the first line. The program calculates the 10 sets of eigenvalues and all real solutions resulting from each set. The intensities predicted from such sets are calculated and compared with the measured intensities and a sum of squared deviations is computed. The chief draw-back of this method is that to apply it completely, one must be able to resolve and measure most of the lines that are theoretically present.

CHAPTER 4

SOME COMMENTS ON THE NMR STUDY OF MOLECULAR INTERACTIONS IN SOLUTION

4.1 INTRODUCTION

Considerable attention has been directed to the study of short-lived complexes of polar solutes (A) and aromatic solvents (B) formed in reactions of the type [41,42,108,109]

$$A + B \rightleftharpoons A \cdots\cdots B \qquad (4.1)$$

occuring in a supposedly inert solvent (S). Though other techniques have also been used, n.m.r. can profitably be chosen for the investigation of such complexes because of the wealth of information that can be obtained.

It has been well known for many years that when polar solutes or non-polar solutes with strongly polar bonds are dissolved in benzene or other aromatic solvents, the solut proton resonance is shifted markedly, often upfield, relative to its position in an inert solvent such as cyclohexane. As the ratio of solvent to solute concentration increases, so the (upfield) aromatic solvent-induced shift (ASIS) also increases due to the equilibrium formation of the complex.

When a solute is in an inert solvent the chemical shift of a nucleus in the former is δ_{free} but this may be changed to δ_c when the solute is fully complexed with an active solvent. In many cases there is a rapid exchange of the solute between the two environments, fully complexed and free, and instead of observing the resonances corresponding to the individual states, a resonance at some intermediate position, δ_{obs}, is observed. Because δ_c and δ_{free} are molecular parameters, δ_{obs} is a time-averaged function given by

$$\delta_{obs} = P_1 \delta_c + P_2 \delta_{free} \qquad (4.2)$$

where P_1 and P_2 are the fractional times that A spends in each state. There has been a practice of defining P_1 and P_2 as the fractional populations of the solute in fully complexed and free states respectively and δ_{obs} has been expressed in the form

$$\delta_{obs} = \frac{n_{AB}}{n_A} \cdot \delta_c + \frac{n_A - n_{AB}}{n_A} \cdot \delta_{free}$$

or alternatively as

$$\delta_{obs} = \frac{n_{AB}}{n_A} (\delta_c - \delta_{free}) + \delta_{free}$$

$$\Delta_{obs} = \frac{n_{AB}}{n_A} \cdot \Delta_c \qquad (4.3)$$

where n_A is the initial number of moles of A taken and n_{AB} is the number of moles of the complex formed at equilibrium Δ_{obs} and Δ_c are defined by the equations

$$\Delta_{obs} = \delta_{obs} - \delta_{free} \qquad (4.4)$$

and

$$\Delta_c = \delta_c - \delta_{free} \qquad (4.5)$$

consequently if equilibrium quotients are used to characterize P_1 and P_2 the values obtained for these are in terms of bulk concentrations rather than time fractions. This approach can be satisfactory only if the quotients are obtained after suitable modifications described later on (see sec. 4.2) in accordance with the molecular basis of eqn. (4.2)

The equilibrium constant, K, for associations of this type should be given by

$$K = \frac{[AB]}{[A][B]} \cdot \frac{\gamma_{AB}}{\gamma_A \gamma_B} \qquad (4.6)$$

where $[AB]$, $[A]$ and $[B]$ are, respectively, the equilibrium concentrations of the complex, free solute and free aromatic solvent, and γ_{AB}, γ_A and γ_B are the corresponding activity coefficients. Often the activity coefficeints are improperly ignored in data processing and this leads to erroneous results as will be mentioned later.

4.2 DATA EVALUATION

Two basic procedures, both based on eqn. (4.3), have been used to process the data for shifts induced in A by B under different conditions for the initial concentration of B. The first is an extrapolation method due originally to Benesi and Hildebrand[110] or some variation thereof[111-3] and the second an iterative procedure such as that used by Creswell and Allred[114].

The simple Benesi-Hildebrand theory assumes a 1:1 equilibrium between the solute (A) and the aromatic solvent (B), of the form given by eqn. (4.1). Neglecting the activity coefficients, the equilibrium quotient, K, is given by

$$K = \frac{[AB]}{[A][B]} \qquad (4.7)$$

If a further approximation is taken by neglecting the amount of aromatic solvent used up in the complex formation under the condition that $[B] \gg [A]$, the following form of the Benesi-Hildebrand equation is obtained:

$$\frac{1}{\Delta_{obs}} = \frac{1}{K\,[B]_o\,\Delta_c} + \frac{1}{\Delta_c} \qquad (4.8)$$

where the different terms carry their usual meanings. If the observed

shifts are measured for a series of samples containing a constant low mole fraction of the solute (A) and different proportions of the aromatic solvent (B) and the inert solvent (S), the plots of Δ_{obs} against $\frac{1}{[B]_o}$ should give a straight line of slope $\frac{1}{K\Delta_c}$ and intercept $\frac{1}{\Delta_c}$. Use of an inert solvent (S) benefits such investigations in three ways. Firstly, the solvent can be chosen to act as a suitable internal reference for shift measurements. Secondly, it allows solid dipolar and solid aromatic materials to be examined. Thirdly, it allows the concentrations of the polar solute to be maintained at a low and constant value so that the effect of possible self-association of the solute can be minimised.

The second (iterative) method, developed by Creswell and Allred, makes use of the equation

$$\Delta_{obs} = \frac{n_{AB}}{n_A} \cdot \Delta_c \qquad (4.3)$$

The authors suggested that a plot of Δ_{obs} against $\frac{n_{AB}}{n_A}$ for assumed values of the equilibrium quotient given, for example when using mole-fractions to define the equilibrium composition of a mixture, by

$$K_x = \frac{n_{AB}\,(n_A + n_B + n_S - n_{AB})}{(n_A - n_{AB})\,(n_B - n_{AB})} \qquad (4.9)$$

in which the different terms carry their usual meanings, should be linear. It is supposed that the correct value of K_x is obtained when a straight line is obtained, corresponding to eqn.(4.3)

It has been a matter of considerable concern [115-7] that when any reaction is investigated, apparent anomalies concerning the values of Δ_c

and the equilibrium quotient have been found. The most significant of these are (a) that when a particular set of experimental data is processed the value of Δ_c obtained is found to depend on the concentration scale employed in the processing method, and (b) that when a particular reaction is studied in different inert solvents, different values of Δ_c are obtained.

Homer et al.[118] have studied the thermodynamics of the method in detail and found that the anomalies arise for two reasons:

(i) the eqn. (4.3) is not strictly valid;

(ii) the concentration range over which the experimental data have been obtained are such that the methods used for data processing become unsound.

The authors have suggested a procedure and the related conditions which must be used in processing the data to avoid these anomalies. On an entirely theoretical basis, they have deduced that:

(i) Meaningful values for equilibrium quotients and Δ_c may be obtained in terms of either mole fractions or molarities. This is possible only when x_B tends towards unity, when parameters become independent of the concentration of B and activity coefficients of all sorts;

(ii) The Benesi-Hildebrand method must be used for data processing, the parameters being obtained from the tangent to the appropriate curve when $x_s = o$;

(iii) Eqn. (4.8) should be modified to account for the variation of the shift of free species with the composition of the mixture and if using the mole fraction scale the normal equilibrium expression must be modified to account for the effect of the size of the inert solvent (S). This effect is a statistical one, i.e. depends on the chance the

solute has of interacting with either an active or inactive solvent molecule. This effect can be accounted for by converting the actual number of moles of the inert solvent into appropriate number of moles of the aromatic solvent which have been replaced. It is accomplished by replacing n_s, the number of moles of the inert solvent, with $n_s \frac{V_s}{V_B}$ where V_s and V_B are the molar volumes of the inert solvent and the aromatic solvent respectively. Jackson[119] has found that making an allowance for the variation of δ_{free} with solvent composition had little effect on the values of parameters, therefore this correction will be neglected in the present investigation;

(iv) On the molar scale, the size-correction for S is not necessary since it is implicit in the scale.

The authors have found that Creswell and Allred method does not have any exact meaning when used over the whole concentration range but ΔH^o calculations by this method are still valid.

Jackson[119] has suggested that only a small portion, ca. 0.005 mole fraction of the total reaction mixture, should be considered as the actual solute and the remainder should be considered as diluent solvent and converted into equivalent moles of the aromatic by multiplying it with the molar volume ratio $\frac{V_A}{V_B}$. This correction will be taken into account while processing data for the present investigation.

There has been yet another erroneous practice of obtaining Δ_c values by extrapolating Δ_{obs} values to $x_B = 1.0$, in a plot of Δ_{obs} against x_B for various samples. Actually $\Delta_c = \frac{K+1}{K} \cdot \Delta_{obs}(x_B = 1.0)$ and this will always be higher than Δ_{obs} unless K is equal to infinity which is unlikely.

It has been customary to discuss the results obtained after such investigations in terms of (a) the nature, (b) stoichiometry, (c) strength and (d) stereochemistry of the interaction. Each one of these points will now be examined in detail though the results discussed should be taken cautiously as many of them are based on fallacious data processing procedures which do not take account of the points mentioned earlier.

4.3 THE NATURE OF THE INTERACTION

Schneider[120], in 1962, observed benzene-induced solvent shifts for a number of polar solutes. He proposed that such aromatic solvent induced shifts could be explained by dipole-induced dipole interaction Corroborative evidence for the proposed type of interaction was forthcoming from the linear plots which were obtained for $\frac{\mu}{V}$ vs. Δ_c, where μ is the dipole-moment and V the molar volume of the solute. Similar linearity between molecular dipole-moments and solvent-induced shifts for methyl protons has been observed in some organometallic compounds of the type $(CH_3)_nSn_{4-n}X$ $(X = Cl, Br, I)$[121]. Abraham[59] has suggested that the bond is purely electrostatic in nature and has attributed the lack of stability to the weak ionic character of C-H bond. Some of the results reported in Chapters 5 and 6 of the present investigation also support the predominantly electrostatic nature of the interaction. Besides the dipole-induced dipole interaction the possibility of a charge-transfer must not be overlooked. However, absorption bands typical of charge transfer were absent in the U.V. spectra of the systems studied by Abraham and he inferred therefore, that charge-transfer was unimportant in the formation of these complexes. Further evidence against any major contribution from charge-

transfer is that the actual degree of electron-transfer appears to be small. Leto[122] and Frenkel[123] suggested that ^1H shifts should change by about 10 ppm for the transfer of every single electron charge, while actual Δ_c values, in most of the cases, hardly exceed 2 ppm. Ronayne et al [47] have found the interaction of amides and ketones with aromatic compounds to be very weak and hence argued against charge-transfer. Homer and Huck[70] have shown that where there can be modifications to the effective location of the aromatic -electrons on complex formation, this is an intramolecular rather than intermolecular process. Recently[124] it has been shown that, for the occurrence of an interaction, the solute need not necessarily possess a permanent dipole as long as it has highly polar bonds. Such 'local' bond-dipoles of the solute induce an electric moment in the polarisable aromatic molecules and complex formation takes place.

4.4 THE STOICHIOMETRY OF THE INTERACTION

It has been widely assumed that the stoichiometry of many aromatic-solute collision complexes is 1:1. Sometimes the conclusion is based on the observation that the solvent shifts at various concentrations of the aromatic solvent in an inert solvent are approximately proportional to the mole fraction of the aromatic solvent. Such linear plots could be fortutious, since if the plots were truely linear complex formation could not be occuring. But it is not unlikely that one may get a linear plot if some internal compensation is involved. However, the concept of 1:1 specific complex derives considerable support from freezing point depression experiments[125] on simple systems, notably chloroform-toluene and chloroform-mesitylene. From dilution studies, Baker and Davis[126]

have suggested that benzene associates with camphor in 1:1 stoichiometry. Klinck et al[127], from their variable temperature n.m.r. studies, have found that the heat of formation (ΔH^{o}) is independent of temperature which indicates the presence of a single 1:1 complex[128]. Had there been a mixture of different type of complexes each having a different value of ΔH^{o}, the plots of log K against $\frac{1}{T}$ would not have been linear, since the different equilibrium quotients will be affected by temperature to different extents. Apparently linear plots have also been obtained during the present investigation. Feeney[129], by a curve-fitting procedure, has tried to prove that the stoichiometry of the complex formed between benzene and some ketones is 1:1. But, once again, it must be pointed out that some of these results are based on fallacious data processing procedures and must be accepted with caution. Recently[130] the notion of a time-averaged cluster of solvent molecules rather than a specific 1:1 complex has been suggested. However, the authors have themselves admitted that the collisions taking place between the solute and solvent molecules are binary in nature but because of the very slow time scale of n.m.r. the interactions between aromatic solvents and camphor solutes will appear as time-averaged cluster. However, it is significant to note in this connection that it is the apparent position of the n.m.r. signal which is expected to be affected by the slow time-scale of n.m.r. technique and not the stoichiometry which is a characteristic of any reaction.

4.5 STRENGTH OF THE INTERACTION

It has been a usual practice to measure the strength of such complexes

in terms of the heat of formation (ΔH^{o}). In most of the cases, the values of ΔH^{o} obtained have been found to be of the order of a few Kjoules/ mole which indicates the weak nature of such interactions. Homer and Cooke[131], after thermodynamic considerations, have related the interaction energy to the equilibrium quotient for the complex formation. The authors are of the opinion that, since the interaction energies are found to vary with temperature via interaction distance which is temperature dependent, they must be directly compared with ΔG^{o} at any temperature and not with the temperature invariant ΔH^{o}.

4.6 THE GEOMETRY OF THE COMPLEX

In the earlier studies[120,132] of benzene-induced solvent shifts, it has been assumed that the solute and benzene solvent molecules prefer to have their molecular planes co-parallel. Sometimes it has been assumed[41] that because of interelectron repulsion the negative end of the solute dipole should be separated as much as possible from the electron rich benzene ring and that both molecules will be constrained to lie in parallel planes, the electron attracting groups of the solute molecule anchored away from the six-fold symmetry axis of the aromatic molecule. But this assumption has been founded on a fallacious argument that because the aromatic molecules are twice as polarisable in the molecular carbon plane than normal to it, the interaction between the solute and the solvent will be greatest in the molecular plane. This argument ignores the angular dependence of the interaction via $(3 \cos^{2}\theta - 1)$ term which in fact favours an alignment along the six-fold axis. Moreover, in the earlier studies, values

of Δ_c, which formed basis for the proposed geometry, were obtained by extrapolating the measured chemical shifts to infinite dilution in aromatic solvent which is invalid (see sec.4.2). Under such circumstances, any conclusions regarding complex-geometry derived on the basis of such extrapolated results, could be misleading. In fact, as it is shown in Chapter 5 of the present investigation, such values may not even represent the correct relative order for different non-equivalent protons.

Homer et al [124] have shown that maximum interaction of a dipole with a non-polar aromatic molecule occurs when the dipole is perpendicular to the benzene ring. This model allows the solute dipolar axis not only to allign along the aromatic six-fold symmetry axis but also at a small angle to it, i.e. the solute molecules can be considered undergoing a wobbling motion about the aromatic symmetry axis. The envelope of the possible orientations is a small cone with a small semi-vertical angle. However, in the investigations referred to above only simple solutes containing a single proton or a group of equivalent protons have been considered. It is just possible that the considerations may not be tenable for unsymmetrical polar solutes containing more than one non-equivalent proton. In fact it was one of the objects behind the present investigation to examine whether the previous considerations are tenable for such solutes containing more than one non-equivalent proton. Moreover, the studies using solutes with more than one non-equivalen proton provide far more information from which to derive information about the complex-geometry than is forthcoming from the use of solutes containing single or a group of equivalent protons. As it is shown in Chapter 5 of this work, the

plane of vinyl bromide molecule is inclined with respect to the plane of benzene ring. Formation of such complexes with solute planes inclined to the benzene ring have been indicated earlier[133-6]. However, it must be pointed out that one is not justified in thinking in terms of universal geometry. As it is shown in the later chapters of the present investigation, the actual geometry of the complex, to a great extent, depends on the nature of the substituents in the solute as well as solvent molecules.

Attempts for deciding a geometry for the complex, by measuring aromatic solvent-induced shifts for more than one non-equivalent proton in the same solute molecule have been made earlier[120,132]. But the conclusions derived from these studies can not be relied upon as unsound methods were adopted for evaluating Δ_c values:

Williamset al,[41] after extensive study have shown that for rigid polar solutes like steroidal ketones, the chemical shift modifications are quite characteristic of the position of different protons in the solute molecule. An important generalisation the so called 'carbonyl plane rule' has been proposed by Williams and Bhacca[137] and independently by Connolly and McCrindle[138]. This rule states that in the specific case of an isolated carbonyl group, the benzene-induced solvent shift will be positive for protons lying behind a plane through the carbonyl carbon atom and perpendicular to the direction of the C = O bond. Protons lying in front of the plane will have a negative shift and those lying very near or in the reference plane will have a small or zero shift. This rule has found a wide application in structural determinations.

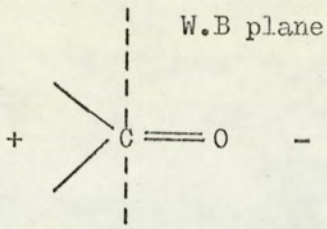

4.7 THE STERIC EFFECTS

To test the existance of a complex between a solute and an aromatic solvent, it has been proposed that the hindrance of this association by steric congestion of either member of the pair could lead to reduced solvent shifts. Hatton and Richards[132] found that the solvent-induced shifts for dimethylformamide in various methyl benzenes decreased as the number of methyl groups in the aromatic solvent species was increased. But, for reasons pointed out earlier (see sec.4.2) solvent-induced shift values obtained by these authors can not be treated as true Δ_c values and, therefore, any conclusions based on them also do not remain valid. Sandoval and Hanna[139] re-investigated the association of dimethylformamide with methyl benzenes and found that the equilibrium quotient (K) increased as the degree of methylation in the aromatic molecule increased while Δ_c had a reverse trend. They have tried to explain the reduction in the value of Δ_c by suggesting a reduction in the ring-current upon methyl substitution. Similar reduction in the values of Δ_c resulting from the methylation of benzene, has also been reported by other workers[136,140]. Such observations have qualitatively been explained by saying that the aromatic solvent molecule may not be able to approach the influenced protons due to steric hindrance. This steric hindrance explanation does not seem to represent the complete picture. Existance of other factors like differing extents of dipole-induced dipole interactions must also

be taken into account. Above all, the earlier results could be misleading as they were obtained by a thermodynamically invalid data evaluation procedure.

4.8 VARIABLE TEMPERATURE STUDIES OF MOLECULAR INTERACTIONS

If solvent-induced shifts are indicative of specific complex formation, one normally expects the equilibrium quotients, derived from solvent-induced shift measurements, to be temperature-dependent. If the activity coefficients of the interacting species are taken to be equal to unity or self-cancelling, the Gibbs Standard Free Energy Change ΔG^{o}_{T} is related to the equilibrium quotient (K) at temperature T by

$$\Delta G^{o}_{T} = - RT\ln K_{x} \qquad (4.10)$$

The equilibrium quotient is expressed in mole fraction units and the equation assumes negligible pressure dependence in the condensed phase. If the value for K_x is deduced using the refined B-H procedure and $x_s = 0$, eqn.(4.10) represents the free energy change when one mole of each of the reacting species combines to form one mole of the complex in a large excess of aromatic solvent. The temperature dependence of ΔG is given classically by the Gibbs-Helmholtz equation

$$\frac{\left[\partial(\Delta G/T)\right]}{\left[\partial(1/T)\right]_p} = \Delta H \qquad (4.11)$$

combining eqn. (4.11) with eqn. (4.10), one gets the following usual expression:

$$\frac{\partial \ln K_x}{\partial(1/T)} = - \frac{\Delta H^{o}}{R} \qquad (4.12)$$

Hence, if lnK is plotted against $\frac{1}{T}$, the slope of the line at any point is equal to $-\frac{\Delta H^{o}}{R}$. The value of ΔH^{o} thus obtained together with the corresponding values of ΔG^{o} obtained from eqn. (4.10) can then be used to obtain the standard entropy change ΔS^{o} for the reaction from the relationship

$$\Delta G^{o} = \Delta H^{o} - T\Delta S^{o} \qquad (4.13)$$

which refers to the reaction at constant temperature T.

Thus by making n.m.r. measurements at various temperatures and then by obtaining the values of the corresponding equilibrium constants, the thermodynamic parameters ΔG^{o}, ΔH^{o} and ΔS^{o} may be evaluated. Apart from the value of parameters in themselves, the constancy of ΔH^{o} with temperature provides helpful evidence[128] in establishing the presence of a single complex. In addition, the values of ΔG^{o} and ΔH^{o} can be used to investigate the nature of the interaction.

Laszlo and Williams [141] measured the shift of steroidel ketones in tolune solutions as a function of temperature. The value of shift obtained by extrapolation (long and of dubious significance) to T = 0^{o}K was considered to be equal to Δ_{c}. The authors have estimated the enthalpy changes and have found that the chemical shift measurements for the 1β - proton and 12α -proton in the 11- androstanone molecule yield the same value of ΔH^{o}, though they have dismissed the results as fortuitous. As it is seen from the results in Chapter 6 and 7 of the present investigation, measurement of solvent-induced shifts for more than one non-equivalent protons in the same solute molecule yield, within experimental error limits, identitical values of ΔH^{o}.

4.9 PROCEDURE ADOPTED TO DETERMINE COMPLEX-GEOMETRY

The results of Johnson and Bovey[142] are available[10] in the form of a comprehensive list of the calculated screenings at various points surrounding the benzene molecule. The co-ordinates of any point relative to the aromatic ring are defined with reference to two axes of which one, the p-axis, is in the plane of the ring and the other, the z-axis, is along the six-fold symmetry axis of benzene molecule. By determining the additional shielding of the hydrogen atoms of the solute due to complex formation, it is possible to fix their positions relative to the ring and consequently the geometry of the complex. However, in most of the cases there will be several different points which correspond to the same experimentally determined additional screening (Δ_c). The procedure adopted to locate the correct position of the solute hydrogen atom in the complex is to plot the appropriate screening contributions listed against p values for selected values of z. Using the experimentally determined values of Δ_c, it is possible to obtain co-ordinates of all points about the ring where the experimental and theoretical screenings are equivalent. A graph is then plotted of the p values against corresponding z values to obtain isoshielding diagrams for all the shifts. Conditions concerning the molecular geometry of the solute molecule and the complex are then applied to decide between the various alternatives.

However, it must be pointed out at this stage that such pictorial representations of the collision complex should be treated cautiously, since they depend on the chemical shift values given by the Johnson-Bovey calculations[142]. These calculations are based on the 'ring

current', which itself has been questioned[143,144], and hence the validity of the J-B approach. Perhaps the magnitude of Δ_c for the varicus complexes is not yet fully understood. Ring current might be playing a predominant role but other factors like charge-transfer and the anisotropy and electric screenings of groups in the solvent molecule may also contribute to Δ_c.

CHAPTER 5

AMBIENT TEMPERATURE STUDIES OF ACRYLONITRILE AND VINYL BROMIDE COMPLEXES WITH BENZENE AND SOME ALKYL SUBSTITUTED BENZENES

5.1 INTRODUCTION

As a result of n.m.r. studies of molecular interactions in solution, two parameters appertaining to the interactions are obtained, namely the equilibrium quotients (K) and the excess shielding (Δ_c) of the solute in the fully complexed state as compared to the free solute. As explained earlier (see sec.4.2) these interactions can be investigated by studying the dependence of the observed solute time-average chemical shift on sample composition. As the ratio of aromatic solvent to solute increases so the chemical shift of solute protons is shifted markedly often upfield, due to an increase in the quantity of the molecular complex formed. Since this shift variation is a direct function of the proportion of the solute complexed, it is possible, by measuring the variation in a series of samples, to obtain the equilibrium quotient for the interaction and also a limiting value for the chemical shift (Δ_c) (see sec.4.2). The information available from the studies using a solute containing a single proton or a group of identitical protons is very limited and inadequate specially in defining the geometry and the stereospecificity of the complex. By measuring the aromatic solvent - induced shifts for a number of non-equivalent protons in the same solute molecule much more information about the different aspects of such complexes should be forthcoming. The work reported herein is directed to this end. Systems composed of vinyl solutes (A) in aromatic hydrocarbons (B) with cyclohexane (S) as inert solvent and internal reference have been studied. The vinyl compounds used as solutes are acrylonitirle and vinyl bromide. A third vinyl solute, vinyl methyl ketone, which contains a labile group, $-COCH_3$, which can adopt different orientations with respect to the rest of the molecule due to rotation about the C-C

bond, and has got a different electronic distribution due to the presence of a carbonyl group, has been dealt with separately in Chapter 7. To avoid any complications due to permanent dipoles, only non-polar aromatic solvents namely benzene, p-xylene, mesitylene, p-diethylbenzene, 1,3,5 - triethylbenzene, p-diisopropylbenzene and 1,3,5 - triisopropylbenzene have been used. These substances were chosen to change the polarisability of the aromatics and steric hindrance of approach to six-fold axis so that the extent of dipole-induced dipole interaction and steric hindrance, the two important type of possible interactions in such systems, could be studied.

5.2 EXPERIMENTAL

The benzene and cyclohexane used were spectrosol grade. Acrylonitrile (Koch-Light pure), vinyl bromide (BDH), mesitylene (BDH), p-diethylbenzene (Aldrich), 1,3,5 - triethylbenzene (Ralph N.Emanuel), p-diisopropylbenzene (Ralph N. Emanuel) and 1,3,5 - triisopropylbenzene (Pfaltz-Bauer) were of the best commercially available quality and were used without further purification. The n.m.r. spectra did not reveal any impurity in the various chemicals used.

The different solute-aromatic solvent systems studied for the present invesitgation were acrylonitrile-benzene, acrylonitirle-p-xylene, acrylonitrile-mesitylene, acrylonitirle-p-diethylbenzene, acrylonitrile-1,3,5-triethylbenzene acrylonitrile-p-diisopropylbenzene, acrylonitrile-1,3,5-triisopropylbenzene, vinylbromide-benzene and vinylbromide - p - xylene.

Some of the ^{1}H spectra were obtained at 60.004 MHz and 306.6^{o}K using a Perkin-Elmer R10 spectrometer. Chemical shifts were measured relative to the internal reference solvent cyclohexane using the conventional sideband technique. The modulation signals were derived from a Muirhead-Wigan-D-890A oscillator and their frequencies measured using a Venner 3336 counter. Each shift was measured six times to minimise random errors and the average taken. When a Varian HA-100D spectrometer became available, spectra for the systems acrylonitrile-mesitylene, acrylonitrile, p-diethylbenzene, acrylonitrile-1,3,5-triethylbenzene, acrylonitrile-p-diisopropylbenzene and acrylonitrile-1,3,5-triisopropylbenzene were recorded on this instrument operating at 100 MHz and 304.2$\pm$ 1^{o}K, the shift frequencies then being measured by an electronic counter (period function) provided with the spectrometer. Small ambient temperature variations on the HA-100D or the temperature difference between the two instruments used will not affect the conclusions significantly, since Δ_c values have been found to be constant, within experimental error limits, over a wide range of temperature (see table 6.8). Small variations in equilibrium quotient values (table 6.8) for a variation of about 2^{o}K in the ambient temperature will also not affect the comparison of results. The chemical shift measurements can be considered accurate to $\pm$ 0.25 Hz on the Perkin-Elmer R10 and $\pm$ 0.1Hz on the Varian HA-100D spectrometer.

The mole fraction of the vinyl compounds was kept low and constant at about 0.04 for the 60.004 MHz instrument and 0.015 for the 100MHz instrument in order to minimise the self-association, the different values being associated with the sensitivity of the instruments. The values indicated represent the lowest concentration at which most of

the lines in the ABC spectrum required for analysis could be measured accurately. The concentrations of the aromatic solvent and cyclohexane were chosen to cover the high mole fraction of the aromatic solvent. The appropriate compositions of the different samples of various solute-aromatic solvent systems are recorded in tables 5.1 to 5.9. For some of the systems, measurements were carried out over the whole range of aromatic mole fraction and the respective sample compositions and Δ_{obs} values have been included in the appropriate tables for future reference.

Spectra were analysed with the aid of the computer program LAOCOON 3, root mean square errors at the convergence and the possible errors in the parameter sets being usually less than 0.05. Some spectra were also analysed by the method employed by Cavanaugh[107].

K_x and Δ_c values were obtained by processing the data on a ICL1905 computer using the program BHCURVEFIT, the gradient and intercept corresponding to equation

$$\frac{1}{\Delta_{obs}} = \frac{1}{K_x \Delta_c x_B} + \frac{1}{\Delta_c} \qquad (4.8)$$

being taken at aromatic mole fraction $x_B = 1.0$. The values of the corrected aromatic mole fraction and the corresponding values of observed solvent-induced shift (Δ_{obs}) for different samples, employed as computer input data are recorded in tables 5.10 to 5.18. In view of the relatively high concentration of solute, the mole fraction of the aromatic solvent was calculated by considering a portion of the solute as inert diluting solvent and making necessary bulk corrections to the actual number of moles of the solute (A) and the inert solvent (S), using the equation:

TABLE 5.1*

Sample composition for the acrylonitrile-benzene-cyclohexane system

Sample	Moles of solute/10^{-3}	Moles of benzene/10^{-2}	Moles of cyclohexane/10^{-3}
A	1.9393	0.0910	45.9708
B	1.8884	0.2458	45.4040
C	1.8865	0.3001	44.0768
D	2.0184	0.4085	43.5646
E	2.1409	0.5537	42.5819
F	2.2955	0.9720	37.5261
G	1.8865	1.4780	33.0240
H	2.2691	2.0117	27.7234
I	2.1051	2.4462	23.6442
J	2.0354	3.0254	18.3460
K	2.0071	3.4204	15.1782
L	1.9224	3.6417	11.8595
M	2.1862	3.8851	8.7725
N	1.9449	4.0724	6.3593
O	2.0561	4.2657	5.8864
P	2.0392	4.3986	3.7238
Q	1.9770	4.4150	2.3051
R	1.9223	4.7106	0.4895

* In this table as well as in some of the subsequent tables, data reported below the dotted line only have been used for the evaluation of K_x and Δ_c.

TABLE 5.2

Sample composition for the acrylonitirle-p-xylene-cyclohexane system.

Sample	Moles of solute / 10^{-3}	Moles of p-xylene/ 10^{-2}	Moles of cyclohexane/10^{-3}
A	1.8771	0.1132	46.9475
B	1.8922	0.2104	45.9339
C	1.8903	0.2998	44.8634
D	2.0618	0.4032	43.7025
E	1.9223	0.5152	42.6949
F	2.1089	1.011	38.0002
G	1.9600	1.4865	32.7852
H	1.9431	1.9852	27.9800
I	2.0203	2.4793	22.8125
J	1.8771	3.0213	18.2177
K	2.0580	3.5009	12.9824
L	2.0919	3.7547	10.6820
M	1.9506	4.0417	8.0181
H	2.1617	4.1463	6.4689
O	1.9544	4.3683	5.0677
P	2.0260	4.4532	3.9520
Q	1.9827	4.4979	2.9587
R	1.9902	4.6001	1.9879
S	1.8865	4.7273	0.5181

TABLE 5.3

Sample composition for the acrylonitirle-mesitylene-cyclohexane system

Sample	Moles of solute $/10^{-3}$	Moles of mesitylene$/10^{-2}$	Moles of cyclohexane$/10^{-3}$
A	1.1572	3.5044	13.5848
B	1.1440	3.7571	10.9256
C	1.2326	3.9946	9.4986
D	1.2156	4.2749	6.5482
E	1.2062	4.4958	4.2087
F	1.2081	4.6914	2.0402
G	1.2420	4.7634	1.5447
H	1.2778	4.7958	0.9351
I	1.2269	4.9803	0.5858

TABLE 5.4

Sample composition for the acrylonitrile-p-diethylbenzene-cyclohexane system

Sample	Moles of solute$/10^{-4}$	Moles of aromatic$/10^{-3}$	Moles of cyclohexane$/10^{-4}$
A	1.2627	6.9915	8.8284
B	1.2627	7.2933	6.5114
C	1.3381	7.3998	4.5984
D	1.3193	7.5026	3.8023
E	1.2627	7.6837	2.8634
F	1.3004	7.7120	2.0130
G	1.0743	7.8081	1.0575

TABLE 5.5

Sample composition for the acrylonitirle-1,3,5-triethylbenzene-cyclohexane system

Sample	Moles of solute/10^{-4}	Moles of aromatic/10^{-2}	Moles of cyclohexane/10^{-4}
A	2.5066	1.1435	32.3075
B	2.5631	1.1978	27.1269
C	2.6008	1.2599	21.6017
D	2.5443	1.3207	15.3517
E	2.5820	1.3492	13.7357
F	2.5820	1.3833	8.6264
G	2.5443	1.4081	6.0124
H	2.7139	1.4491	2.4240
I	2.5820	1.4713	0.8912

TABLE 5.6

Sample composition for the acrylonitrile-p-diisopropylbenzene-cyclohexane system

Sample	Moles of solute/10^{-4}	Moles of aromatic/10^{-2}	Moles of cyclohexane/10^{-3}
A	8.1983	3.7489	11.4294
B	7.6329	4.0090	8.9568
C	7.8025	4.2575	6.4092
D	7.2748	4.3880	4.8907
E	7.5952	4.5124	4.0435
F	7.9533	4.7055	1.9451
G	7.6894	4.7529	1.3890
H	8.4432	4.5000	0.5525

TABLE 5.7

Sample composition for the acrylonitrile-1,3,5-triisopropyl-benzene-cyclohexane system

Sample	Moles of solute/10^{-4}	Moles of aromatic/10^{-2}	Moles of cyclohexane/10^{-4}
A	4.7305	1.8757	57.3075
B	4.8624	1.9929	45.8294
C	4.6174	2.1171	32.4857
D	4.8247	2.1911	24.6197
E	4.7493	2.2416	19.7837
F	4.6740	2.2901	15.4705
G	4.8436	2.3550	9.8146
H	4.6928	2.3790	6.8203
I	4.8247	2.4081	5.0380
J	4.7117	2.4207	2.0675

TABLE 5.8

Sample composition for the vinyl bromide-benzene-cyclohexane system.

Sample	Moles of solute/10^{-3}	Moles of aromatic/10^{-2}	Moles of cyclohexane/10^{-3}
A	2.3719	0.1133	46.9558
B	2.1288	0.2112	46.0385
C	2.0681	0.3041	45.0083
D	2.3822	0.4030	44.0280
E	2.0840	0.5020	43.2664
F	1.9260	1.0130	37.9848
G	1.9493	1.4934	33.0525
H	2.0531	2.0069	27.9610
I	1.9241	2.4915	23.3781
J	2.0475	3.0326	18.0169
K	1.9325	3.5140	13.6514
L	1.8895	4.007	8.0204
M	2.0671	4.2476	5.9696
N	2.0138	4.3956	4.0934
O	1.7679	4.4159	2.9538
P	1.8061	4.7575	0.4836

TABLE 5.9

Sample composition for the vinyl bromide-p-xylene-cyclohexane system

Sample	Moles of solute/10^{-3}	Moles of aromatic/10^{-2}	Moles of cyclohexane/10^{-3}
A	1.9605	0.0957	46.6160
B	2.0680	0.2009	45.9636
C	2.1578	0.2987	44.9263
D	2.0091	0.4045	43.7607
E	2.0792	0.5042	42.6200
F	1.9876	1.0124	37.6877
G	2.3298	1.5073	32.9884
H	1.9483	2.0252	27.7293
I	2.0016	2.4615	23.7702
J	1.9596	2.9520	18.2010
K	2.0709	3.4919	13.0169
L	1.8801	3.7284	10.7462
M	1.9811	3.9744	8.1904
N	2.0325	4.1478	6.4912
O	1.9409	4.3094	4.8788
P	1.9493	4.4346	3.4066
Q	1.9465	4.5864	2.0936
R	1.8652	4.7276	0.4967

TABLE 5.10

Aromatic solvent mole fraction (x_B) and Δ_{obs} values at 60.004MHz and 306.6°K for various samples in acrylonitirle-benzene-cyclohexane system.

Sample	Mole fraction (x_B)	Δ_{obs}(Hz)		
		H_1	H_2	H_3
A	-	1.74	1.90	1.61
B	-	4.42	4.71	4.21
C	-	5.67	5.47	4.82
D	-	7.10	7.32	6.62
E	-	9.31	9.73	8.38
F	-	15.52	15.96	13.60
G	-	22.79	23.22	19.45
H	-	27.81	28.57	23.76
I	-	32.26	33.59	27.55
J	-	37.15	38.57	31.68
K	0.6345	39.97	41.90	34.59
L	0.6991	41.79	43.92	35.90
M	0.7624	43.81	46.11	37.30
N	0.7988	44.72	47.34	38.05
O	0.8338	45.49	48.13	38.54
P	0.8824	46.31	49.39	39.47
Q	0.9152	47.27	50.60	40.13
R	0.9624	48.51	51.61	41.00

TABLE 5.11

Aromatic mole fraction (x_B) and Δ_{obs} values at 60.004MHz and 306.6°K for various samples in the acrylonitrile-p-Xylene-cyclohexane system.

Sample	Molefraction (x_B)	Δ_{obs}(Hz)		
		H_1	H_2	H_3
A	-	2.57	2.37	1.99
B	-	4.50	4.36	3.73
C	-	6.36	6.06	5.27
D	-	8.00	7.62	6.82
E	-	10.15	9.68	8.61
F	-	17.21	16.51	14.61
G	-	23.21	22.27	19.48
H	-	28.44	27.31	23.81
I	-	32.53	31.38	27.25
J	-	36.28	35.16	30.54
K	0.7387	38.89	37.88	32.76
L	0.7834	40.30	39.27	33.82
M	0.8354	41.84	40.85	35.06
N	0.8607	42.43	41.44	35.62
O	0.8905	43.32	42.48	36.41
P	0.9096	43.75	42.79	36.76
Q	0.9272	44.27	43.52	37.13
R	0.9449	44.64	43.78	37.52
S	0.9725	45.36	44.62	38.01

TABLE 5.12

Aromatic mole fraction (x_B) and Δ_{obs} values at 100MHz and 305.0°K for various samples in the acrylonitirle-mesitylene-cyclohexane system.

Sample	Mole fraction (x_B)	Δ_{obs} (Hz)		
		H_1	H_2	H_3
A	0.7605	67.04	61.85	55.29
B	0.8075	69.11	63.95	57.00
C	0.8353	70.15	64.97	57.93
D	0.8847	72.32	67.27	59.73
E	0.9232	73.99	68.83	61.15
F	0.9582	75.50	70.53	62.58
G	0.9659	75.75	70.68	62.73
H	0.9752	76.09	71.01	62.96
I	0.9819	76.54	71.45	63.40

TABLE 5.13

Aromatic mole fraction (x_B) and Δ_{obs} values at 100MHz and 303.3°K for various samples in the acrylonitrile-p-diethylbenzene - cyclohexane system.

Sample	Mole fraction (x_B)	Δ_{obs} (Hz)		
		H_1	H_2	H_3
A	0.9148	72.80	68.77	59.68
B	0.9371	73.60	69.51	60.32
C	0.9536	74.29	70.24	60.91
D	0.9611	74.50	70.42	61.03
E	0.9702	74.94	70.85	61.33
F	0.9774	74.91	70.82	61.33
G	0.9871	75.36	71.29	61.79

TABLE 5.14

Aromatic mole fraction (x_B) and Δ_{obs} values at 100MHz and 303.9°K for various samples in the acrylonitrile-1,3,5-triethylbenzene-cyclohexane system.

Sample	Mole fraction (x_B)	Δ_{obs}(Hz)		
		H_1	H_2	H_3
A	0.8564	66.85	59.59	53.86
B	0.8808	67.91	60.62	54.83
C	0.9061	69.04	61.65	55.76
D	0.9328	70.05	62.55	56.58
E	0.9406	70.66	63.11	57.09
F	0.9611	71.34	63.66	57.40
G	0.9718	71.83	64.11	58.02
H	0.9859	72.29	64.44	58.33
I	0.9922	72.54	64.71	58.61

TABLE 5.15

Aromatic mole fraction (x_B) and Δ_{obs} values at 100MHz and 304.2°K for various samples in the acrylonitirle-p-diisopropylbenzene - cyclohexane system.

Sample	Mole fraction (x_B)	Δ_{obs}(Hz)		
		H_1	H_2	H_3
A	0.8475	63.65	58.68	51.50
B	0.8831	65.29	60.24	52.95
C	0.9170	67.09	61.93	54.50
D	0.9366	67.86	62.63	55.09
E	0.9476	68.35	63.13	55.51
F	0.9730	69.18	63.86	56.06
G	0.9799	69.98	64.66	56.92

TABLE 5.16

Aromatic mole fraction (x_B) and Δ_{obs} values at 100MHz and 304.1°K for various samples in the acrylonitrile-1,3,5-triisopropylbenzene - cyclohexane system

Sample	Mole fraction (x_B)	Δ_{obs} (Hz)		
		H_1	H_2	H_3
A	0.8747	65.72	54.83	51.08
C	0.9313	68.78	57.15	53.70
D	0.9476	69.25	57.47	54.02
F	0.9665	70.02	58.10	54.72
G	0.9775	70.28	58.20	54.95
H	0.9833	70.50	58.36	55.11

TABLE 5.17

Aromatic mole fraction (x_B) and Δ_{obs} values at 60.004MHz and 306.6°K for various samples in the vinyl bromide-benzene-cyclohexane system.

Sample	Mole fraction (x_B)	Δ_{obs} (Hz)		
		H_1	H_2	H_3
A	-	0.89	0.60	0.38
C	-	2.07	2.31	1.38
F	-	6.62	7.16	4.48
G	-	9.45	10.20	6.22
H	-	11.65	13.22	7.87
I	-	14.25	15.85	9.14
K	0.6614	18.32	20.56	11.47
L	0.7827	20.24	22.90	12.40
M	0.8291	20.88	23.72	12.83
N	0.8724	21.39	24.50	13.07
O	0.9142	21.87	25.01	13.23
P	0.9623	22.39	25.72	13.48

TABLE 5.18

Aromatic mole fraction (x_B) and Δ_{obs} values at 60.004 MHz and 306.6°K for various samples in the vinyl bromide-p-xylene-cyclohexene system.

Sample	Mole fraction (x_B)	Δ_{obs} (Hz)		
		H_1	H_2	H_3
A	-	0.94	1.05	0.63
B	-	1.75	1.80	1.23
C	-	2.50	2.62	1.67
D	-	3.31	3.47	2.27
E	-	4.22	4.23	2.74
F	-	7.54	7.49	4.85
G	-	10.32	10.21	6.74
H	-	12.84	12.40	8.46
I	-	14.73	14.42	9.40
J	-	16.74	16.50	10.66
K	0.7360	18.37	18.11	11.85
L	0.7817	19.24	18.87	12.22
M	0.8284	19.96	19.69	12.66
N	0.8597	20.47	20.19	12.84
O	0.8906	20.90	20.71	13.17
P	0.9172	21.33	21.06	13.40
Q	0.9415	21.79	21.58	13.68
R	0.9713	22.18	22.00	13.81

$$x_B = \frac{n_B}{\left[n_A-(n_A + n_B + n_S) \times 0.005\right]\frac{V_A}{V_B} + n_B + n_S \frac{V_S}{V_B}} \qquad (5.1)$$

where n_A, n_B and n_S are, respectively, the number of moles of the solute (A), aromatic solvent (B) and the inert solvent (S) initially taken, and V_A, V_B and V_S are the corresponding molar volumes at the appropriate temperature. The rest of the solute, (0.005 mole fraction) considered to be involved in the complex formation was neglected while calculating the mole fraction (x_B) of the aromatic solvent, since this assumption is implicit in the B -- H theory itself. The densities of the various species forming the basis of bulk corrections are recorded in table 5.19. The densities at the required temperatures were obtained from linear plots of the data given in the literature[145-9]. In the case of 1,3,5-triethylbenzene and 1,3,5-triisopropylbenzene, where no reliable density data at different temperatures are available. values corrected for 293.2°K were used. In view of the small amount of correction, it is not expected to affect the results significantly.

TABLE 5.19 - Densities of various substances at different temperatures

	Density/$(10^{-3}Kgm^{-3})$		
	293.2°K	298.2°K	303.2°K
Cyclohexane[145]	0.77855	0.77389	0.76922
Benzene[145]	0.87901	0.87370	0.86837
p-Xylene[145]	0.86105	0.86669	0.85233
Mesitylene[145]	0.86518	0.86111	0.85704
p-Diethylbenzene[145]	0.86196	0.85794	0.85390
1,3,5-Triethylbenzene[146]	0.8621	-	-
p-Diisopropylbenzene[145]	0.85676	0.85290	0.84903
1,3,5 - Triisopropylbenzene[147]	0.8545	-	-
Acrylonitrile[148]	0.8060	0.8004	-
Vinyl bromide[149,a]	1.4933	1.4738	1.4542

a. For the liquid at saturation pressure.

5.3 RESULTS AND DISCUSSIONS

The values of K_x and Δ_c obtained after processing the data are recorded in table 5.20. A perusal of the table brings forward some interesting regularities which will be discussed in turn.

5.3.a Equilibrium Quotient Values

In a compact and monofunctional molecule like acrylonitrile or vinyl bromide it is rather unlikely that independent interactions could be taking place at the three protons. The effect of complexation of the three sites is expected to proceed in phase and therefore, in different samples of the same series, the percentage complexation should be identitical for all the sites. This can be elucidated by the following calculation:

TABLE 5.20

The values of K_x and Δ_c for different protons in various solute-aromatic solvent systems

System	Proton	K_x	Δ_c(ppm)
Acrylonitrile-benzene	H_1	1.5214	1.355
	H_2	1.2553	1.572
	H_3	1.8740	1.059
Acrylonitrile-p-xylene	H_1	0.996	1.533
	H_2	0.8088	1.687
	H_3	0.9718	1.305
Acrylonitrile-mesitylene	H_1	0.8187	1.708
	H_2	0.6791	1.779
	H_3	0.7188	1.525

CONT.

Table 5.20 (cont.)

System	Proton	K_x	Δ_c(ppm)
Acrylonitrile-p-diethylbenzene	H_1	1.2657	1.357
	H_2	1.1745	1.328
	H_3	1.3212	1.091
Acrylonitrile-1,3,5,-triethylbenzene	H_1	0.8538	1.583
	H_2	0.8539	1.412
	H_3	0.8345	1.294
Acrylonitrile-p-diisopropyl-benzene	H_1	0.6365	1.817
	H_2	0.6035	1.734
	H_3	0.5768	1.570
Acrylonitrile-1,3,5-triisopropylbenzene	H_1	2.3596	1.009
	H_2	3.3955	0.759
	H_3	2.1151	0.812
Vinyl bromide-benzene	H_1	1.5789	0.649
	H_2	1.0275	0.863
	H_3	2.2211	0.330
Vinyl bromide-p-xylene	H_1	0.5722	1.035
	H_2	0.4131	1.281
	H_3	0.6308	0.608

If Δ_{obs}^{1} and Δ_{obs}^{2} are the observed solvent-induced shifts for two different protons in the same solute, for a certain sample in the series, Δ_c^{1} and Δ_c^{2} are the corresponding solvent-induced shifts in the fully complexed states, n_A is the number of moles of the solute initially taken, and n_{AB} is the equilibrium number of moles of the complex formed, then from eqn. (4.3) , for the first proton

$$\Delta_{obs}^{1} = \frac{n_{AB}}{n_A} \cdot \Delta_c^{1} \qquad (5.2)$$

Similarly for the second proton

$$\Delta_{obs}^{2} = \frac{n_{AB}}{n_A} \cdot \Delta_c^{2} \qquad (5.3)$$

From equns. (5.2) and (5.3) one gets

$$\frac{\Delta_{obs}^{1}}{\Delta_{obs}^{2}} = \frac{\Delta_c^{1}}{\Delta_c^{2}} \qquad (5.4)$$

i.e. the ratio of observed solvent-induced shifts (Δ_{obs}) for different protons in the same solute will be equal to the ratio of the respective Δ_c values and should be a constant for the different samples in a series; a fact which is substantiated by the data reported in table 5.21. This in effect means that the equilibrium quotient values (K_x) obtained after processing the data for the three different protons should be indentical. As it is apparent from the data reported in table 5.20, in most of the systems studied, the K_x values for the three different protons are faily close to each other, within experimental error limits. This constancy of the ratio of Δ_{obs} values for different protons throughout the series and the similar values of equilibrium quotients for the different protons in the same solute-aromatic solvent system provide strong justification for assuming a 1:1 complex formation in the systems studied for the present investigation and hence for the treatment of data.

TABLE 5.21*

Ratio of Δ_{obs} values for the different proton-pairs in various samples of acrylonitrile-benzene-cyclohexane system.

Sample	Aromatic Molefraction	Δ_{obs} ratio		
		$H_1:H_2$	$H_1:H_3$	$H_2:H_3$
K	0.6345	0.954	1.156	1.211
L	0.6991	0.952	1.164	1.223
M	0.7624	0.950	1.175	1.236
N	0.7988	0.945	1.175	1.244
O	0.8338	0.945	1.180	1.249
P	0.8824	0.938	1.173	1.251
Q	0.9152	0.934	1.178	1.261
R	0.9624	0.940	1.183	1.259

* Based on the data reported in Table 5.10

It must be pointed out at this stage that when any comparison of equilibrium quotient (K_x) or Δ_c values for different aromatic solvents is made, it implies a comparison of values obtained for the same solute.

For all the protons in acrylonitrile, the highest values for K_x is obtained by using 1,3,5-triisopropyl benzene as the aromatic solvent. It seems to be due to the fact that in this case the increased polarisability and the introduction of bulkier side chains, which function as 'traps' in holding the solute molecule tightly, facilitate the formation of collision complex. This is further substantiated by the ΔS^o values reported in Chapter 6 of the present investigation. However, the dependence of K_x on the nature of the aromatic molecule is obviously

(see table 5.20) quite complicated.

Equilibrium quotient (K_x) value at a temperature T is related, by equation

$$-\Delta G^{o}_{T} = RT\ln K_x \qquad (4.10)$$

to the change in standard free energy and hence to the other thermodynamic parameters (ΔH^{o} and ΔS^{o}) of the system. Homer and Cooke[131] have shown that the interaction energy for such complex formations is related to these thermodynamic parameters. Since the thermodynamic parameters themselves have been studied at a later stage of the present investigation discussion of the equilibrium quotient values will be deferred until later. For the time being, the discussions will be based on the Δ_c values.

5.3.b. The Effect of the nature of the solute on Δ_c

A comparison of Δ_c values for the different portons in acrylonitrile and vinyl bromide solutes, induced by benzene or p-xylene (with little) steric hindrance) shows that the Δ_c value for a proton in acrylonitrile is much higher than the value for the same proton in vinyl bromide. In this connection it has to be noted that acrylonitrile has a fairly high value of dipole moment c a.3.89D[150] as compared to vinyl bromide c a.1.407D[151] . It seems that highly polar acrylonitrile is able to polarise the aromatic solvent molecule to a greater extent which results in a higher electrostatic attraction working on the solute molecule towards the benzene ring. Due to this increased electostatic attraction, the solute molecule, presumably, approaches the aromatic ring more closely and hence provides the higher value for

Δ_c with this solute.

5.3.c. The Effect of Alkyl Substitution in the Benzene Ring on Δ_c values, in General.

Homer and Cooke[131] have studied the relationship between the interaction energy of solute-aromatic solvent complex formation and the polarisability of the aromatic solvent. It is well known that the polarisability as well as the molar volume of the aromatic hydrocarbons increases as the bulk of the substituted alkyl group increases. In fact, there is almost a linear relationship between polarisability (along six-fold axis) and the molar volume (Fig.5.1). In view of this, it was thought worthwhile to plot Δ_c values for the different protons for various acrylonitrile-aromatic solvent systems against the molar volume of the latter (Fig.5.2). An examination of Fig (5.2) reveals the following regularities:

(i) As the number of methyl groups increases in going from benzene to mesitylene, the Δ_c values for all the three vinyl protons increase;

(ii) When ethyl groups are introduced as substituents in place of methyl groups, there is a sudden drop in the value of Δ_c. But once again 1,3,5-triethylbenzene induces a higher value of Δ_c than does p-diethylbenzene;

(iii) The Δ_c values obtained with 1,3,5-triisopropylbenzene are the lowest;

(iv) Since Δ_c for H_1, H_2 and H_3 are different, it suggests some stereospecificity of complex formation.

Any effect, such as electrostatic attraction between the solute and

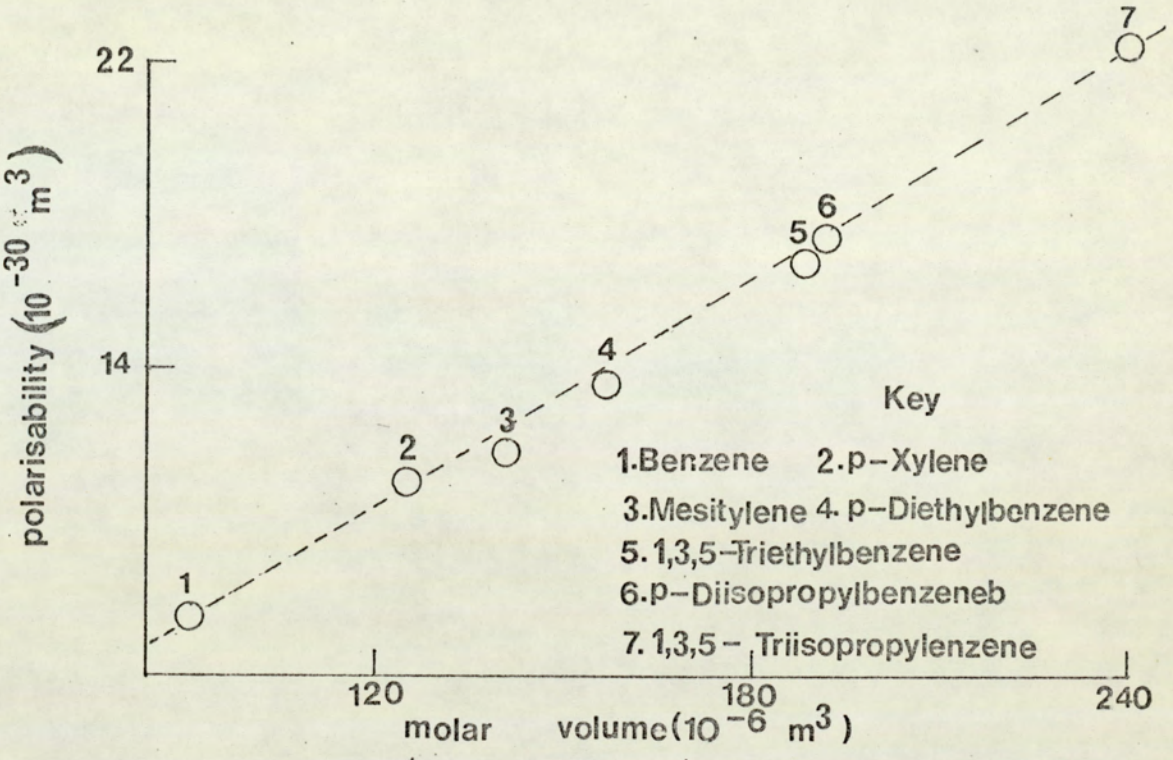

Fig. 5.1 The relationship between the polarisability and the molar volume of the aromatic solvents

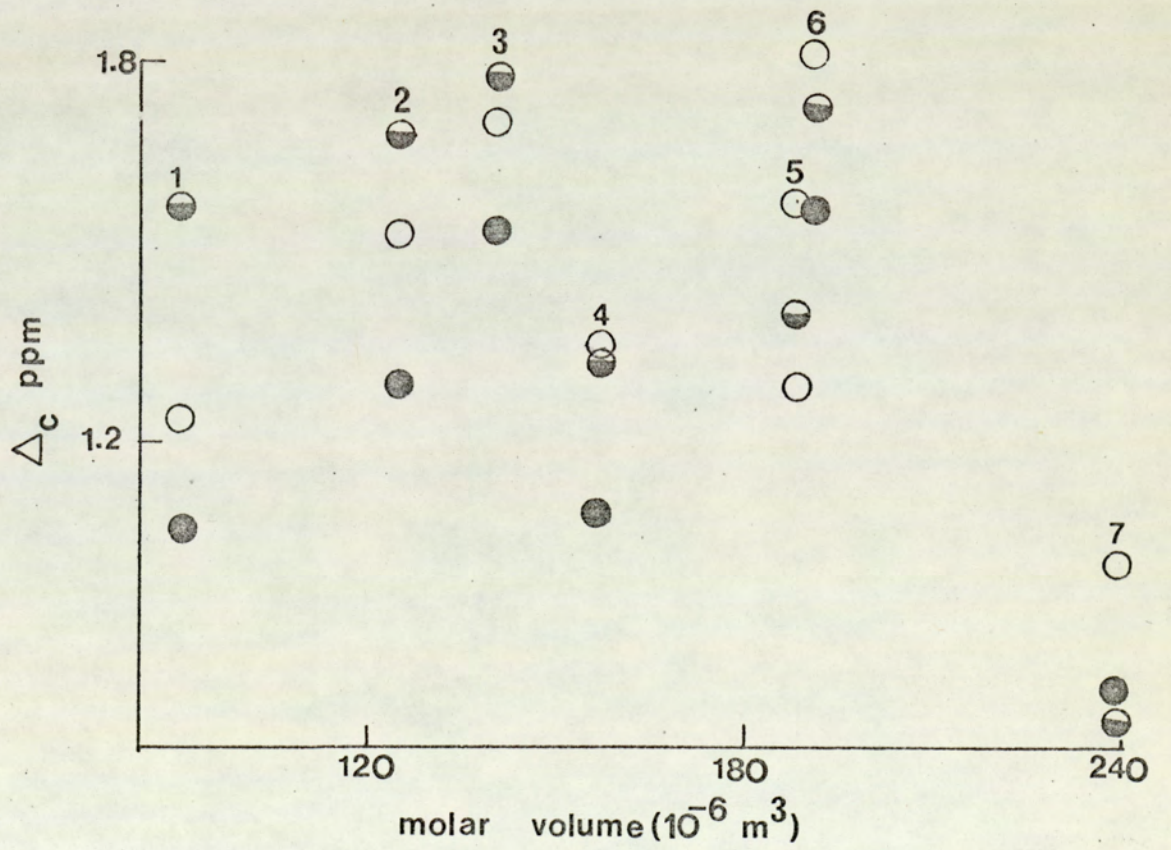

Fig. 5.2 The Variation of the Δ_c values for the protons H_1 ○, H_2 ◒ and H_3 ● in acrylonitrile with the molar volume of the aromatic solvents (numbered as in Fig.5.1)

aromatic solvent molecules due to dipole-induced interaction, which can make the solute molecule approach close to the benzene ring will enhance the value of Δ_c while steric hindrance due to bulky groups substituted in either the aromatic solvent or the polar solute will have a tendency to reduce Δ_c values. Actually, the two effects will compete with each other and the nett effect will be a sum total of the two. It would appear that both the effects, electrostatic attraction (due to increased polarisability) and the steric hindrance, will be enhanced by the substitution of alkyl groups in the benzene ring. However, the enhancement of the two effects may not be proportional. In fact, steric hindrance will, to a great extent, depend on factors like length of the alkyl chain, branching in the chain etc. This is substantiated by the variations in the Δ_c values noticed for different alkyl substituted benzenes.

A progressive rise in the value of Δ_c due to the increased methylation of the benzene molecule suggests that it is the increased dipole-induced dipole interaction (i.e. electrostatic attraction between the solute and the aromatic solvent molecules) due to increased polarisability of the aromatic solvent which is having an edge over steric hindrance in these cases. In fact, steric hindrance itself may not be very pronounced for methyl substituted benzenes due to the comparatively small bulk and length of the side chain and may not change significantly from one member to the next higher member in the series. However, when one goes from mesitylene to p-diethylbenzene, there is a sudden drop in the value of Δ_c which is quite anticipated in view of the pronounced steric hindrance due to increased length and the bulk of the side chain which is not compensated by a proportional rise in the polarisability. Once again, the next higher member in the

series, 1,3,5-triethylbenzene, shows a higher value of Δ_c which could be due to a significant rise in the polarisability of the aromatic solvent molecules and therefore a closer approach by the solute while steric hindrance does not change much. Higher values of Δ_c obtained with p-diisopropyl benzene as compared with p-diethylbenzene can also be explained on similar grounds. However, p-diisopropyl benzene induces Δ_c which is higher than that induced by 1,3,5-triethylbenzene (which has almost similar molar volume). In this connection it should be noted that 1,3,5-triethylbenzene has substituents at three positions, while p-diisopropyl has only two positions substituted which are fairly remote (1 and 4). Since in the formation of such stereospecific complexes Δ_c will depend on factors which affect the access of solute molecule to the aromatic solvent molecule, presumably, the far separated alkyl groups in p-diisopropyl benzene offer a better chance of such access and hence the higher values of Δ_c in this case. 1,3,5-triisopropyl benzene induces the lowest values of Δ_c for all the three protons which appears to be a bit exceptional. However, it could not be surprising in view of the maximum overcrowding of the benzene ring in this case. In the end it must be said that the phenomenon is highly specific and complicated and precise generalisations are rather difficult.

5.3.d. The Effect of Alkyl Substitution in the Benzene Ring on the Relative Values of Δ_c for the Three Protons

The order of Δ_c values for the three protons in acrylonitrile induced by various aromatic solvents is given in table 5.22.

TABLE 5.22

Order of Δ_c values for the different protons in acrylonitrile

Aromatic Solvent	Order for H_1, H_2 and H_3
Benzene	$H_2 > H_1 > H_3$
p-Xylene	$H_2 > H_1 > H_3$
Mesitylene	$H_2 > H_1 > H_3$
p-Diethylbenzene	$H_1 > H_2 > H_3$
1,3,5-Triethylbenzene	$H_1 > H_2 > H_3$
p-Diisopropylbenzene	$H_1 > H_2 > H_3$
1,3,5,-Triisopropylbenzene	$H_1 > H_3 > H_2$

It clearly emerges from the table 5.22 that it is proton H_2 which is most susceptible to the interactions taking place in the system. It is very likely that this extreme sensitivity of Δ_c values for H_2 could be due to its having a unique position, being farthest from the negative end of the solute dipole and closest to the aromatic ring.

It is interesting to note in this connection that for p-xylene and mesitylene Δ_{obs} values for the three protons are in the following order:

$$H_1 > H_2 > H_3$$

However, as the mole fraction of the aromatic solvent in the system, and hence the percentage complexation, increase, Δ_{obs} for H_2 tends to approach Δ_{obs} for H_1 and the corresponding Δ_c values, obtained after data processing, are in the reverse order (Fig 5.3)

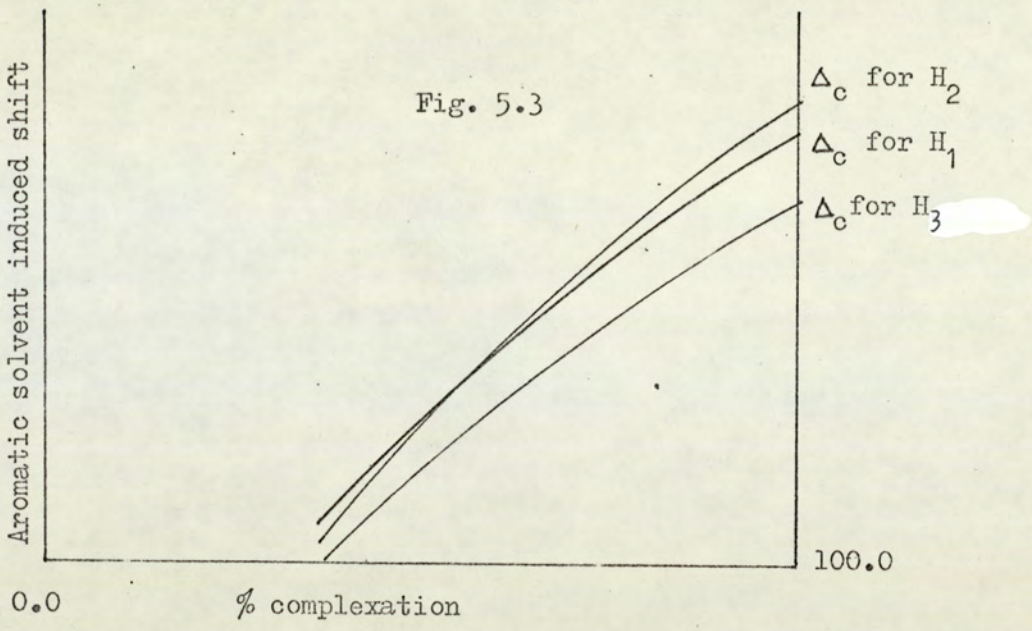

This observation is important in view of the fact that there has been a practice to use Δ_{obs} values obtained after extrapolation to $x_B = 1.0$ in place of Δ_c which could be misleading. The Δ_{obs} value for any proton will depend on two factors (eqn.4.3), the percentage complexation and the Δ_c value. Since it is rather unlikely that percentage complexation should be different for the different protons, presumably, Δ_c must vary from sample to sample in the same series but by a small amount which is not reflected in the Δ_{obs} ratios.

5.3.e. Geometry of the (Solute-Benzene) Complex

Since the shielding values corresponding to different points around alkyl substituted benzenes are not yet available, determination of complex-geometry involving these aromatic solvents will not be attempted and the attention will be confined to the consideration of a geometry involving benzene only. Theoretically, relationships[142] correlating the influence of the 'ring-current' of benzene at a point (p,z) in a cylindical co-ordinate system, based on the centre and six-fold axis of benzene molecule, and solvent-induced shift Δ_c, permit calculation of spacial relationships in a postulated 1:1 stereospecific

collision complex of solute and benzene. It has been said in earlier studies[120] that in such complexes, the solute molecule tends to adopt a preferred orientation over the benzene ring such that the planes of the two molecules are co-parallel. If the two molecules have their planes parallel and there are no bulky substitutents in either of them, all the three protons will be at a distance corresponding to van der Waals contact between the solute and benzene molecules and for this Z = 3.70Å for all of them. Using the experimentally determined Δ_c values induced by benzene the p-values for all the three protons in vinyl bromide and acrylonitrile corresponding to Z = 3.70 Å have been obtained from isoshielding diagrams (Fig 5.4 ,see sec.4.9) and are recorded in table 5.23. If these values are correct, there should be a point (lying on the six-fold symmetry axis) in the plane of the vinyl solute molecule which can satisfy all the three distances (ps) to the three protons in the solute molecule.

TABLE 5.23

Benzene-induced Δ_c values for the three protons in acrylonitrile and vinyl bromide and corresponding p-values for the co-parallel configuration (Z = 3.70Å = 2.662 ring radi.

Solute	Proton	Δ_c (ppm)	p(r.r.)
Acrylonitrile	H_1	1.355	not consistent at all
	H_2	1.572	not consistent at all
	H_3	1.059	not consistent at all
Vinyl bromide	H_1	0.649	1.115
	H_2	0.863	0.660
	H_3	0.330	1.800

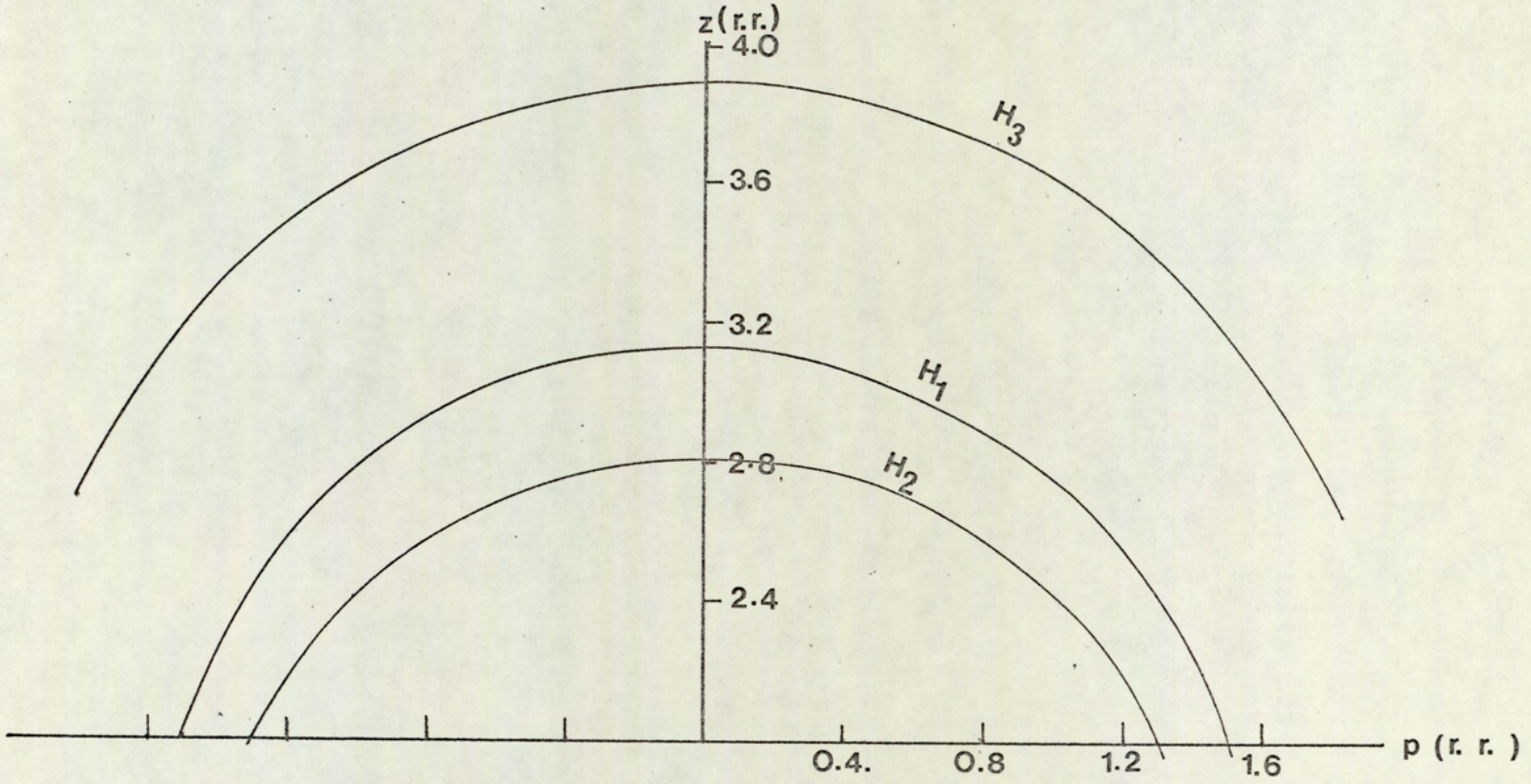

Fig. 5.4 Isoshielding diagrams corresponding to Δ_c values induced by benzene for the individual protons in vinyl bromide molecule.

A search for such a point was attempted by drawing the solute molecule to the scale on the basis of molecular parameters given in the table 5.24[152,153]. No such point seems to exist, showing that the co-parallel orientation of the solute and benzene molecules in the complex is not consistent with the geometry of the solute molecule and the experimentally determined values of Δ_c.

TABLE 5.24

Molecular parameters for acrylonitrile[152] and vinyl bromide[153] molecules

a. Bond-lengths (Å)

Compound	C–H	C = C	C – C	C ≡ N	C – Br
Acrylonitrile	1.086_3	1.338_9	1.425_6	1.163_7	–
Vinyl bromide	1.07	1.34	–		1.89

b. Bond-angles (radians)

Compound	$\angle CCH_2$ and $\angle CCH_3$	$\angle CCH_1$	$\angle CCX$(X = CN or Br)
Acrylonitrile	2.094	2.124	2.140
Vinyl bromide	2.094	2.094	2.124

As it has been pointed out elsewhere,[154] analytically five parameters are required in order to fix the stereochemistry of the complex; two are required to specify the centre of mass of the solute, in relation to that of benzene, and three to specify the orientation of the molecule about that point. In the present case, since the number of observable quantities (the three solvent induced shifts) is less than

the analytically required unknown parameters (5), a unique solution is not possible. More than one stereochemistry for vinyl bromide-benzene complex is consistent with the benzene-induced shifts (Δ_c) and the geometry of the solute molecule. As indicated earlier, the one geometry of the complex most likely to occur will have proton H_2 at a distance corresponding to van der Waals contact with the benzene ring and the electronegative Br atom projecting farthest and above the benzene ring so as to avoid the electrostatic repulsion from the ring electrons. Keeping this consideration in mind, an attempt has been made to determine a tentative geometry for the complex. Different possible sets of p and z values corresponding to the experimentally determined values of Δ_c for all the three protons in vinyl bromide have been extrapolated from the tables given elsewhere[10] and isoshielding diagrams (Fig.5.4) have been plotted (see sec.4.9). The values of p and z for the three protons in the most likely arrangement of the vinyl bromide and benzene molecules in the complex and consistent with the geometry of the solute molecule are given in table (5.2 5). It is difficult to represent the actual three-dimensional structure of the complex on paper. However, the arrangement has been illustrated (Fig.5.5) by presenting the front and side-views of the solute molecule in relation to the benzene ring.

TABLE 5.25

Co-ordinates (p,z) for the three protons in vinyl bromide solute for a postulated structure of vinyl bromide-benzene complex

Proton	p(r.r.)	z(r.r.)
H_1	0.870	2.854
H_2	1.200	2.194
H_3	1.462	3.240

As it has been said earlier (see sec.4.9) such pictorial representations of the collision complex should be treated cautiously since they depend on the chemical shift values given by Johnson-Bovey[142] calculations. The authors compiled the tables considering only the 'ring-current' of benzene molecule and as the idea of ring 'ring-current' has been questioned [143,144] so must the validity of the J-B approach itself. Values of Δ_c for H_1, H_2 and H_3 of acrylonitrile obtained with benzene and some other aromatic solvent are collectively (not individually) too high to assign a geometry to acrylonitirle-aromatic complex, based on 'ring-current' shielding values, that is consistent with the experimentally determined Δ_c values for the three protons and the molecular parameters of the solute molecule. Perhaps the magnitude of Δ_c for the various complexes is not yet fully understood. Whilst a ring-current might be playing a predominant role other factors like charge-transfer and the amisotropic and electrical screenings by groups in the solvent molecule may also contribute to Δ_c.

Nevertheless, in view of the different values of Δ_c for the three protons induced by an aromatic solvent, it seems that the solute and the aromatic solvent do tend to adopt preferred relative orientations in the complex. Since the relative magnitude of Δ_c for the three protons is found to depend on the nature of the substituents in the aromatic molecule, this preferred orientation also seems to differ from system to system. As it is shown in Chapter 7 of the present investigation, the relative magnitude of Δ_c for the three vinyl protons may depend on the nature of the substituent in the solute molecule as well (see table 7.11). All this leads one to think that such complex

formations are highly stereospecific in nature. They are stereo-specific in the sense that:

(i) for any solute-aromatic solvent pair, the solute tends to adopt a preferred time-average orientation;

(ii) the preferred orientation may itself vary from one aromatic solvent to the other;

(iii) it may also depend on the nature of the substituents in the solute molecule.

Under such circumstances perhaps one is not justified in thinking in terms of a universal geometry for all the systems. It is anticipated that some more information will be forthcoming from the consideration of thermodynamic parameters for complex formation and this will be discussed at a later stage (Chapter 6.)

CHAPTER 6

STUDIES OF MOLECULAR INTERACTIONS OF ACRYLONITRILE AND VINYL BROMIDE WITH BENZENE AND ALKYL SUBSTITUTED BENZENES AT VARIOUS TEMPERATURES

6.1 INTRODUCTION

If solvent-induced shifts are indicative of specific complex formation, one normally expects the equilibrium quotients, derived from solvent-induced shift measurements to be temperature-dependent. It is evident, therefore, that by performing the n.m.r. measurements at various temperatures, and thereby obtaining the values of corresponding equilibrium quotients, the thermodynamic properties ΔG^{o}, ΔH^{o} and ΔS^{o} may readily be deduced (see sec.4.8). Apart from the values of the latter in themselves, the constancy of ΔH^{o} with temperature provides helpful evidence[128] in establishing the presence of a single complex (or isomeric complexes) and the values of various thermodynamic parameters obtained throw light on the nature of the complex and the factors which affect its formation.

6.2 EXPERIMENTAL AND RESULTS

The samples (in the acrylonitrile-benzene, acrylonitrile-p-xylene, acrylonitrile-mesitylene, acrylonitrile-p-diethylbenzene, acrylonitrile-1,3,5-triethybenzene, acrylonitrile-p-diisopropylbenzene, acrylonitrile-1,3,5-triisopropylbenzene, vinyl bromide-benzene and vinyl bromide-p-xylene systems) used in the studies at various temperature were the same as used in ambient temperature studies. Measurements were carried out at four other temperatures (in addition to the ambient temperature) for all the systems except acrylonitrile-p-diethylbenzene and acrylonitrile-1,3,5-triethylbenzene for which measurements could be made at only one more temperature due to paucity of time. ^{1}H n.m.r. spectra were obtained using the Perkin-Elmer R10 spectrometer for the systems acrylonitrile-benzene,

acrylonitrile-p-xylene, vinyl bromide-benzene and vinyl bromide-p-xylene, and from the Varian HA - 100D for the systems acrylonitrile mesitylene, acrylonitrile-p-diethylbenzene, acrylonitrile-1,3,5-triethylbenzene, acrylonitrile-p-diisopropyl benzene and acrylonitrile-1,3,5 - triisopropylbenzene. At any pre-set temperature, the variation in temperature from sample to sample was less than $\pm$ 0.2°K for both the instruments.

Chemical shift measurements and the analyses of the spectra were done in a manner similar to that described earlier (see sec.5.2) and the results are reported in tables 6.1 - 6.9. Values of K_x and Δ_c were obtained by processing the data on a ICL 1905 computer using the program BHCURVEFIT, the gradient and the intercept being taken at $x_B = 1.0$, after making necessary corrections to the mole fraction of the aromatic solvent (see sec.4.2 and 5.2). The values of K_x and Δ_c obtained after processing the data are given in table 6.10. Values from table 5.20, obtained from ambient temperature studies, are also included in table 6.10 for comparision.

Values for the thermodynamic parameters, ΔH°, ΔG° and ΔS° were obtained after processing the equilibrium quotient values at different temperatures on a computer program PARATHERM and are recorded in talbe 6.11.

6.3 DISCUSSION

6.3.a. General

The values of Δ_c do not show any regular variation with temperature.

TABLE 6.1

Aromatic mole fraction (x_B) and Δ_{obs} values at 60.004MHz and different temperatures for the acrylonitrile-benzene-cyclohexane system.

Temperature (^oK)	Sample	x_B	Δ_{obs} (Hz)		
			H_1	H_2	H_3
292.9	D	-	8.18	8.24	6.97
	G	-	25.00	25.56	21.47
	I	-	35.07	36.26	30.05
	J	-	39.85	41.43	34.13
	K	0.6345	42.81	44.76	36.71
	L	0.6992	44.98	46.78	38.03
	M	0.7624	46.45	48.75	39.57
	N	0.7988	47.47	49.87	40.28
	O	0.8339	48.20	50.61	40.84
	P	0.8825	49.32	52.06	41.70
	Q	0.9152	50.13	52.75	42.34
	R	0.9625	51.31	54.06	42.93
320.1	D	-	6.84	6.92	5.75
	G	-	21.06	21.62	18.19
	I	-	30.30	31.57	26.11
	J	-	34.80	36.16	29.91
	K	0.6344	37.17	39.35	32.19
	L	0.6991	39.49	41.36	33.69
	M	0.7623	41.17	43.33	35.20
	N	0.7987	42.15	44.46	36.00
	O	0.8338	42.88	45.42	36.63
	P	0. 8824	44.18	46.56	37.36
	Q	0.9151	44.91	47.66	38.11
	R	0.9623	46.00	48.88	39.12

cont.....

TABLE 6.1 (cont.)

Temperature (^oK)	Sample	x_B	Δ_{obs} (Hz)		
			H_1	H_2	H_3
330.7	D	-	6.24	6.34	5.37
	G	-	19.80	21.47	17.07
	I	-	28.49	29.70	24.48
	J	-	32.94	34.52	28.21
	K	0.6344	35.70	37.52	30.43
	L	0.6991	37.54	39.39	31.99
	M	0.7623	39.15	41.32	33.41
	N	0.7987	40.22	42.36	34.16
	O	0.8337	40.89	43.31	34.80
	P	0.8823	41.99	44.56	35.70
	Q	0.9150	42.81	45.49	36.26
	R	0.9623	43.91	46.67	37.20
340.7	D	-	5.81	5.92	4.85
	G	-	18.54	19.07	15.99
	I	-	26.97	28.09	23.07
	J	-	31.18	32.88	26.88
	K	0.6344	33.84	35.76	29.05
	L	0.6990	35.64	37.68	30.52
	M	0.7622	37.33	39.69	31.93
	N	0.7986	38,28	40.70	32.66
	O	0.8337	38,86	41.52	33.39
	P	0.8823	40.26	42.65	34.26
	Q	0.9150	41.00	43.96	35.04
	R	0.9623	41.90	44.97	35.56

TABLE 6.2

Aromatic mole fraction (x_B) and Δ_{obs} values at 60.004MHz and various temperatures for the acrylonitrile-p-xylene-cyclohexane system.

Temperature (^oK)	Sample	x_B	Δ_{obs} (Hz)		
			H_1	H_2	H_3
294.2	E	-	11.20	10.59	9.30
	H	-	30.48	28.99	25.59
	K	0.7393	41.36	39.91	34.76
	L	0.7839	42.76	41.32	35.82
	M	0.8359	44.17	42.90	37.18
	N	0.8610	44.74	43.50	37.58
	O	0.8909	45.87	44.42	38.34
	P	0.9099	46.07	44.77	38.79
	Q	0.9274	46.65	45.34	39.09
	R	0.9451	47.02	45.81	39.50
	S	0.9727	47.80	46.67	40.07
321.6	E	-	8.93	8.80	7.91
	H	-	26.07	25.22	22.02
	K	0.7380	36.03	35.57	30.53
	L	0.7828	37.38	36.84	31.56
	M	0.8349	38.95	38.34	32.79
	N	0.8602	39.48	38.84	33.33
	O	0.8902	40.50	39.75	33.98
	P	0.9092	40.77	40.13	34.29
	Q	0.9269	41.30	40.65	34.69
	R	0.9447	41.70	41.22	35.11
	S	0.9724	42.37	41.81	35.66

CONT.

TABLE 6.2 (cont.)

Temperature (°K)	Sample	x_B	Δ_{obs} (Hz)		
			H_1	H_2	H_3
332.6	E	-	8.64	8.07	7.04
	H	-	24.47	23.34	20.42
	K	0.7375	34.27	33.25	28.70
	L	0.7823	35.58	34.66	29.75
	M	0.8345	37.01	36.08	30.97
	N	0.8598	37.52	36.66	31.38
	O	0.8899	38.39	37.73	32.22
	P	0.9090	38.70	37.98	32.45
	Q	0.9267	39.20	38.43	32.87
	R	0.9445	39.75	38.87	33.17
	S	0.9723	40.42	39.85	33.85
341.0	E	-	8.09	7.63	6.59
	H	-	23.14	22.42	19.44
	K	0.7370	32.60	31.92	27.44
	L	0.7819	33.86	33.23	28.40
	M	0.8342	35.35	34.81	29.69
	N	0.8596	35.89	35.16	30.10
	O	0.8896	36.78	36.20	30.83
	P	0.9088	37.10	36.49	31.15
	Q	0.9265	37.61	37.02	31.55
	R	0.9443	38.09	37.43	31.80
	S	0.9722	38.66	38.33	32.43

TABLE 6.3

Aromatic mole fraction (x_B) and Δ_{obs} values at 100.0MHz and various temperatures for the acrylonitrile-mesitylene-cyclohexane system.

Temperature (^oK)	Sample	x_B	Δ_{obs} (Hz)		
			H_1	H_2	H_3
286.9	A	0.7614	76.60	70.88	62.90
	B	0.8083	77.51	72.67	64.72
	C	0.8359	78.81	74.17	65.56
	D	0.8852	80.92	76.11	67.78
	E	0.9236	82.62	77.81	69.08
	F	0.9584	84.35	79.59	70.58
	G	0.9661	84.49	79.92	70.71
	H	0.9754	85.10	80.36	71.26
	I	0.9820	85.26	80.61	71.40
315,7	A	0.7600	63.02	58.48	52.05
	B	0.8071	65.22	60.67	53.72
	C	0.8348	66.06	61.56	54.68
	D	0.8844	68.17	63.56	56.50
	E	0.9230	69.85	65.26	57.85
	F	0.9580	71.38	66.80	59.19
	G	0.9658	71.71	67.11	59.45
	H	0.9751	71.95	67.38	59.68
	I	0.9818	72.32	67.78	60.00

CONT.

TABLE 6.3 (Cont.)

Temperature (^{o}K)	Sample	x_B	Δ_{obs} (Hz)		
			H_1	H_2	H_3
329.5	A	0.7593	59.31	55.25	49.01
	B	0.8065	61.42	57.43	50.88
	C	0.8343	62.63	58.64	51.98
	D	0.8840	64.66	60.66	53.63
	E	0.9227	66.41	62.40	55.09
	F	0.9579	67.78	63.90	56.39
	G	0.9656	68.14	64.18	56.72
	H	0.9750	68.53	64.62	57.05
	I	0.9817	68.82	64.91	57.27
339.2	A	0.7586	56.19	52.66	46.59
	B	0.8059	57.94	54.41	48.00
	C	0.8338	58.95	55.43	48.85
	D	0.8837	60.89	57.33	50.53
	E	0.9224	62.49	58.91	51.88
	F	0.9577	63.92	60.41	53.16
	G	0.9655	64.20	60.67	52.32
	H	0.9749	64.56	61.00	53.56
	I	0.9816	64.73	61.18	53.76

TABLE 6.4

Aromatic mole fraction (x_B) and Δ_{obs} values at 100.0MHz for the acrylonitrile-p-diethylbenzene-cyclohexane system.

Temperature (°K)	Sample	x_B	Δ_{obs} (Hz)		
			H_1	H_2	H_3
330.2	A	0.9141	62.66	60.08	51.59
	B	0.9366	63.53	60.95	52.22
	C	0.9532	64.03	61.51	52.71
	D	0.9608	64.51	61.92	53.09
	F	0.9772	65.02	62.48	53.52
	G	0.9870	65.29	62.71	53.69

TABLE 6.5

Aromatic mole fraction (x_B) and Δ_{obs} values at 100.0MHz for the acrylonitrile-1,3,5-triethylbenzene-cyclohexane system.

Temperature (°K)	Sample	x_B	Δ_{obs} (Hz)		
			H_1	H_2	H_3
330.3	B	0.8808	58.48	53.16	47.39
	C	0.9061	59.56	54.17	48.33
	D	0.9328	60.56	55.12	49.19
	E	0.9406	60.97	55.50	49.57
	F	0.9611	61.73	56.16	50.18
	G	0.9718	62.22	56.61	50.55

TABLE 6.6

Aromatic mole fraction (x_B) and Δ_{obs} values at 100.0MHz and various temperatures for the acrylonitrile -p-diisopropylbenzene-cyclohexane system.

Temperature (^oK)	Sample	x_B	Δ_{obs} (Hz)		
			H_1	H_2	H_3
292.8	B	0.8834	71.42	64.85	57.47
	C	0.9172	72.89	66.31	58.74
	D	0.9368	73.97	67.16	59.55
	E	0.9478	74.39	67.63	59.96
	F	0.9732	75.19	68.41	60.57
	G	0.9799	76.06	69.14	61.25
315.2	A	0.8470	59.36	55.19	48.26
	B	0.8827	60.87	56.62	49.52
	C	0.9167	62.45	58.10	50.82
	D	0.9364	63.39	59.02	51.56
	E	0.9474	63.81	59.51	52.11
	G	0.9798	65.07	60.58	52.94
325.1	A	0.8466	55.76	52.22	45.44
	B	0.8823	57.09	53.43	46.52
	C	0.9164	58.83	55.03	47.85
	D	0.9362	59.76	56.00	48.71
	E	0.9473	60.02	56.23	48.91
	G	0.9797	61.09	57.31	49.79
	H	0.9883	61.61	57.77	50.25

TABLE 6.6 (cont.)

Temperature (°K)	Sample	x_B	Δ_{obs} (Hz)		
			H_1	H_2	H_3
331.2	A	0.8463	53.69	50.56	43.80
	B	0.8821	55.38	52.04	45.16
	C	0.9163	56.81	53.45	46.37
	D	0.9361	57.77	54.27	47.05
	E	0.9472	58.22	54.76	47.49
	G	0.9797	59.36	55.76	48.38
	H	0.9882	59.81	56.31	48.88

TABLE 6 . 7

Aromatic mole fraction (x_B) and Δ_{obs} values at 100.0MHz and various temperatures for the acrylonitrile-1,3,5-triisopropylbenzene-cyclohexane system.

Temperature (°K)	Samples	x_B	Δ_{obs} (Hz)		
			H_1	H_2	H_3
293.7	A	0.8747	69,72	57.39	54.10
	B	0.9018	71.06	58.45	55.09
	C	0.9318	72.98	59.81	56.72
	D	0.9476	73.39	60.11	57.05
	F	0.9665	73.91	60.41	57.55
	G	0.9775	74.62	60.99	58.11
	H	0.9833	74.53	61.05	58.00
	I	0.9866	74.42	60.77	57.78

TABLE 6.7 (cont.)

Temperature (°K)	Sample	x_B	Δ_{obs} (Hz)		
			H_1	H_2	H_3
311.8	A	0.8747	61.87	52.06	48.25
	B	0.9018	63.33	53.23	49.40
	C	0.9313	64.67	54.34	50.58
	D	0.9476	65.04	54.56	60.86
	F	0.9665	65.76	55.10	51.46
	H	0.9833	66.30	55.58	51.98
322.0	A	0.8747	57.89	49.29	45.20
	B	0.9018	58.90	50.18	46.08
	C	0.9313	60.55	51.49	47.51
	D	0.9476	60.87	51.62	47.61
	F	0.9665	61.62	52.18	48.30
	G	0.9775	61.85	52.48	48.52
	H	0.9833	62.02	52.59	48.60
	J	0.9923	62.27	52.78	48.83
332.0	A	0.8747	53.75	46.29	42.11
	C	0.9313	56.40	48.46	44.28
	D	0.9476	56.62	48.62	44.41
	E	0.9577	57.04	48.93	44.83
	F	0.9665	57.66	49.40	45.24
	G	0.9833	58.12	49.78	45.65
	I	0.9866	57.95	49.63	45.50
	J	0.9923	58.20	49.86	45.79

TABLE 6.8

Aromatic mole fraction (x_B) and Δ_{obs} values at 60.0004MHz and different temperatures for the vinyl bromide-benzene-cyclohexane system.

Temperature (°K)	Sample	x_B	Δ_{obs}(Hz)		
			H_1	H_2	H_3
279.2	A	-	1.14	1.21	0.84
	C	-	2.80	2.80	1.99
	F	-	9.17	8.76	5.48
	G	-	11.37	12.34	7.51
	H	-	14.21	15.58	9.29
	I	-	16.88	18.61	10.89
	J	-	18.65	20.71	11.41
	L	0.7835	23.42	26.50	14.47
	M	0.8300	23.92	27.13	14.71
	N	0.8734	24.52	28.01	14.90
	O	0.9152	24.96	28,59	15.06
	P	0.9633	25.47	29.27	15.28
290.0	A	-	0.46	0.63	0.23
	C	-	2.32	2.55	1.81
	F	-	7.44	8.10	5.05
	G	-	9.83	10.93	6.25
	H	-	13.23	14.68	8.67
	I	-	15.64	17.40	10.14
	J	-	18.03	20.17	11.52
	K	0.6618	19.99	22.44	12.68
	L	0.7832	21.94	24.90	13.62
	M	0.8297	22.48	25.53	13.95
	N	0.8730	23.06	26.31	14.17
	O	0.9148	23.48	26.88	14.38
	P	0.9629	24.06	27.66	14.55

TABLE 6.8 (cont.)

Temperature (°K)	Sample	x_B	Δ_{obs} (Hz)		
			H_1	H_2	H_3
315.9	A	-	0.81	0.91	0.50
	C	-	2.15	2.19	1.47
	F	-	6.28	6.96	4.20
	G	-	9.04	9.89	6.03
	H	-	11.48	12.59	7.50
	I	-	13.68	15.11	8.80
	J	-	15.92	17.69	10.06
	K	0.6612	17.66	19.74	11.15
	L	0.7825	19.63	22.11	12.17
	M	0.8289	20.21	22.74	12.53
	O	0.9139	21.17	23.90	13.00
	P	0.9620	21.82	24.76	13.26
331.1	A	-	0.79	0.73	0.40
	C	-	1.71	1.94	1.26
	F	-	5.72	6.16	3.75
	G	-	8.07	8.94	5.18
	H	-	10.34	11.46	6.70
	I	-	12.46	13.81	8.02
	J	-	14.53	16.21	9.18
	K	0.6608	16.35	18.26	10.42
	L	0.7820	18.15	20.31	11.20
	M	0.8282	18.71	21.14	11.50
	N	0.8715	19.18	21.72	11.78
	O	0.9131	19.70	22.17	11.98
	P	0.9614	20.20	23.00	12.26

TABLE 6.9

Aromatic mole fraction (x_B) and Δ_{obs} values at 60.004MHz and various temperatures for the vinyl bromide-p-xylene-cyclohexane system.

Temperature (°K)	Sample	x_B	Δ_{obs}(Hz)		
			H_1	H_2	H_3
291.2	D	-	3.90	3.94	2.66
	H	-	14.36	14.06	9.43
	K	0.7370	20.26	19.83	13.02
	L	0.7826	21.21	20.73	13.49
	M	0.8293	21.95	21.54	13.95
	N	0.8606	22.34	21.91	14.26
	O	0.8913	22.85	22.46	14.54
	P	0.9178	23.39	23.00	14.75
	Q	0.9421	23.72	23.38	15.04
	R	0.9718	24.32	23.95	15.33
321.2	D	-	3.13	3.05	2.10
	H	-	11.98	11.65	7.58
	K	0.7350	17.15	16.98	10.90
	L	0.7807	17.94	17.75	11.42
	M	0.8276	18.70	18.56	11.87
	N	0.8589	19.24	18.99	12.06
	O	0.8899	19.69	19.49	12.39
	P	0.9165	20.13	19.85	12.63
	Q	0.9409	20.48	20.34	12.89
	R	0.9708	20.88	20.82	13.16

CONT.

TABLE 6.9 (cont.)

Temperature (^{o}K)	Sample	x_B	Δ_{obs} (Hz)		
			H_1	H_2	H_3
331.7	D	-	2.86	2.81	1.80
	H	-	11.23	10.96	7.34
	K	0.7342	16.43	16.08	10.33
	L	0.7800	17.05	16.89	10.87
	M	0.8269	17.85	17.67	11.37
	N	0.8583	18.26	17.99	11.49
	O	0.8893	18.70	18.51	11.77
	P	0.9160	19.24	19.05	12.11
	Q	0.9404	19.52	19.41	12.25
	R	0.9704	19.87	19.83	12.56
341.1	D	-	2.66	2.74	1.76
	H	-	10.58	10.45	6.86
	K	0.7335	15.54	15.35	9.90
	L	0.7794	16.16	16.04	10.23
	M	0.8263	16.81	16.74	10.67
	N	0.8577	17.24	17.16	10. 85
	O	0.8888	17.66	17.61	11.19
	P	0.9155	18.02	17.96	11.35
	Q	0.9400	18.36	18.48	11.62
	R	0.9700	18.72	18.80	11.77

TABLE 6.10

Values of K_x and Δ_c at various temperatures for the different protons in various solute-aromatic solvent systems.

Proton	Temperature (^oK)	K_x	Δ_c(ppm)
a. Acrylonitrile-benzene-cyclohexane system			
H_1	292.9	1.7439	1.356
	306.6	1.5214	1.323
	320.1	1.4255	1.323
	330.7	1.1704	1.379
	340.7	1.0834	1.369
H_2	292.9	1.3735	1.561
	306.6	1.2553	1.572
	320.1	0.9936	1.665
	330.7	0.9272	1.650
	340.7	0.8761	1.638
H_3	292.9	2.0677	1.076
	306.6	1.8740	1.059
	320.1	1.5022	1.098
	330.7	1.4046	1.067
	340.7	1.3063	1.067
b. Acrylonitrile-p-xylene-cyclohexane system			
H_1	294.2	1.0761	1.556
	306.6	0.9996	1.533
	321.6	0.9350	1.483
	332.6	0.8269	1.508
	342.0	0.7297	1.554

CONT.

TABLE 6.10.b (cont.)

Proton	Temperature (°K)	K_x	Δ_c(ppm)
H_2	294.2	0.9263	1.640
	306.6	0.8088	1.687
	321.6	0.7196	1.693
	332.6	0.6736	1.671
	342.0	0.6491	1.644
H_3	294.2	1.0932	1.300
	306.6	0.9718	1.305
	321.6	0.8629	1.302
	332.6	0.8199	1.269
	342.0	0.7769	1.255
	c. Acrylonitrile-mesitylene-cyclohexane system		
H_1	286.9	0.8769	1.844
	305.0	0.8187	1.708
	315.7	0.7601	1.692
	329.5	0.7162	1.666
	339.2	0.6157	1.721
H_2	286.9	0.7122	1.959
	305.0	0.6791	1.779
	315.7	0.6471	1.743
	329.5	0.5916	1.766
	339.2	0.5222	1.808

TABLE 6.10.c. (cont.)

Proton	Temperature (°K)	K_x	Δ_c(ppm)
H_3	286.9	0.8244	1.597
	305.0	0.7188	1.525
	315.7	0.6832	1.494
	329.5	0.6480	1.473
	339.2	0.5671	1.506
d. Acrylonitrile-p-diethylbenzene-cyclohexane system			
H_1	303.3	1.2657	1.357
	330.2	0.8829	1.403
H_2	303.3	1.1745	1.328
	330.2	0.7939	1.429
H_3	303.3	1.3212	1.091
	330.2	0.8993	1.143
e. Acrylonitrile-1,3,5-triethylbenzene-cyclohexane system			
H_1	303.9	0.8538	1.583
	330.3	0.6500	1.606
H_2	303.9	0.8539	1.412
	330.3	0.6238	1.499
H_3	303.9	0.8345	1.294
	330.3	0.5700	1.418

TABLE 6.10 (cont.)

Proton	Temperature (^{o}K)	K_x	Δ_c(ppm)
	f. Acrylonitrile-p-diisopropylbenzene-cyclohexane system		
H_1	292.8	0.7862	1.742
	303.9	0.6365	1.817
	315.2	0.6162	1.730
	325.1	0.5941	1.666
	331.2	0.4878	1.840
H_2	292.8	0.7497	1.628
	303.9	0.6035	1.734
	315.2	0.5777	1.679
	325.1	0.5631	1.616
	331.2	0.5000	1.701
H_3	292.8	0.7636	1.570
	303.9	0.5768	1.570
	315.2	0.5817	1.462
	325.1	0.5829	1.374
	331.2	0.4818	1.514
g. Acrylonitrile-1,3,5-triisopropyl benzene-cyclohexane system.			
H_1	293.7	2.8871	1.008
	304.2	2.3596	1.009
	311.8	2.0577	0.990
	322.0	1.5587	1.026
	333.0	1.2737	1.043

CONT.

TABLE 6.10.g. (cont.)

Proton	Temperature	K_x	Δ_c(ppm)
H_2	293.7	3.6859	0.778
	304.2	3.3955	0.759
	311.8	2.4922	0.782
	322.0	1.8940	0.809
	333.0	1.6414	0.804
H_3	293.7	2.6350	0.804
	304.2	2.1511	0.812
	311.8	1.5335	0.864
	322.0	1.6283	0.791
	333.0	1.2292	0.832
h. Vinyl bromide-benzene-cyclohexane system.			
H_1	279.2	1.6481	0.692
	290.0	1.5789	0.664
	306.6	1.4078	0.649
	315.9	1.2907	0.650
	331.1	1.1724	0.635
H_2	279.2	1.1924	0.913
	290.0	1.1693	0.869
	306.6	1.0275	0.863
	315.9	0.8552	0.913
	331.1	0.8033	0.878

CONT.

TABLE 6.10.h. (cont.)

Proton	Temperature(^{o}K)	K_x	Δ_c(ppm)
H_3	279.2	3.2899	0.335
	290.0	3.1221	0.324
	306.6	2.2211	0.330
	315.9	2.0239	0.334
	331.1	1.3607	0.361
i. Vinyl bromide-p-xylene-cyclohexane system			
H_1	291.2	0.6686	1.024
	306.6	0.5722	1.035
	321.2	0.5357	1.018
	331.7	0.5135	0.997
	341.1	0.4655	1.004
H_2	291.2	0.4492	1.311
	306.6	0.4131	1.281
	321.2	0.3662	1.320
	331.7	0.4016	1.177
	341.1	0.3149	1.340
H_3	291.2	0.6775	0.643
	306.6	0.6308	0.608
	321.2	0.6021	0.593
	331.7	0.5619	0.587
	341.1	0.4872	0.613

TABLE 6.11

Values of thermodynamic parameters at 298.2°K for the complexes formed by acrylonitrile and vinyl bromide with benzene and alkyl substituted benzenes

Proton	$-\Delta H^{\circ}$(kJ mole^{-1})	$-\Delta G^{\circ}$(kJ mole^{-1})	$-\Delta S^{\circ}$(J K^{-1} mole^{-1})
	a. Acrylonitrile-benzene-cyclohexane system		
H_1	8.297	1.276	23.548
H_2	8.414	0.669	25.974
H_3	8.427	1.678	22.627
	b. Acrylonitrile-p-xylene-cyclohexane system		
H_1	6.460	0.163	21.125
H_2	6.188	-0.322	21.845
H_3	5.937	-0.109	19.539
	c. Acrylonitrile-mesitylene-cyclohexane system		
H_1	5.075	-0.448	18.531
H_2	4.544	-0.925	18.351
H_3	5.289	-0.674	20.012
	d. Acrylonitrile-p-diethylbenzene-cyclohexane system		
H_1	11.146	0.770	34.794
H_2	12.117	0.602	38.627
H_3	11.903	0.887	36.936

CONT.

TABLE 6.11 (cont.)

Proton	$-\Delta H^{o}$(kJ mole^{-1})	$-\Delta G^{o}$(kJ mole^{-1})	$-\Delta S^{o}$(J K^{-1} mole^{-1})
e. Acrylonitrile-1,3,5-triethylbenzene-cyclohexane system			
H_1	8.619	-0.230	29.677
H_2	9.920	-0.205	33.970
H_3	12.046	-0.222	41.150
f. Acrylonitrile-p-diisopropylbenzene-cyclohexane system			
H_1	8.268	-0.803	30.435
H_2	7.289	-0.946	27.631
H_3	7.460	-0.950	28.213
g. Acrylonitrile-1,3,5-triisopropylbenzene-cyclohexane system			
H_1	17.272	2.427	49.785
H_2	16.820	2.983	46.413
H_3	15.121	2.096	43.668
h. Vinyl bromide-benzene-cyclohexane system			
H_1	5.188	0.937	14.255
H_2	6.427	0.100	21.213
H_3	13.004	2.276	35.978
i. Vinyl bromide-p-xylene-cyclohexane system			
H_1	5.519	-1.159	22.418
H_2	4.749	-2.071	22.874
H_3	4.891	-1.017	19.824

They may of course vary slightly but perhaps the variations have been masked by experimental errors.

The values of K_x show a regular fall with rise in temperature, except in a few isolated instances. In fact, the K_x values in themselves are usually small and will be highly sensitive to experimental errors and the isolated cases of irregular behaviour of K_x values with temperature could be due to this reason.

As illustrated by a typical diagram (Fig 6.1) the plots of log K_x against the reciprocal of absolute temperature are apparently linear in all the systems studied and therefore indicate that, over the temperature range studied, the enthalpy of association (ΔH^o) is practically independent of temperature which suggests that only 1:1 complexes are being formed.

The values of ΔG^o, ΔH^o and ΔS^o are of the order of magnitude expected for the formation of weak complexes. It is most significant that the values of thermodynamic parameters obtained after processing the data for the different protons in the same solute molecule are similar, within the limits of experimental error, a fact which provides further justification for assuming that only one type of complex is being formed (i.e. of the type 1:1).

A comparison of ΔG^o values for the different protons in the two solutes, acrylonitrile (dipole moment = 3.89D[150]) and vinyl bromide (dipole moment = 1.41D[151]), obtained by using benzene (or p-xylene) as aromatic solvent shows that the ΔG^o values are in the same order

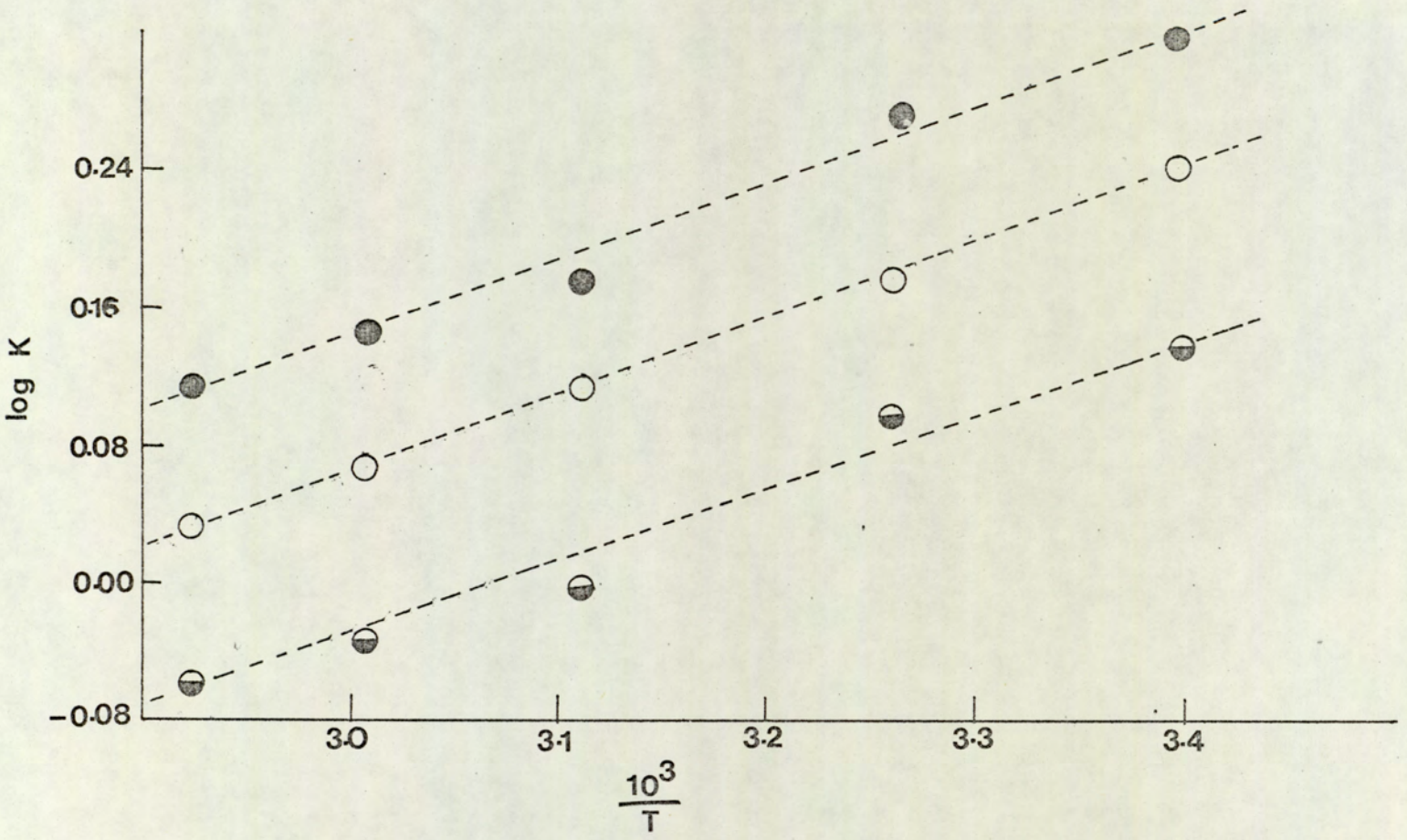

Fig. 6.1 The variation of log K with the reciprocal of absolute temperature for the protons H_1 ○ , H_2 ⊖ and H_3 ● in the acrylonitrile-benzene-cyclohexane system.

as the respective dipole moments of the solutes, for all the protons except H_3 in vinyl bromide. The values of Δ_{obs} for H_3 in vinyl bromide are of very small order of magnitude (10Hz) and are therefore highly sensitive to experimental errors. It is not unlikely that the irregularity shown in the thermodynamic parameters for this proton could be due to this, specially in view of the extreme sensitivity of the data processing procedure for the evaluation of K_x. The correlation between ΔG^o values and the solute dipole moments is in accordance with the view put forward by Homer et al[131] and indicates that dipole-induced dipole interactions are playing a significant role in complex formation.

A perusal of the table 6.11 shows that, for acrylonitrile, as one goes from benzene to mesitylene all the three parameters, ΔH^o, ΔG^o and ΔS^o, have a tendency to become less negative. However, when measurements are made with alkyl benzenes containing bulkier groups, the thermodynamic parameters show a tendency to become more negative again. The values of the thermodynamic parameters are plotted (Fig.6.2) against the molar volume of the aromatic solvent which is almost linearly related (see sec. 5.3.c. and Fig 5.1) to its polarisability. The plot (Fig.6.2) shows some sort of alternating behaviour. Values of-ΔG^o for the different alkyl-substituted benzenes are in the following order:

benzene > p-xylene > mesitylene < p-diethylbenzene > 1,3,5-triethyl benzene > p-diisopropyl benzene < 1,3,5-triisopropyl benzene.

Values of-ΔG^o for the other solute vinyl bromide, obtained with

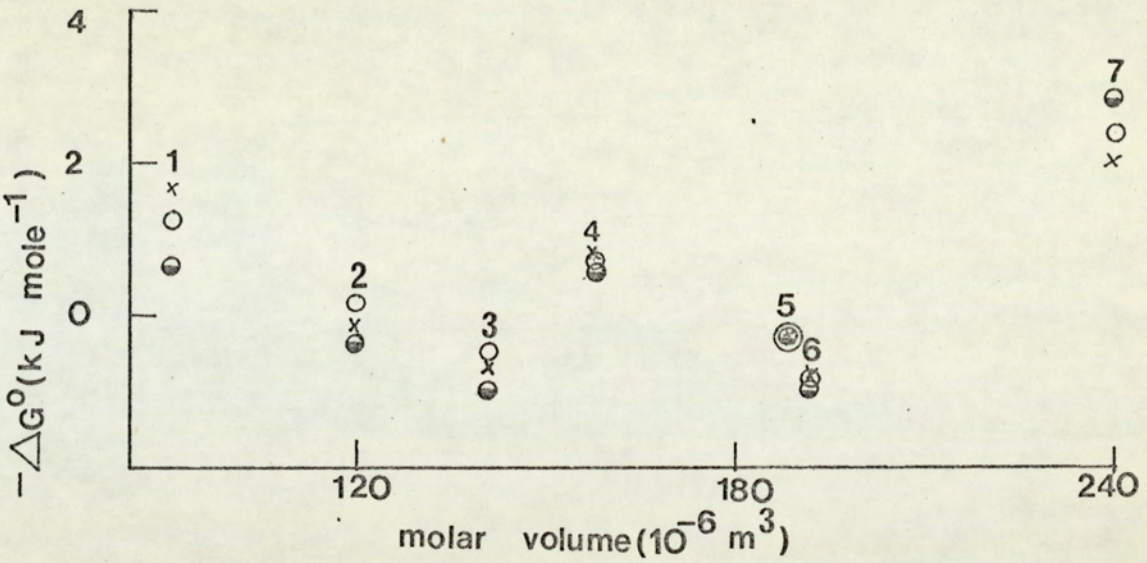

Fig. 6.2.a. The variation of-ΔG^{o} for the protons H_1 ○, H_2 ⊖ and H_3 ✕ in acrylonitrile solute with the molar volume of the aromatic solvents (numbered as in Fig. 6.2.b.)

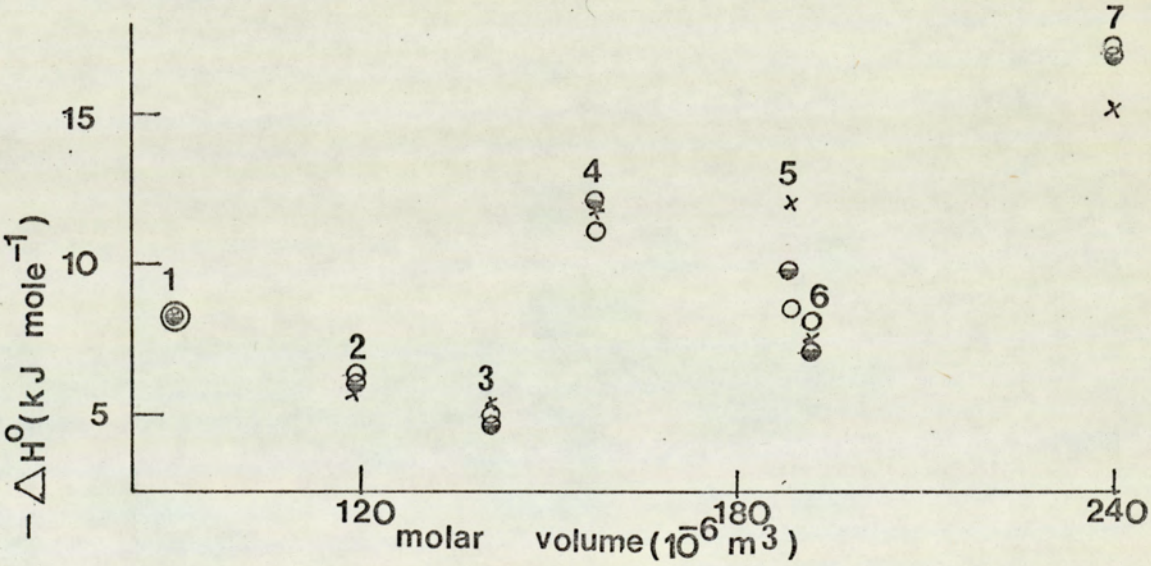

Fig. 6.2.b. The variation of-ΔH^{o} for the protons H_1 ○ , H_2 ⊖ and H_3 ✕ in the acrylonitrile solute with the molar volume of the aromatic solvents 1. benzene, 2. p-xylene, 3. mesitylene, 4. p-diethylbenzene, 5. 1,3,5-triethylbenzene, 6, p-diisopropylbenzene and 7. 1,3,5-triisopropylbenzene.

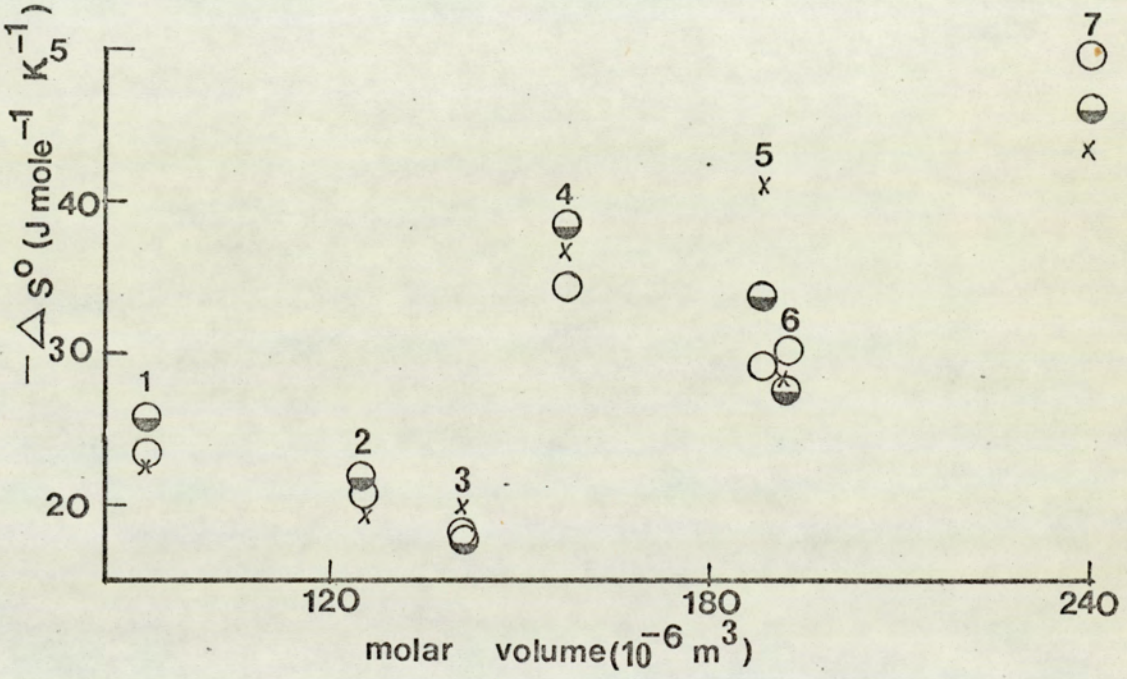

Fig. 6.2.c. The variation of $-\Delta S^{\circ}$ for the protons H_1 ○, H_2 ◒ and H_3 X in the acrylonitrile solute with molar volume of the aromatic solvents (numbered as in Fig. 6.2.b.)

benzene and p-xylene as aromatic solvents, show a similar order, i.e. benzene > p-xylene.

The other two thermodynamic parameters, ΔH^{o} and ΔS^{o}, tend to become more negative as the equilibrium quotient for the complex formation increases which shows that the solute and the aromatic solvent are subject to more physical restraint as the equilibrium quotient increases. The order of ΔH^{o} and ΔS^{o} values for different aromatic solvents with a particular solute is similar to that observed for ΔG^{o} but departures from the behaviour in isolated cases have also been noticed. This once again emphasizes the proposals put forward by Homer et al[131] that ΔG^{o} (not ΔH^{o}) should be treated as a true measure of the interaction energy. However, ΔH^{o} and ΔS^{o}, among themselves, vary in a similar fashion from one aromatic solvent to the other.

6.3.b. Analysis of the Equilibrium Quotient Values

In fact, in the formation of such collision complexes, the extent of complex formation, i.e. K_x and therefore the thermodynamic parameters, may depend on the probability of the solute molecule approaching the solvent molecule, within a certain 'sphere of influence' around it and spending, on the average, some time in a preferred orientation. This probability will itself depend on a number of factors, e.g., the polarisability of the aromatic solvent molecule, dipole moment of the solute molecule, the steric environments of the aromatic solvent and solute molecules, etc. It is just possible that a certain aromatic molecule may have a higher polarisability than another but the

chances of complex being formed could be in the reverse order if the former aromatic solvent has a steric environment which can not be penetrated by the solute molecule. Even among the alkyl substituted benzenes, the presence of substituents in suitably orientated locations (the suitability depending also on the geometry of the solute molecule) may help in holding the solute molecule for a longer time over the aromatic solvent molecule rather than inhibiting its approach. All this leads one to think that the polar solute-aromatic solvent interactions are going to be highly specific in nature and the equilibrium quotient and the thermodynamic parameters may show some sort of alternating behaviour for the different alkyl-substituted benzenes.

It clearly emerges from what has been said the values of equilibrium quotients for the different solute-aromatic solvent systems may consist of mainly two terms; first a polarisability term (x) which will make a positive contribution towards the value of the equilibrium quotient and can be weighted according to the respective molar volumes, since polarisability has been shown to be linearly related to the corresponding molar volumes (see Fig. 5.1), and second the steric term due to the presence of substituted alkyl groups in the aromatic solvent which can be weighted in proportion to $(V_A - V_B)$, the difference in the molar volume of a particular aromatic solvent and benzene. The steric term itself can be considered to have two types of contributions, first a positive contribution (y) due to the 'trap' effect of the alkylgroups and second a negative contribution (z) due to steric hindrance (blocking effect) experienced by the solute molecule in approaching the solvent molecule. Thus, the equilibrium quotient for any solute-aromatic solvent system can be expressed in the form :

$$K_x = V_A\ x + (V_A - V_B)(y - z) \qquad (6.1)$$

Since the steric effect is being measured in relation to benzene, it can be considered zero for benzene and the corresponding equilibrium quotient expression reduces to

$$K_1 = 0.903x \qquad (6.2)$$

For p-xylene and mesitylene, the methyl groups do not project significantly above the benzene ring and the 'trap' effect due to them can be considered negligible. The corresponding equilibrium quotients can, respectively, be expressed as

$$K_2 = 1.250x + (1.250 - 0.903)z \qquad (6.3)$$

$$K_3 = 1.405\ x + (1.405 - 0.903)z \qquad (6.4)$$

For p-diethylbenzene, 1,3,5-triethylbenzene, p-diisopropyl benzene and 1,3,5-triisopropyl benzene all the terms in eqn. (6.1) will be non-vanishing and the corresponding equilibrium quotient values are respectively

$$K_4 = 1.572x + (1.572 - 0.903)(y - z) \qquad (6.5)$$

$$K_5 = 1.882x + (1.882 - 0.903)(y - z) \qquad (6.6)$$

$$K_6 = 1.913x + (1.913 - 0.903)(y - z) \qquad (6.7)$$

$$K_7 = 2.392x + (2.392 - 0.903)(y - z) \qquad (6.8)$$

Values of the factors x,y and z can be evaluated and compared from the equilibrium quotient values at 306.6°K obtained for proton H_1 in acrylonitrile with various aromatic solvents. Eqns. (6.2) - (6.8) take the form

$$1.521 = 0.903x \qquad (6.9)$$

$$1.000 = 1.250x - 0.347z \qquad (6.10)$$

$$0.819 = 1.405x - 0.502z \qquad (6.11)$$

$$1.217 = 1.572x + 0.669(y-z) \qquad (6.12)$$

$$0.854 = 1.882x + 0.979(y-z) \qquad (6.13)$$

$$0.636 = 1.913x + 1.010(y-z) \qquad (6.14)$$

$$2.360 = 2.392x + 1.489(y-z) \qquad (6.15)$$

From eqn. (6.9)

$$x = 1.684 \qquad (6.16)$$

By substituting x = 1.684 into eqns. (6.10) and (6.11) respectively

$$z = 3.814 \qquad (6.17)$$

and $$z = 3.082 \qquad (6.18)$$

It is significant to note at this stage that fairly close values of z obtained for two different aromatic solvents indicate the soundness of the approach. After substituting an average value of z ca. 3.133 into eqns. (6.12) - (6.15), the values of y for p-diethyl benzene, 1, 3, 5 - triethyl benzene, p-diisopropyl benzene and 1, 3, 5 - triisopropyl benzene are, respectively

$$y = 0.996 \qquad (6.19)$$

$$y = 0.768 \qquad (6.20)$$

$$y = 0.753 \qquad (6.21)$$

and $$y = 2.013 \qquad (6.22)$$

Once again the values of y obtained for the first three aromatic solvents can be considered fairly close, in view of the fact that some other interactions might also be playing a minor role which has been neglected in all these calculations. Other interactions seem definitely involved in the case of 1, 3, 5 - triisopropyl benzene and could be the reason for its exceptional behaviour.

An average value for y, 0.839 was obtained from eqns. (6.19) - (6.21)

and the three different contributions to the equilibrium quotient values for proton H_1 in acryloritrile with various aromatic solvents were caluclated and are given in table 6.12

Table 6.12

Various contributions to the equilibrium quotient values for H_1 (at 306.6°k) in acrylonitrile , obtained with various aromatic solvents.

Aromatic Solvent	Polarisability factor	'Trap' factor	Blocking Factor	Calculated K	Experimental K
Benzene	1.521	0	0	1.521	1.521
p-Xylene	2.105	0	-1.087	1.018	1.000
Mesitylene	2.360	0	-1.573	0.793	0.819
p-Diethyl-benzene	2.647	0.561	-2.096	1.112	1.217
1,3,5-Triethyl-benzene	3.169	0.821	-3.067	0.923	0.845
p-Diisopropyl-benzene	3.221	0.847	-3.164	0.904	0.636
1,3,5-Triiso-propylbenzene	4.028	1.249	-4.664	0.613	2.360

A graph of the various oontributions, and the caluculated and the experimental equilibrium quotient values against the molar volume of the aromatic solvent was plotted (Fig 6.3). The two values of the equilibrium quotients are fairly close except in the case of 1, 3, 5 - triisopropyl benzene which can not be understood at this stage.

6.3.C. Analysis of the Δ_c Values.

Sometimes the value of Δ_c for a solute-aromatic solvent complex has

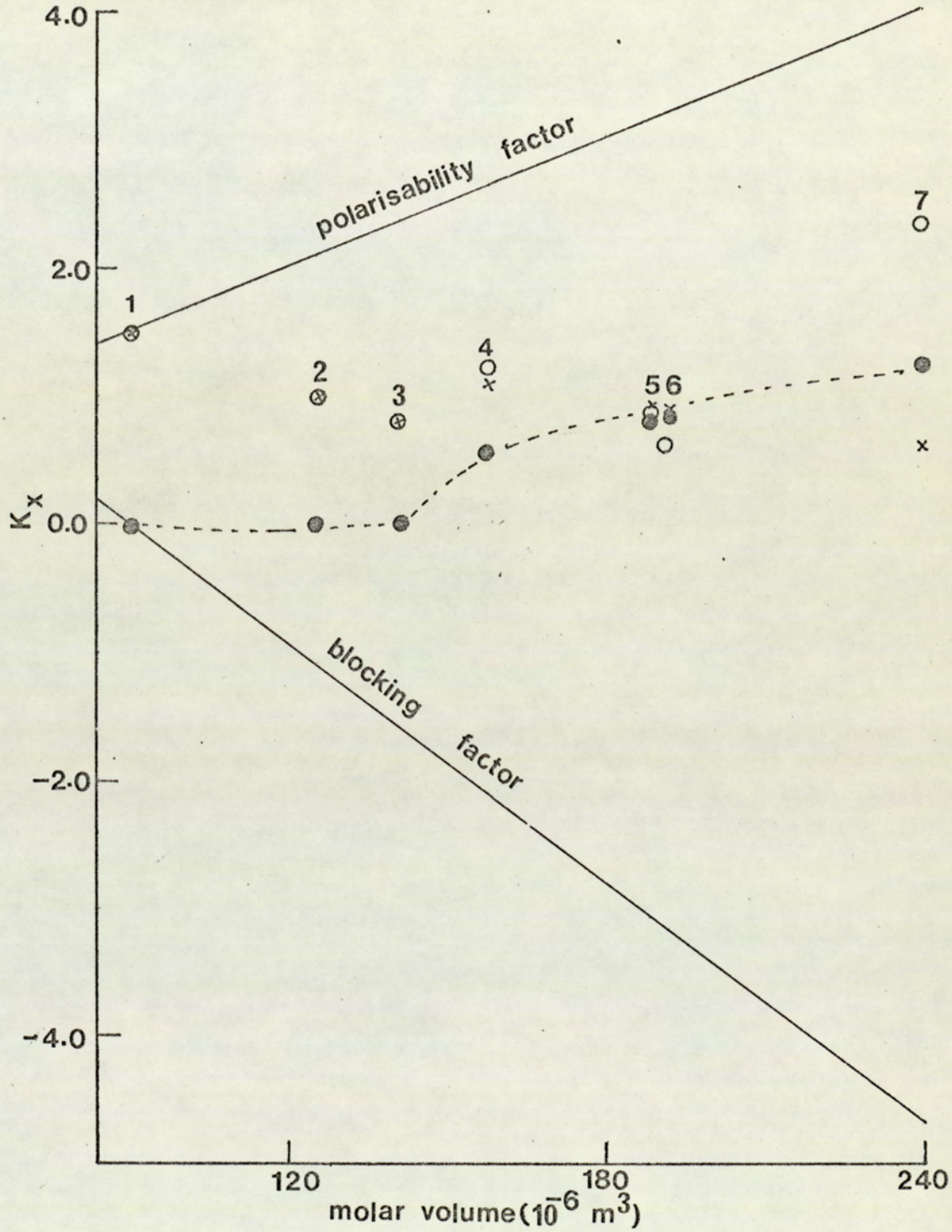

Fig. 6.3 The polarisability factor, the blocking factor and the 'trap' factor ● , and the experimental ○ and calculated X values of the equilibrium quotient for the proton H_1 in the acrylonitrile solute obtained with different aromatic solvents (numbered as in Fig. 6.2.b.).

been taken as a measure of the strength of the interaction. As is apparent from Figs 5.2 and 6.3, the curve representing the variation of Δ_c values for a particular solute proton obtained with different aromatic solvents is almost a mirror image of the curve representing the variation of the corresponding equilibrium quotient (and related thermodynamic) values. Under such circumstances, the previous contentions concerning the strength of interactions become quite misleading.

Of the various factors involved in these interactions, the polarisability of the aromatic solvent is expected to enhance the Δ_c values while the steric effects should tend to reduce it. In fact, Δ_c is expected to depend, to a certain extent, on the time the solute molecule spends in a particular orientation. For example, a proton in a solute molecule which is held too rigicly in a particular orientation with respect to the aromatic solvent molecule may have lower values of Δ_c than in a complexed state where it has greater freedom to adopt a variety of orientations in the time averaging process which lead to the enhanced shielding. The arguments in the preceeding section illustrate the importance of steric effects and these may be the reason for the almost inverse variation of Δ_c and K_x values with the molar volume of the aromatic solvent.

The point can be illustrated in quantative terms by expressing the Δ_c values for one of the protons, say H_1 in acrylonitrile obtained with various aromatic solvents, as a sum of three terms (as for K_x), a positive contribution (x') from the polarisability of the aromatic solvent weighted in proportion to the molar volume of the aromatic solvent, a 'trap' factor (y') and a blocking factor (z') which is

expected to make a negative contribution towards Δ_c. The latter two factors are weighted in proportion to the difference in the molar volumes of the particular aromatic solvent and benzene, i.e.

$$\Delta_c = V_A \cdot x + (V_A - V_B)(y - z) \qquad (6.23)$$

After substituting the actual values of Δ_c (from table 5.20) for benzene, p-xylene, mesitylene, p-diethyl benzene, 1,3,5 - triethyl benzene, p-diisopropyl benzene and 1,3, 5 - triisopropyl benzene, the eqn. (6.23) can respectively be written as

$$1.355 = 0.903x' + (0.903 - 0.903)(y' - z') \qquad (6.24)$$

$$1.533 = 1.250x' + (1.250 - 0.903)(y' - z') \qquad (6.25)$$

$$1.708 = 1.405x' + (1.405 - 0.903)(y' - z') \qquad (6.26)$$

$$1.357 = 1.572x' + (1.572 - 0.903)(y' - z') \qquad (6.27)$$

$$1.583 = 1.882x' + (1.882 - 0.903)(y' - z') \qquad (6.28)$$

$$1.817 = 1.913x' + (1.913 - 0.903)(y' - z') \qquad (6.29)$$

$$1.009 = 2.392x' + (2.392 - 0.903)(y' - z') \qquad (6.30)$$

From eqn. (6.24)

$$x = 1.501$$

Since the methyl groups in p-xylene and mesitylene do not project significantly above the benzene ring, the corresponding 'trap' factors (y') can be considered negligible. After substituting $x' = 1.501$ in eqns. (6.25) and (6.26) one gets for p-xylene and mesitylene respectively

$$z = 0.988$$

$$z = 0.797$$

An average of the two values for z' ca.0.8925 is substituted in eqns (6.27) - (6.30) and the values of 'trap' factors, y'_4, y'_5, y'_6 and y'_7, for p-diethyl benzene, 1,3,5 - triethyl benzene, p-diisopropyl benzene and 1,3,5 - triisopropyl benzene, respectively, are

$y_4' = 0.603$

$y_5' = 0.375$

$y_6' = 0.151$

$y_7' = 0.840$

Negative values for y' in the Δ_c expression as opposed to the positive values for the corresponding term in the K_x expression are quite anticipated in view of the opposite behaviours of Δ_c and K_x with the molar volume of the aromatic solvent. The negative values of y' in eqn. (6.23) emphasize the fact, stated earlier, that the loss of freedom of movement for the solute in the complex tends to reduce the values of Δ_c by precluding regions of higher shielding. It is rather difficult to correlate the values of y' for the various aromatic solvents as it will involve specific and different effects of the substituents in complex formation.

CHAPTER 7

NMR STUDIES OF THE MOLECULAR INTERACTIONS BETWEEN VINYL METHYL KETONE AND BENZENE

7.1 INTRODUCTION

Chapters 5 and 6 deal with the study of molecular interactions between aromatic solvents, and vinyl bromide and acrylonitrile. These solutes are simple in the sense that they have a rigid structure and do not have any possibility of conformational changes. However, if the vinyl solute possesses a group, like $COCH_3$ in vinyl methyl ketone, which can adopt different orientations with respect to the rest of the molecule, due to rotation about C-C bond, further interesting observations associated with complex formation are expected. By the measurement of chemical shifts in tolune at different temperatures, the possibility of conformational changes for vinyl methyl ketone, as a result of solute-aromatic solvent interaction, has been suggested.[155] It is difficult to decide the nature of the interactions causing the conformational changes. However, in view of the fact that tolune is a polar solvent, it is possible that the observed confirmational changes are due to dipole-dipole interaction or simply due to a dipole-induced dipole interaction. Therefore, it was thought worthwhile to study the interaction of vinyl methyl ketone with the non-polar aromatic solvent benzene to investigate, amongst other things, the importance of the dipole-induced interaction. Apart from conformational differences, vinyl methyl ketone differs further from the two previously studied vinyl solutes in the respect that it has a slightly different type of electronic distribution due to the presence of a carbonyl group in the molecule. In view of these points, it warranted separate consideration.

7.2 EXPERIMENTAL

The benzene and cyclohexane used for the studies were spectrosol grade and vinyl methyl ketone was obtained from Kodak and used without further purification. The n.m.r. spectra did not show evidence of impurities in any of the solutions. A series of samples, containing different proportions of benzene and cyclohexane but a constant low mole fraction ca. 0.04 of vinyl methyl ketone, was prepared gravimetrically. The compositions of the different samples are recorded in Table 7.1

The ^1H spectra were obtained by using a Perkin- Elmer R10 spectrometer operating at 60.004MHz and 306.6°K . The spectra were calibrated by the usual side band technique using a Muirhead-Wigan D-890A oscillator and a Venner 3336 frequency counter. A minimum of six scans were taken for each sample and the frequencies used for analysing the spectra represented an average of these measurements.

Measurements were also made at four other temperatures namely 281.2°, 291.2°, 321.7° and 335.0°K.

The ABC spectra from the solute were analysed using the computer program LAOCOON 3, the total root mean square (RMS) error and the probable errors in the parameters being bellow 0.05. The chemical shifts (in the form of Δ_{obs}) obtained by this procedure are given in tables 7.2-7.6.

The parameters K_x and Δ_c were evaluated by processing the data on the computer program BHCURVEFIT, the gradient and the intercept being taken

TABLE 7.1

Sample composition for the vinyl methyl ketone-benzene-cyclohexane system.

Sample	Moles of solute/10^{-3}	Moles of Benzene/10^{-2}	Moles of cyclohexane/10^{-3}	x_B
A	2.0474	0.2087	46.6932	-
B	1.8419	0.2960	44.9822	-
C	2.0845	0.4080	43.8474	-
D	2.0374	0.4860	42.9765	-
E	1.9760	0.9877	37.9075	-
F	1.9346	1.4816	33.1096	-
G	2.0174	1.9827	27.6961	-
H	1.8719	2.5081	22.9539	-
I	2.0745	2.9907	18.0478	-
J	2.0431	3.4894	13.0965	0.6652
K	2.0431	3.7820	10.2602	0.7282
L	1.9418	4.0256	8.1476	0.7785
M	2.0374	4.1284	6.5233	0.8119
N	2.1059	4.3332	5.0986	0.8461
O	1.9732	4.4436	3.7559	0.8786
P	1.8947	4.5916	2.0758	0.9194
Q	1.9760	4.7370	0.4967	0.9580

TABLE 7.2

Δ_{obs} values at 60.004MHz and 281.2°K for various samples in vinyl methyl ketone-benzene-cyclohexane system.

Sample	Δ_{obs}(Hz)			
	H_{methyl}	H_1	H_2	H_3
J	17.30	9.48	22.43	19.77
K	18.13	9.60	23.40	20.65
L	18.68	9.68	24.20	21.34
M	18.88	9.73	24.74	21.75
N	19.13	9.59	25.15	22.10
O	19.57	9.62	25.63	22.43
P	19.89	9.46	26.10	22.82
Q	20.07	9.17	26.55	23.20

TABLE 7.3

Δ_{obs} values at 60.004MHz and 291.2°K for various samples in vinyl methyl ketone-benzene-cyclohexane system.

Sample	Δ_{obs}(Hz)			
	H_{methyl}	H_1	H_2	H_3
J	16.71	9.02	20.99	18.26
K	17.37	9.15	22.19	19.19
L	17.93	9.35	23.00	19.92
M	18.07	9.30	23.38	20.25
N	18.40	9.27	23.90	20.51
O	18.72	9.26	24.32	20.94
P	19.06	9.13	24.95	21.49
Q	19.23	8.98	25.32	21.67

TABLE 7.4

Δ_{obs} values at 60.004MHz and 306.6°K for various samples in vinyl methyl ketone-benzene-cyclohexane system.

Sample	Δ_{obs} (Hz)			
	H_{methyl}	H_1	H_2	H_3
A	*	0.99	1.66	1.44
B	*	1.32	2.44	2.15
C	*	1.68	3.14	2.75
D	*	1.94	3.66	3.23
E	*	3.71	6.84	5.98
F	*	5.18	9.92	8.64
G	*	6.30	12.57	10.92
H	12.59	7.46	15.23	13.24
I	13.99	8.09	17.21	14.90
J	15.45	8.59	19.32	16.54
K	16.18	8.68	20.43	17.35
L	16.81	8.93	21.21	17.97
M	16.93	8.97	21.51	18.31
N	17.16	8.90	21.97	18.62
O	17.60	8.94	22.48	19.00
P	17.87	9.00	22.97	19.38
Q	18.14	8.80	23.45	19.70

* Could not be measured due to overlap with cyclohexane spinning side bands.

TABLE 7.5

Δ_{obs} values at 60.004MHz and 321.7°K for various samples in vinyl methyl ketone-benzene-cyclohexane system.

Sample	Δ_{obs}(Hz)			
	H_{methyl}	H_1	H_2	H_3
J	14.18	8.11	17.80	15.25
K	14.96	8.58	18.86	16.07
L	15.51	8.72	19.56	16.68
M	15.97	8.64	20.11	16.89
N	16.16	8.69	20.56	17.22
O	16.37	8.80	21.01	17.64
P	16.96	8.78	21.55	17.94
Q	17.07	8.67	21.91	18.29

TABLE 7.6

Δ_{obs} values at 60.004MHz and 335.0°K for various samples in vinyl methyl ketone-benzene-cyclohexane system.

Sample	Δ_{obs}Hz)			
	M_{methyl}	H_1	H_2	H_3
J	13.24	7.84	16.77	13.79
K	14.00	7.86	17.65	14.60
L	14.49	7.97	18.49	15.12
M	14.77	8.19	18.86	15.45
N	15.01	8.31	19.22	15.82
O	15.29	8.36	19.76	16.12
P	15.68	8.45	20.41	16.49
Q	15.95	8.32	20.65	16.82

TABLE 7.7*

Values of K_x and Δ_c for the vinyl methyl ketone–benzene complex

Proton	Temperature (°K)	K_x	Δ_c(ppm)
H_{methyl}	281.2	2.2939	0.487
	291.2	1.9595	0.492
	306.6	1.6230	0.497
	321.7	1.5687	0.475
	335.0	1.4886	0.452
H_2	281.2	1.4313	0.766
	291.2	1.4248	0.731
	306.6	1.1435	0.747
	321.7	1.0425	0.732
	335.0	0.8935	0.749
H_3	281.2	1.8933	0.600
	291.2	1.7339	0.580
	306.6	1.4895	0.559
	321.7	1.2896	0.552
	335.0	1.2030	0.523

* Δ_{obs} values for H_1 could not be processed to give meaningful values of K_x and Δ_c.

corresponding to $x_B = 1.00$, and the values obtained are given in Table 7.7. For reasons explained earlier, the benzene mole fraction required as input data was obtained after including a portion of the solute as inert solvent (see sec. 5.2) and making the necessary bulk corrections (eqn. 5.1). As reliable density data for vinyl methyl ketone at different temperatures were not available, $\frac{V_A}{V_B}$ values at 293.2°K were used throughout the calculations. However, in view of a very small amount of vinyl methyl ketone being present in the system, this is not expected to affect the results significantly. The molar volume ratio, $\frac{V_S}{V_B}$, for benzene and cyclohexane remains fairly constant within the temperature range studied therefore the value at 293.2°K was also used throughout the calucations. Data necessary for the bulk corrections are given in Table 7.8[145,156].

TABLE 7.8

Densities of various substances used

Compound	Density/$(10^{-3}$Kgm$^{-3})$ at 293.2°K
Benzene[145]	0.87901
Cyclohexane[145]	0.77855
Vinyl methyl ketone[156]	0.8636

7.3 RESULTS AND DISCUSSION

7.3.a The Values of Δ_{obs} and the Possibility of Conformation Changes

A perusal of the Tables 7.2 - 7.6 shows that as the proportion of the

aromatic solvent in the mixture and therefore, the amount the complex formed, increases, Δ_{obs} values for the different type of protons (except H_1) increases progressively. By reducing the temperature, the Δ_{obs} values increase, obviously due to enhanced complex formation. However, for the proton H_1, the Δ_{obs} values do increase in the initial stages but at very high mole fractions of the aromatic solvent they become constant or even start decreasing, a tendency which becomes more marked if the temperature is reduced (Fig.7.1.) This behaviour is clearly illustrated by considering the ratio of Δ_{obs} values for different protons given in table 7.9.

TABLE 7.9*

The Δ_{obs} ratios for the different proton pairs in various samples for vinyl methyl ketone-benzene-cyclohexane system.

Sample	$H_{methyl}:H_1$	$H_2:H_1$	$H_3:H_1$	$H_2:H_{methyl}$	$H_3:H_{methyl}$	$H_2 : H_3$
J	1.799	2.249	1.926	1.251	1.071	1.168
K	1.863	2.353	1.998	1.263	1.072	1.178
L	1.882	2.375	2.012	1.262	1.069	1.180
M	1.887	2.397	2.041	1.271	1.082	1.175
N	1.928	2.469	2.093	1.280	1.085	1.180
O	1.968	2.514	2.125	1.277	1.080	1.185
P	1.986	2.553	2.154	1.285	1.085	1.185
Q	2.061	2.664	2.238	1.293	1.086	1.190

* Based on the data reported in Table 7.4

As it is apparent from the Table 7.9, the Δ_{obs} ratios, except those involving H_1, show only small variations (the significance of this is

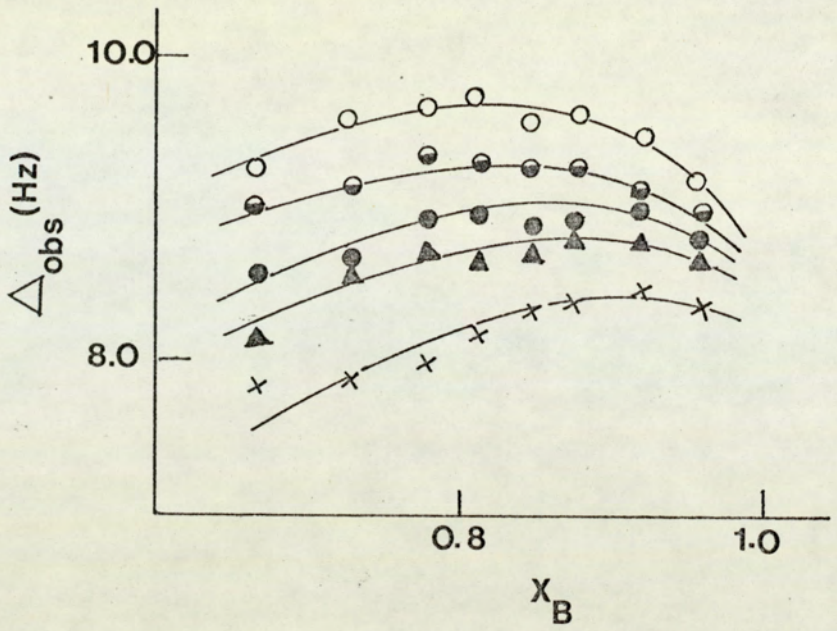

Fig. 7.1 The variation of the Δ_{obs} values for the proton H_1 in the vinyl methyl ketone solute with the mole fraction of benzene at 281.2° ○ , 291.2° ◒ , 306.6° ● , 321.7° ▲ and 335.7°K ×

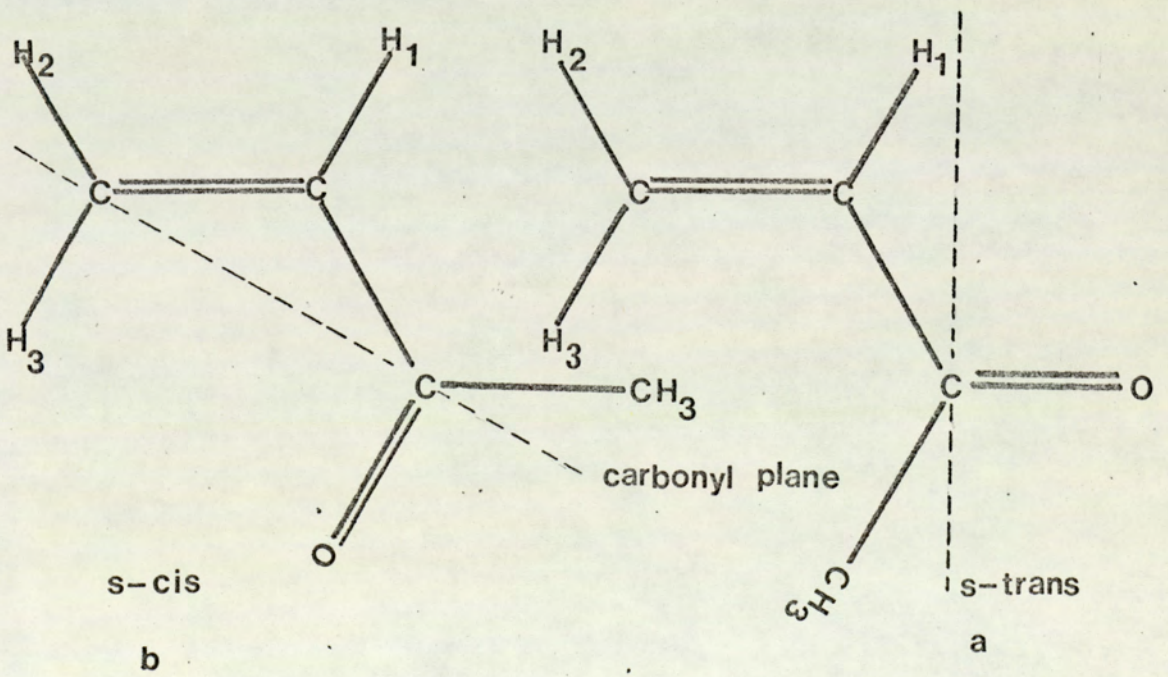

Fig. 7.2 s-cis and s-trans conformers of the vinyl methyl ketone molecule.

explained at the end of this section). However, the Δ_{obs} ratios involving H_1 and any other proton show a significant variation from sample to sample due to the fact that Δ_{obs} for H_1 tend to decrease after reaching a mxaimum value while the Δ_{obs} values for the others continue rising (almost proportionally). This behaviour of Δ_{obs} ratios involving H_1 indicates that, perhaps, vinyl methyl ketone molecule is undergoing some conformational changes which will now be discussed in detail.

Homer et al[70] have established that in solute-aromatic solvent complexes of the type considered here, the solute has a tendency to adopt a time-average orientation over the benzene ring such that the dipolar axis of the solute molecule lies along the six-fold symmetry axis of the benzene ring and the negative end of the dipole is farthest from the benzene ring. Evidence given in the earlier chapters lends support to this idea. By microwave spectral studies[157], it has been shown that though there are four possible orientations of the dipole moment for vinyl methyl ketone, the one almost along the C=O bond is the most plausible. It has also been indicated by infrared studies[158] that vinyl methyl ketone may exist as a mixture of different conformers at room temperature; two co-planar forms, s-trans (Fig 7.2.a) and s-cis (Fig7.2.b) together with other non-planar forms.

On the basis of considerations just mentioned one would expect the following order of aromatic solvent-induced shift values for the different protons for the s-trans structure.

$$H_3 > H_2 > H_{methyl} > H_1$$

and for the s-cis structure

$$H_1 > H_{methyl} > H_2 > H_3$$

If the actual structure is a mixture of the two conformers, the order of aromatic solvent-induced shifts will depdend on the relative contribution of the two forms. In the present investigation, H_1 has been found to have the least value of aromatic solvent-induced shift which, according to the proposals of Homer et al[70] indicates that the s-trans structure is making the major contribution to the actual time-averaged structure of the complex. Since this small value of Δ_{obs} for H_1 tends to decrease as the mole fraction of the aromatic solvent in the system increases, it seems that the s-trans character increases with the mole fraction of the aromatic in the system. Such conformational changes by changing the nature of the medium have been attributed[159,160] to the difference in the dielectric constants of the solvents. The proportion of the more polar conformer is expected to be higher in a medium of higher dielectric constant (ϵ). It has been indicated previously[161] that of the two vinyl methyl ketone conformers, the s-trans is more polar. In view of this, some shift in conformational equilibrium towards the s-trans form is quite anticipated, when the proportion of benzene (ϵ = 2.284[146]) in the mixture increases against cyclohexane (ϵ = 2.023[146]). Decreasing the temperature has a similar effect, presumably, due to the fact that the s-trans form is energetically a favoured one[155]. The actual order of Δ_c values for the protons H_2 and H_3 can not be predicted from these considerations unless the direction of the dipolar axis for vinyl methyl ketone molecule is precisely known.

It is significant to note at this stage that the order of aromatic

solvent-induced shift values for the different protons present in the two structures of vinyl methyl ketone, obtained by the considerations just described, is in conformity with the one predicted on the basis of an empirical rule, the carbonyl plane rule, given elsewhere[137, 138]. According to this rule if a reference plane is drawn through the carbon of the C = O bond (Fig 7.2), benzene complexes preferentially behind the reference plane because the negative oxygen of the carbonyl group inhibits complex formation with it. On account of the shielding effect of benzene, protons on the opposite side of oxygen show an upfield (+ ve), those on the same side as oxygen a downfield (- ve) and those very near the plane show a small positive or negative aromatic solvent-induced shift and are very sensitive to any conformational changes. In view of this rule the proton H_1 in vinyl methyl ketone molecule is expected to have the smallest (+ve) solvent shift(Δ_c)-induced for the s-trans conformer and the highest (+ve) Δ_c for the s-cis conformer which supports the conclusions based on the proposals of Homer et al[70].

If such conformational changes do indeed occur they are expected to be affected by any steric hindrance due to bulky substituents in either the solute or the aromatic solvent. To investigate this and substantiate the present conclusions, one sample each in p-xylene and mesitylene was prepared and the chemical shifts for the three vinyl protons in vinyl kethyl ketone were measured from samples containing the same mole fraction ca. 0.96 of the aromatic solvent. Table 7.10 records the Δ_{obs} values at 60.004 MHz.

It is apparent from the table that the H_1 shift (Δ_{obs}) in mesitylene is greater than that in

TABLE 7.10

Aromatic solvent induced shifts (Δ_{obs}) at 60.004MHz for the different vinyl protons in vinyl methyl ketone

Aromatic Solvent	Δ_{obs} (Hz)		
	H_1	H_2	H_3
Benzene	8.80	23.45	19.70
p- Xylene	12.69	21.79	20.56
Mesitylene	13.00	19.91	19.86

p-xylene which is again greater than in benzene, indicating that there is a small conversion to s-trans form in mesitylene and p-xylene, presumbly due to restricted rotation in presence of the alkyl substituents. This reduced s-trans character cannot be due to reduced dielectric constants since the extent of s-trans character and the dielectric constant (ϵ) for p-xylene ($\epsilon = 2.327$[145]) and mesitylene ($\epsilon = 2.248$[145]) are in the reverse order.

Though the variation of Δ_{obs} ratios between H_1 and any other proton with the mole fraction of the aromatic solvent is indicative of conformational changes, any change in conformational equilibrium over a narrow range of aromatic mole fraction is probably small. This is substantiated from the fact that Δ_{obs} ratios involving protons other than the sensitive H_1 show only small changes (see table 7.9). In view of this is can be assumed that only one type of complex i.e. 1:1 (but with isomers) is being formed and Δ_{obs} values for H_2, H_3 and H_{methyl} can be processed to derive meaningful values for the parameters K_x

and Δ_c (the meaning of these "average" parameters will be discussed later.) Marked variations reflected in the ratios involving H_1 (which is closest to the carbonyl group) are perhaps due to the fact that Δ_{obs} for H_1 itself is small and even small changes in it will be significant. Since the Δ_{obs} values for H_1 tend to decrease at high mole fraction of benzene, they could not be processed to yield meaningful values of K_x and Δ_c.

The values for K_x and Δ_c, obtained after processing the data are given in table 7.7. Though these values represent only a time-average of the values for the two isomeric complexes, they can be used for the determination of a time-average configuration for the complex. From such a time-average structure it is possible to estimate the relative contributions of the two isomers which can be subsequently used in evaluating the K_x and Δ_c parameters for the individual complexes.

7.3.b. <u>The Time-Average Geometry of the Complex</u>

It has been shown earlier (see sec. 5.3.d and 5.3.e) that the order of Δ_c values for the different protons in the same solute, therefore the geometry of the complex, depends on the nature of the aromatic solvent. The study of the vinyl methyl ketone-benzene system shows that the complex geometry may depend on the nature of the substituents in the solute as well.

The orders of Δ_c values for the different protons in acrylonitrile, vinyl bromide and vinyl methyl ketone, induced by benzene, are given in table 7.11

TABLE 7.11

Order of Δ_c values for the different protons in acrylonitrile, vinyl bromide and vinyl methyl ketone.

Solute	Order of Δ_c values
Acrylonitrile	$H_2 > H_1 > H_3$
Vinyl bromide	$H_2 > H_1 > H_3$
Vinyl methyl ketone	$H_2 > H_3 > H_{methyl} > H_1$*

* The maximum observed value

The difference in the relative values of Δ_c for vinyl methyl ketone benzene suggests that the vinyl methyl ketone-benzene complex has a time-average geometry different from the vinyl bromide-benzene and acrylonitrile-benzene complexes. This is not surprising in view of different contributions from the two rotamers. On the basis of the arguments put forward by Homer et al[70] and the carbonyl plane rule[137, 138], it has been concluded, qualitatively, that the solute molecule has predominantly s-trans character. Now an attempt will be made to estimate the relative contributions of the two rotamers in quantitative terms.

In the case of vinyl methyl ketone, the oxygen forms the negative end and the positive charge is predominantly localised on the carbon of the carbonyl group. After complexing with benzene, for obvious reasons, the oxygen tends to lie as far from the benzene ring as possible and H_2 and H_3 closest to it. This arrangement may be used as a criterion

in attempting to find a tentative time-average configuration for the complex based on the experimentally observed values of Δ_c given in table 7.7. Isoshielding diagrams (Fig 7.3) corresponding to the experimentally determined values of Δ_c for H_2, H_3 and H_{methyl} have been plotted as described earlier (see sec. 4.9 and also 5.3.e). The values of p and z co-ordinates for the different protons in the most likely arrangement of vinyl methyl ketone in the complex are given in table 7.12. For the methyl protons, free rotation about C-C bond has been assumed and the co-ordinates represent the centre (projection of C-C line on the plane containing methyl protons) for the three protons. As the actual molecular parameters for the vinyl methyl ketone molecule were not available in the literature, the values given in the table 7.13, based on the values reported[152] for similar molecules acrolein ($CH_2 = CH - CHO$) and acetone ($CH_3 - CO - CH_3$), were used in the calculations

TABLE 7.12

Co-ordinates for the various protons in vinyl methyl ketone solute for a postulated structure of vinyl methyl ketone-benzene complex.

Proton	p(r.r.)	z(r.r.)
H_1	0.68	3.74
H_2	1.32	2.20
H_3	1.48	2.32
H_{methyl}	1.36	2.76

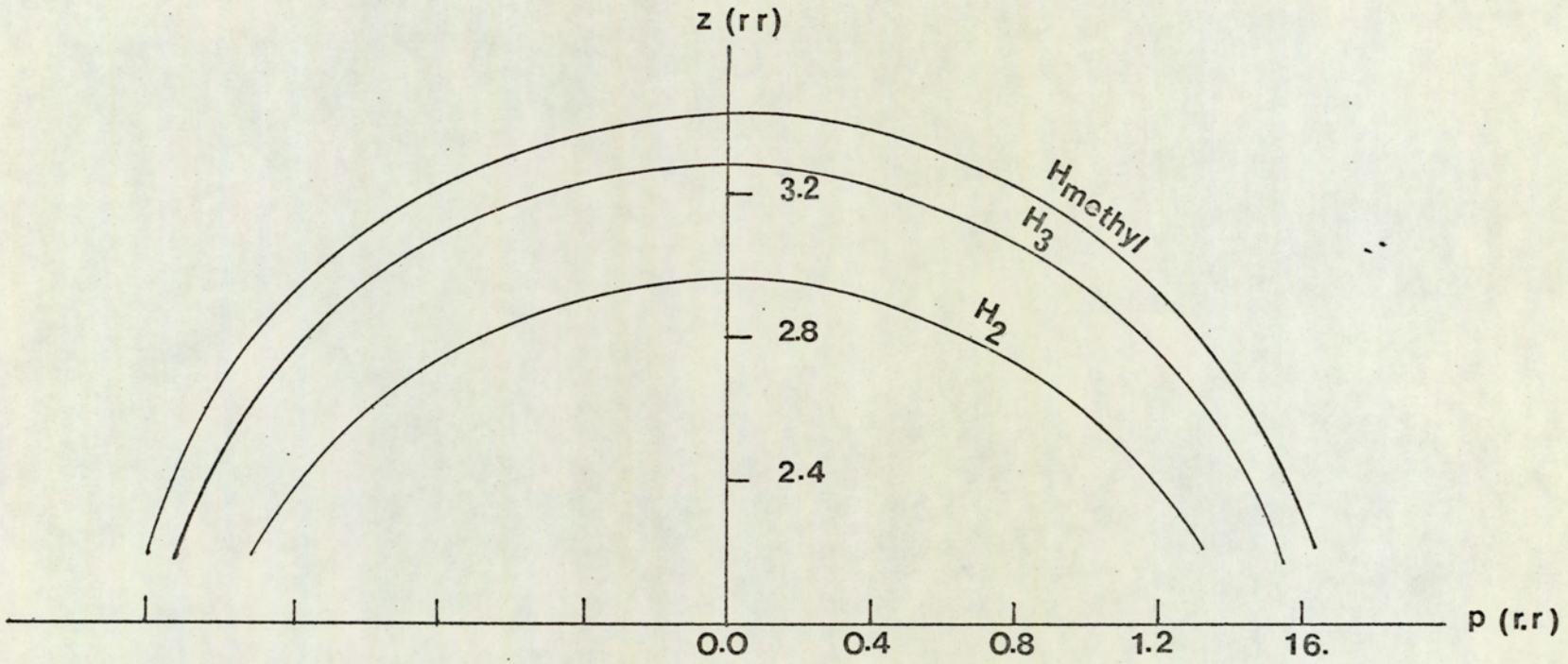

Fig. 7.3 Isoshielding diagrams corresponding to Δ_c values induced by benzene for the protons H_{methyl}, H_2 and H_3 in the vinyl methyl ketone molecule.

TABLE 7.13

Molecular parameters for vinyl methyl ketone used in the calculation of complex geometry.

a. Bond-lengths (Å)

C – H	C = C	= C – C =	C = O	C – C
1.09	1.36	1.46	1.22	1.52

b. Bond angles (radians)

All ∠ C = CH	∠ CCO	∠ C – CH
2.059	2.129	1.911

It was found that in the postulated time-average configuration the plane containing the $COCH_3$ group deviates from the planar s-trans structure by about 1.134 radians which in effect means that the time-average contribution of the s-trans rotamer in the complex is about 64%; zero deviation is equivalent to 100% s-trans character and deviation by 2π radians is equivalent to zero contribution from the s-trans form. These results confirm the qualitative interpretations made earlier.

7.3.c. Values of K_x and Δ_c

The K_x values for H_2, H_3 and H_{methyl} given in table 7.7 are in fair agreement. It has been pointed out elsewhere [128,162] that if more than one isomeric 1:1 complex is being formed, the experimentally observed equilibrium quotient K is a sum of the equilibrium quotients

for the individual complexes, i.e.

$$K = \sum_i K_i \qquad (7.1)$$

As it has been described in the previous section, in the fully complexed state at room temperature, the s-trans form makes about 64% contribution to the actual structure of vinyl methyl ketone in the complex, which in effect means that the equilibrium quotient for the complex formation with the s-trans structure is 64% of the observed equilibrium quotient and that with the s-cis structure is 36%. A higher equilibrium quotient with the more polar s-trans structure of the solute once again emphasizes the importance of dipole-induced dipole interactions in such solute-aromatic solvent systems.

It has also been said in the previous studies[162] that the $\Delta_{c(i)}$ values corresponding to the different isomeric 1:1 complexes are related to the experimentally observed Δ_c^{Expt} value by the relationship

$$\Delta_c^{Expt} = \frac{\sum_i K_i \Delta_{c(i)}}{\sum_i K_i} \qquad (7.2)$$

Unfortunately the Δ_c values for the individual isomeric complexes can not be obtained simply on the basis of this equation even if the individual K_i are known. The problem can be illustrated by taking a concrete example of proton H_2 for vinyl methyl ketone-benzene system. The observed K_x (at 306.6°K) and Δ_c for the proton are, respectively, 1.1435 and 0.747 ppm. Keeping in view that the s-trans and s-cis structures are making, respectively, 64% and 36% contributions to the actual time-average structure of the complex, eqn. 7.2 takes the form

$$0.747 = (1.1435 \times 0.64)\ \Delta_c^{trans} + (1.1435 \times 0.36)\Delta_c^{cis} \qquad (7.3)$$

which means that an infinite set of values for Δ_c^{trans} and Δ_c^{cis} are

possible.

7.3.d. Studies at Various Temperatures

Values of K_x and Δ_c obtained by processing the Δ_{obs} data at different temperatures are given in table 7.7. The values of K_x show a consistent decline with rise in temperature indicating a reduced complexation. The values of Δ_c are almost constant within the limits of experimental error. In view of the presence of conformational equilibrium, one would have expected some dependence of Δ_c values on temperature. However, such variations may not be apparent if the relative proportions of the rotamers do not change significantly, specially when the ΔH^o values for the different isomers do not differ much. Presumably, this is the situation in the present case. This contention is also supported by the fact that in an earlier study[155], the rotamers could not be separated even by varying the temperature over a wide range.

A plot of log K_x against the reciporcal of absolute temperature is apparently linear (Fig 7.4), within the limits of experimental error. The values of K_x at various temperatures have been processed using the computer program PARATHERM to obtain the thermodynamic parameters ΔH^o, ΔG^o and ΔS^o. Values of these parameters, given in table 7.14, are once again indicative of formation of weak complexes. Values of parameters obtained after processing the data for the various protons are of similar magnitude which shows that only isomeric 1:1 complexes are being formed.

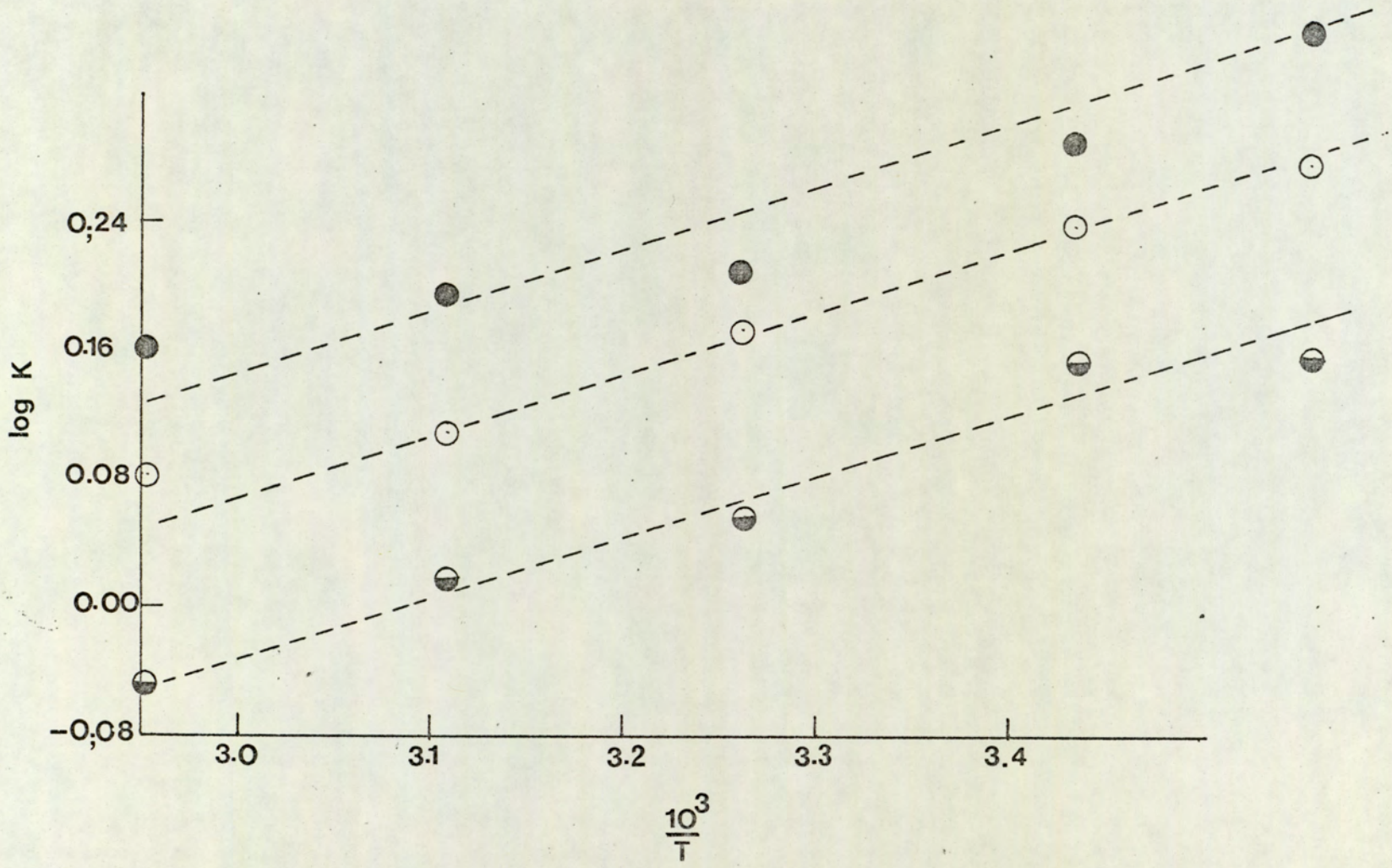

Fig. 7.4 The variation of log K with the reciprocal of absolute temperature for the protons H_2 ◒, H_3 ○ and H_{methyl} ● in the vinyl methyl ketone-benzene-cyclohexane system.

TABLE 7.14

Thermodynamic parameters at 298.2°K for the vinyl methyl ketone - benzene complex.

Proton	$-\Delta H^{o}$(KJ mole^{-1})	$-\Delta G^{o}$(KJ mole^{-1})	$-\Delta S^{o}$(J K^{-1} mole^{-1})
H_{methyl}	6.167	1.561	15.456
H_2	7.138	0.561	22.050
H_3	6.832	1.176	18.979

In situations where more than one isomeric complexes are being formed, the apparent ΔH^{o} has been said[128] to be related to the actual ΔH_i values for the individual isomers and corresponding K_i values by the relationship

$$\Delta H^{o} = \frac{\Sigma K_i \Delta H_i^{o}}{\Sigma K_i} \qquad (7.4)$$

However, in systems where the proportion of different isomers does not change significantly with temperature the calculations will eventually lead to identitcal ΔH^{o} values for the different isomeric complexes which will also be equal to the experimentally observed value. Therefore, no attempt to calculate ΔH^{o} for the individual isomers was made.

CHAPTER 8

SPIN-SPIN COUPLING CONSTANTS

In the recent past, interest has been shown[41] in the study of solvent and temperature effects on the spin-spin soupling constants (J). Some regular variations have been noticed for H-F coupling constants. However, studies of solvent and temperature effects on proton-proton coupling constants have received comparatively little attention, perhaps, due to the fact that J_{HH} values in themselves are small and any variations in them are liable to be lost in the experimental errors. Normally, rigid molecules are used for the study of such effects in order to avoid any variations due to the rotation abound C-C bonds. The solutes used here in this investigation fall in this category and offer an opportunity to study the variation of proton-proton coupling constants with solvent and temperature.

In a previous study[163] of some vinyl compounds ($CH_2 = CHX$), the various proton-proton coupling constants were found not to show any regular and significant variation except the geminal coupling constant, J_{gem} ($H_2 - H_3$) which showed some tendency to decrease in going from cyclohexane ($\epsilon = 2.02$) to dimethylformamide ($\epsilon = 36.70$). The variations were said to be an effect of the dielectric constant of the medium. Values of the coupling constants obtained under different conditions during the present investigation are reported in tables 8.1 - 8.8.

A perusal of the tables 8.1 - 8.3 shows that, apparently, there is no significant variation in the values of the various coupling constants with temperature. This seems to be due to the fact

TABLE 8.1

Values of spin-spin coupling constants (J) for different proton pairs in acrylonitrile obtained under various conditions.

Solvent	Temperature (^{o}K)	Coupling constant (Hz)		
		J_{cis}	J_{trans}	J_{gem}
Cyclohexane[a]	292.9	11.67	17.73	1.08
	306.6	11.62	18.02	1.14
	320.1	11.47	17.82	1.15
	330.7	11.49	17.86	1.13
	340.7	11.60	17.87	1.14
Benzene[b]	292.9	11.69	17.79	1.05
	306.6	11.73	18.00	0.97
	320.1	11.59	17.98	0.95
	330.7	11.70	17.87	0.95
	340.7	11.66	17.87	0.99
p-Xylene[c]	294.2	11.66	18.02	1.07
	306.6	11.67	17.85	1.05
	321.6	11.76	17.97	1.06
	332.6	11.68	17.87	1.03
	342.0	11.65	18.01	1.02
Mesitylene[d]	286.9	11.67	17.78	1.02
	305.0	11.58	17.81	1.02
	315.7	11.62	17.88	1.08
	329.5	11.58	17.81	1.02
	339.2	11.62	17.86	1.05

CONT.

TABLE 8.1 (cont.)

Solvent	Temperature (°K)	Coupling constant (Hz)		
		J_{cis}	J_{trans}	J_{gem}
p-Diethylbenzene[e]	303.3	11.60	17.82	1.05
	330.2	11.65	17.80	1.03
1,3,5-Triethyl-benzene[f]	303.9	11.59	17.79	0.99
	330.3	11.64	17.84	1.05
p-Diisopropyl-benzene[g]	292.8	11.65	17.92	1.07
	304.2	11.70	17.91	1.06
	315.2	11.65	17.83	1.03
	305.1	11.61	17.89	1.06
	331.2	11.55	17.82	1.05
1,3,5-Triisopropyl benzene[h]	293.7	11.61	17.87	1.06
	304.2	11.61	17.86	1.03
	311.8	11.66	17.85	1.05
	322.0	11.65	17.87	0.99

a. 4 mole% solution of acrylonitrile in cyclohexane

b. Sample R in table 5.1

c. Sample S in table 5.2

d. Sample I in table 5.3

e. Sample G in table 5.4

f. Sample I in table 5.5

g. Sample H in table 5.6

h. Sample J in table 5.7

TABLE 8.2

Values of spin-spin coupling constants (J) for different proton pairs in vinyl bromide under various conditions.

Solvent	Temperature (°K)	Coupling constent (Hz)		
		J_{cis}	J_{trans}	J_{gem}
Cyclohexane[a]	291.2	7.26	15.06	-1.59
	306.6	7.22	15.11	-1.60
	321.2	7.13	15.04	-1.52
	331.7	7.16	15.16	-1.52
Benzene[b]	279.2	7.31	14.95	-1.90
	290.0	7.26	14.75	-1.85
	306.6	7.09	14.95	-1.86
	315.9	7.35	14.85	-1.84
	341.1	7.11	15.01	-1.80
p-Xylene[c]	291.2	7.00	15.06	-1.81
	306.6	7.27	15.05	-1.72
	321.2	7.21	15.05	-1.72
	331.7	7.05	15.08	-1.74
	341.1	7.14	15.09	-1.71

a. 4 mole% solution of vinyl bromide in cyclohexane

b. Sample P in table 5.8 c. Sample R in table 5.9

TABLE 8.3

The values of spin-spin coupling constants (J) for different proton pairs in vinyl methyl ketone under various conditions.

Solvent	Temperature (^{o}K)	Spin-spin coupling constant (Hz)		
		J_{cis}	J_{trans}	J_{gem}
Cyclohexane[a]	281.2	10.70	17.81	1.09
	291.2	10.79	17.82	1.09
	306.6	10.73	17.72	1.10
	321.7	10.77	17.91	1.16
	335.0	10.70	17.70	1.22
Benzene[b]	281.2	10.68	17.77	0.86
	291.2	10.61	17.69	0.99
	306.6	10.70	17.77	0.98
	321.7	10.77	17.77	0.92
	335.0	10.67	17.91	1.02
p-Xylene[c]	304.2	10.72	17.77	1.04
Mesitylene[d]	304.0	10.71	17.70	1.05

a. 4 mole% solution of vinyl methyl ketone in cyclohexane

b. Sample Q in table 7.1

c. 3 mole% solution of vinyl methyl ketone in p-xylene (96 mole%? and cyclohexane (1 mole%)

d. 3 mole% solution of vinyl methyl ketone in mesitylene (96 mole%) and cyclohexane (1 mole%)

TABLE 8.4

Values of spin-spin coupling constants (J) at 306.6°K for the different proton pairs in acrylonitrile for various samples in the acrylonitrile-benzene-cyclohexane system.

Sample *	Coupling constant (Hz)		
	J_{cis}	J_{trans}	J_{gem}
A	11.61	17.88	1.19
B	11.60	18.16	1.13
C	11.58	17.84	1.24
D	11.68	17.92	1.06
E	11.59	18.03	0.99
F	11.68	17.89	1.07
G	11.65	17.76	1.13
H	11.60	17.65	1.13
I	11.71	17.82	1.02
J	11.64	17.87	1.11
K	11.68	17.95	1.02
L	11.63	17.80	0.98
M	11.54	17.84	0.94
N	11.66	17.86	1.03
O	11.68	17.73	0.95
P	11.82	17.88	0.89
Q	11.77	17.86	0.85
R	11.73	18.00	0.97

* Refer to table 5.1

TABLE 8.5

Values of spin-spin coupling constants (J) at 306.6°K for the different proton pairs in acrylonitrile for various samples in the acrylonitrile-p-xylene-cyclohexane system.

Sample *	Coupling constant (Hz)		
	J_{cis}	J_{trans}	J_{gem}
A	11.42	17.69	1.20
B	11.67	17.86	1.10
C	11.54	17.83	1.14
D	11.62	17.85	1.13
E	11.66	18.04	1.21
F	11.67	17.94	1.13
G	11.65	17.89	1.09
H	11.65	17.91	1.08
I	11.63	17.84	1.06
J	11.63	17.89	1.10
K	11.64	17.98	1.10
L	11.57	17.84	0.96
M	11.67	17.94	1.15
N	11.73	17.93	1.02
O	11.60	17.82	1.10
P	11.60	17.85	1.05
Q	11.75	17.94	1.05
R	11.67	17.86	1.01
S	11.67	17.85	1.05

* Refer to table 5.2

TABLE 8.6

Values of spin-spin coupling constant (J) at 306.6°K for the different proton pairs in vinyl bromide for various samples in vinyl bromide-benzene-cyclohexane system.

Sample *	Coupling constant (Hz)		
	J_{cis}	J_{trans}	J_{gem}
A	7.30	15.29	-1.66
C	7.25	15.08	-1.53
F	7.37	14.89	-1.59
G	7.31	14.87	-1.83
H	7.06	14.94	-1.64
I	7.21	15.05	-1.68
K	7.03	15.07	-1.68
L	7.31	14.88	-1.77
P	7.09	14.95	-1.86

* Refer to table 5.8

TABLE 8.7

Values of spin-spin coupling constants (J) at 306.6°K for the different proton pairs in vinyl bromide for various samples in vinyl bromide-p-xylene-cyclohexane system.

Sample *	Coupling constant (Hz)		
	J_{cis}	J_{trans}	J_{gem}
A	6.99	15.02	-1.40
B	7.25	15.11	-1.58
C	7.13	15.16	-1.56
D	7.18	15.08	-1.56
E	7.24	15.10	-1.55
F	7.04	15.20	-1.61
G	7.38	15.05	-1.61
H	7.19	15.14	-1.61
I	7.07	15.12	-1.66
J	7.21	15.06	-1.69
K	7.10	14.97	-1.72
L	7.19	15.09	-1.66
M	7.20	15.09	-1.73
N	7.16	15.02	-1.69
O	7.05	14.99	-1.66
P	7.05	15.12	-1.80
Q	7.25	15.10	-1.78
R	7.22	15.05	-1.72

* Refer to table 5.9

TABLE 8.8

Values of spin-spin coupling constants (J) at 306.6°K for the different proton pairs in vinyl methyl ketone for various samples in vinyl methyl ketone-benzene-cyclohexane system.

Sample *	Coupling constant (Hz)		
	J_{cis}	J_{trans}	J_{gem}
A	10.77	17.72	1.11
B	10.72	17.79	1.15
C	10.71	17.79	1.07
D	10.73	17.76	1.16
E	10.76	17.85	1.08
F	10.71	17.78	1.09
G	10.77	17.78	1.09
H	10.71	17.75	1.09
I	10.70	17.77	1.05
J	10.67	17.73	1.09
K	10.64	17.86	1.05
L	10.65	17.82	1.09
M	10.74	17.75	0.98
N	10.75	17.76	1.03
O	10.68	17.72	1.00
P	10.78	17.73	0.95
Q	10.70	17.77	0.98

* Refer to table 7.1

that the thermal excitation of the vibrational or torsional modes, over the small range of temperature used for the present studies, may not be significant particularly when the solute is present in a complexed state[41].

J_{cis} and J_{trans} do not show significant variation even with the change of the solvent and whatever variations are noticed (table 8.1 - 8.8), they seem to be within the limits of experimental error. However, J_{gem} shows a tendency to decrease in going from cyclohexane to an aromatic solvent. There is, apparently, no significant variation in the coupling constant values obtained with the various aromatic solvents (see table 8.1 - 8.3). The behaviour seems to be consistent with the dielectric constant view mentioned earlier. While the dielectric constant for cyclohexane is appreciably different from that for any of the aromatic solvents, it does not differ much from one aromatic solvent to the other (see table 8.9)

TABLE 8.9

Values of the dielectric constant (ϵ) for various solvents

Solvent	ϵ
Cyclohexane	2.02
Benzene	2.28
p-Xylene	2.24
Mesitylene	2.25
p-Diethylbenzene	2.24
p-Diisopropylbenzene	2.22

CHAPTER 9

GENERAL CONCLUSIONS

GENERAL CONCLUSIONS

From the ^1H n.m.r. studies reported herein of molecular interactions between polar solutes containing more than one non-equivalent proton and aromatic solvents, several facts regarding the various aspects of such interactions, e.g. their nature and strength, the stoichiometry and geometry of the complexes formed and the steric factors which influence complex formation, have emerged.

The almost similar values of equilibrium quotients and related thermodynamic parameters for the different non-equivalent protons in the same solute obtained with a particular aromatic solvent, and the constancy of ΔH^o values with temperature strongly indicate the formation of only one type, 1:1, complex. However, the possibility of isomeric 1:1 complexes, in the case where conformational changes are possible, is not ruled out.

Different values of Δ_c for the different non-equivalent protons in the same solute obtained with a particular aromatic solvent indicate that the solute tends to adopt a preferred time-average orientation over the aromatic ring such that the negative end of the solute dipole is farthest away from the aromatic ring. However, this time average orientation seems to depend on the nature of the substituents in the aromatic solvent as well as the solute molecules.

The values of the thermodynamic parameters obtained for the various polar solute-aromatic solvent systems are indicative of the formation of weak complexes. The idea of estimating the strength of the interaction

from Δ_c values seems to be misleading.

As the analysis of equilibrium quotient and related thermodynamic parameter values as well as Δ_c values shows, dipole-induced dipole interactions appear to be playing an important role in the formation of polar solute-aromatic solvent complexes (increasing both K_x and Δ_c with the plarisability of the aromatic.) However, dipole-induced dipole interactions are not overwhelmingly important. Steric effects due to the presence of alkyl groups substituted in the aromatic ring play very significant roles. The steric effects may affect the equilibrium quotient values in two ways; they can enhance it due to a 'trap' effect as well as reduce it by blocking the approach of the solute molecule towards the aromatic solvent molecule. The values of Δ_c usually show a fall (relative to the benzene complex) due to enhanced steric effects. The steric effects seem to be highly specific in nature and together with the polarisation effect give rise to an alternating dependence of the value of various parameters on the molar volume of the aromatic solvent.

The spin-spin coupling constants for the vinyl proton pairs are found not to show any significant variation with concentration or temperature except J_{gem} which tends to decrease on changing from cyclohexane to an aromatic solvent.

REFERENCES

1. W. Pauli, Naturwisschaften, (1924), 12, 741.
2. O. Stern, Z. Phys., (1921), 7, 249; W. Gerlach and O.Stern, Ann. Phys. Leipzig, (1924,)74, 673.
3. I. I. Rabi, S. Millman, P. Kusch and J. R. Zacharias, Phys. Rev., (1939), 55, 526.
4. N. F. Ramsey, "Molecular Beams", Oxford University Press, (1956).
5. C. J. Gorter, Physica, (1936), 3, 995.
6. C. J. Gorter and L. F. J. Broer, Physica, (1942),9, 591.
7. E. M. Purcell, H. C. Torrey and R. V. Pound, Phys. Rev., (1946), 69, 37.
8. F. Bloch, W. W. Hansen and M. Packard, Phys. Rev., (1946),69,127.
9. J. A. Pople, W. G. Schneider and H. J. Bernstein, "High Resolution Nuclear Magnetic Resonance", McGraw-Hill Book Co., N.Y.,(1959).
10. J. W. Emsley, J. Feeney and L. H. Sutcliffe, "High Resolution Nuclear Magnetic Resonance Spectroscopy, Vol.I", Pergamon Press, Oxford, (1965).
11. J. W. Emsley, J. Feeney and L. H. Sutcliffe, "High Resolution Nuclear Magnetic Resonance Spectroscopy, Vol.II", Pergamon Press, Oxford(1965).
12. L. M. Jackman, "Applications of Nuclear Magnetic Resonance Spectroscopy in Organic Chemistry", Pergamon Press, London, (1959).
13. S. G. Starling and A. J. Woodall, "Physics" 2nd Edition, Longmans, London, (1957).
14. L. Pauling and E. B. Wilson, Jr., "Introduction to Quantum Mechanics" McGraw-Hill Book Co. Inc., N.Y., (1935).
15. E. M. Purcell, Phys. Rev., (1946),69, 681.
16. A. Einstein, Phys. Z., (1917),18, 121.

17. W. A. Anderson, Phys. Rev., (1956), 104, 850.

18. N. Bloembergen, E. M. Purcell and R. V. Pound, Phys. Rev., (1948), 73, 679.

19. F. Bloch, Phys. Rev., (1946), 70, 460.

20. R. K. Wangsness and F. Bloch, Phys. Rev., (1953),89, 728.

21. F. Bloch, Phys. Rev., (1956),102, 104.

22. G. V. D. Tiers, J. Phys. Chem. (1961), 65, 1916.

23. R. V. Pound, Phys. Rev., (1950), 79, 685.

24. N. Bloembergen, "Nuclear Magnetic Relaxation", W. A. Benzamin, N.Y. (1961).

25. W. D. Knight, Phys. Rev., (1949), 76, 1259.

26. W. G. Proctor and F. C. Yu, Phys. Rev., (1950), 77, 717.

27. W. C. Dickinson, Phys. Rev., (1950), 77, 736.

28. G. V. D. Tiers, J. Phys. Chem., (1958), 62, 1151.

29. W. E. Lamb, Phys. Rev., (1941), 60, 817.

30. N. F. Ramsey, Phys. Rev., (1950), 78, 699.

31. N. F. Ramsey, Phys. Rev, (1952), 86, 243.

32. A. Saika and C. P. Slichter, J. Chem. Phys., (1954),22, 26.

33. A. D. Buckingham and J. A. Pople, Discuss. Farad. Soc.,(1956) 22, 17.

34. S. Mohanty and H. J. Bernstein, J. Chem. Phys., (1971),54, 2254.

35. J. A. Pople, Proc. Roy. Soc., (1957), A239, 541.

36. J. A. Pople, Proc. Roy. Soc., (1957),A239, 550.

37. T. P. Das and R. Bersohn, Phys. Rev., (1956),104, 476.

38. C. P. Slichter, "Principles of Magnetic Resonance", Haper and Row, N.Y., (1963).

39. H. M. McConnell, J. Chem.Phys., (1957),27, 226.

40. J. A. Pople, J.Chem.Phys., (1956),24, 1111.

41. P. Laszlo, "Progress N.M.R. Spectroscopy, Vol.III", Pergamon Press, Oxford, (1967).

42. J. Ronayne and D. H. Williams, "Annual Review of N.M.R. Spectroscopy, Vol.II", Academic Press, London, (1969).

43. A. D. Buckingham, T. Schaefer and W. G. Schneider J. Chem.Phys., (1960), 32, 1227.

44. W. C. Dickinson, Phys.Rev., (1951),81, 717.

45. D. J. Frost and G. E. Hall, Mol.Phys.,(1966),10, 191.

46. A. A, Bothner-By and R. E. Glick, J.Chem.Phys., (1957) 26, 1651.

47. J. Ronayne and D. H. Williams, J.Chem.Soc. (B), (1967), 540.

48. J. Rpnayne, and D. H. Williams, J.Chem.Soc. (C), (1967),2642.

49. M. D. Johnston, Jr., F. P. Gasparro, and I. D. Kuntz, Jr., J.Am. Chem. Soc., (1969), 19, 5715.

50. R. E. Klinck and J. B. Stothers, Can.J.Chem., (1962), 40, 1071.

51. R. E. Klinck and J. B. Stothers, Can.J.Chem., (1962),40, 2329.

52. R. E. Klinck and J. B. Stothers, Can.J.Chem., (1966),44, 37.

53. D. H. Williams, J. Ronayne and R. G. Wilson, Chem.Comm.,(1967),1089.

54. R. G. Wilson and D. H. Williams, J.Chem.Soc.(B), (1968),1163.

55. T. Winkler and W.von Phillipsborn, Helv.Chim. Acta, (1968),51,183.

56. K. D. Bartle, D. W. Jones and R. S. Mathews, J.Chem.Soc(A), (1969), 876.

57. T. Winkler and W. von Phillipsborn, Helv.Chim.Acta, (1969),52,796.

58. M. J. Stephen, Mol.Phys., (1958), 1, 223.

59. R. J. Abraham, Mol.Phys., (1961), 4, 369.

60. J. Homer and D. L. Redhead, J.Chem.Soc. Farad.TransII, (1972), 68, 793.

61. J. K. Becconsall, Mol.Phys.,(1968), 15, 129.

62. J. K. Becconsall, T. Winkler and W. von Phillipsborn, Chem. Comm.,

(1969), 430.

63. J. K. Becconsall, Mol. Phys. (1970), 18, 337.

64. A. A. Bothmer-By, J.Mol.Spectros, (1960), 5, 52.

65. B. B. Howard, B. Linder and M. T. Emerson, J.Chem.Phys., (1962), 36, 458.

66. N. Lumbroso, T. K. Wu and B. P. Dailey, J.Phys. Chem.,(1963), 67, 2469.

67. P. de Mongolfier, J.Chim.Phys., (1967),64, 639.

68. F. H. A. Rummens, W. T. Raynes and H. J. Bernstein, J.Phys. Chem., (1968), 72, 2111.

69. W. T. Raynes and M. A. Raza, Mol.Phys., (1969), 17, 157.

70. J. Homer and P. J. Huck, J.Chem.Soc. (A), (1968), 277.

71. A. D. Buckingham, Can.J.Chem., (1960), 38, 300.

72. P. Diehl and R. Freeman, Mol.Phys., (1961),4, 39.

73. J. Homer, Tetrahedron, (1967), 23, 4065.

74. P. J. Huck, Ph.D. Thesis, University of Aston in Birmingham (1968).

75. W. G. Proctor and F. C. Yu, Phys.Rev., (1951), 81, 20.

76. M. Barfield and D. M. Grant, "Advance in Magnetic Resonance, Vol.I", Academic Press, N.Y., (1965).

77. H. S. Gutowsky, D. W. McCall and C. P. Slichter, J.Chem.Phys., (1953), 21, 279.

78. E. L. Hahn and D. E. Maxwell, Phys. Rev., (1951), 84, 1246.

79. N. F. Ramsey and E. M. Purcell, Phys. Rev., (1952), 85, 143.

80. A. L. Bloom and M. E. Packard, Science, (1955), 122, 738.

81. H. Primas and H. H. Günthard, Rev. Sci. Instruments, (1957), 28, 510.

82. Chem. Eng. News, (1964), 23, 55.

83. H. S. Gutowsky, D. W. McCall and C. P. Slichter, J.Chem.Phys., (1953), 21, 279.

84. E. L. Hahn and D. E. Maxwell, Phys. Rev., (1952), 88, 1070.

85. H. M. McConnell, A. D. McLean and C. A. Reilly, J.Chem.Phys., (1955), 23, 1152.

86. E. B. Wilson, J.Chem.Phys., (1957), 27, 60.

87. W. A. Anderson, Phys. Rev., (1956), 102, 151.

88. N. K. Banerjee, T. P. Das and A. K. Saha, Proc. Roy. Soc. (London) (1954), A226, 490.

89. K. B. Wiberg and B. J. Nist, "The Interpretation of NMR Spectra," W. A. Benjamin, N.Y., (1962).

90. J. D. Roberts, " An Introduction to the Analysis of Spin-Spin Splitting in High Resolution Nuclear Magnetic Resonance Spectra", W. A. Benjamin, N.Y., (1961).

91. R. J. Abraham, "Analysis of High Resolution N.M.R.Spectra", Elsevier, Amsterdam, (1971).

92. C. N. Banwell and N. Sheppard, Mol.Phys., (1960),3, 351.

93. R.W. Fressenden and J.S. Waugh, J.Chem.Phys.,(1959), 31, 996.

94. J.D. Swalen and C.A. Reilly, J.Chem.Phys.,(1962),37, 21.

95. R.A.Hoffman, J.Chem.Phys.,(1960),33, 1256.

96. Y. Arata, H.Shimizu and S.Fujiwara,J.Chem.Phys.(1962),36, 1951.

97. S.S.Castellano and A.A.Bothner-By,J.Chem.Phys.(1964),41, 3863.

98. J.A.Musso and A.Isaia, J.Chim.Phys.(1969), 66, 1676.

99. S. Castellano and J.S.Waugh, J.Chem.Phys.,(1961), 34, 295.

100. R.J.Abraham and S.Castellano, J.Chem.Soc.(B), (1970),49.

101. T.Schaefer and W.G.Schneider, Can.J.Chem.,(1960),38, 2066.

102. R.T.Hobgood, R.E.Mayo and J.H.Goldstein, J.Chem.Phys.(1963),39,2501.

103. R.Freeman, J.Chem.Phys.,(1964),40, 3571.

104. S.Castellano and J.S.Waugh, J.Chem.Phys.,(1962),37, 1951.

105. W. Brügel,Th.Ankel and F.Kruckeberg,Z.Electrochem.(1960),64,1121.

106. Ralph E.Mayo and J.H.Goldstein,J.Mol.Spectros,(1964),14, 173.

107. J.R.Cavanaugh,J.Chem.Phys., (1963),39, 2378.

108. R. Foster,"Organic Charge-Transfer Complexes",Academic Press, New York, (1969).

109. R. Foster,"Progress in NMR Spectroscopy,Vol.4", Pergamon, Oxford, (1969).

110. H.A.Benesi and J.H.Hildebrand,J.Am.Chem.Soc.,(1949),71, 2703.

111. M.W.Hanna and A.L.Ashbough, J.Phys.Chem.,(1964), 68, 811.

112. R.Foster and C.A.Fyfe, Trans.Farad,Soc.,(1965), 61, 1626.

113. R.L.Scott, Rec. Trav. Chim,(1956), 75, 787.

114. C.J.Creswell and A.L.Allred, J.Phys.Chem.,(1962),66, 1469.

115. R.Foster, Rec.Trav.Chim.,(1970),89, 1149.

116. I.D.Kuntz,Jr.,F.P.Gasparro,M.D.Johnston,Jr. and R.P.Taylor, J.Am.Chem.Soc., (1968), 90, 4778.

117. P.J.Trotter and M.W.Hanna,J.Am.Chem.Soc.,(1966),88, 3724.

118. J.Homer,M.H.Everdell, C.J.Jackson, and P.M.Whitney, J.Chem. Soc.Farad.Trans.II,(1972),68, 874.

119. C.J.Jackson,Ph.D.Thesis, University of Aston in Birmingham(1971).

120. W.G.Schneider,J.Phys.Chem.,(1962),66, 2653.

121. T.L.Brown andK.Stark, J.Phys.Chem.,(1965),69, 2679.

122. J.R.Leto, F.A.Cotton and J.S.Waugh, Nature(1957), 180, 978.

123. G. Frenkel, R.E.Carter,A.McLachlan and J.H.Richards, J.Am.Chem. Soc., (1960), 82, 5846.

124. J.Homer and M.C.Cooke,J.Chem.Soc. (A),(1969),773.

125. L.W.Reeves and W.G.Schneider, Can.J.Chem.,(1957), 35, 251.

126. K.M.Baker and B.R.Davis,J.Chem.Soc.(B), (1968),261.

127. Gurudata, R.E.Klinck and J.B.Stothers, Can.J.Chem.(1967),45,213.

128. L.E.Orgel and R.S.Mulliken, J.Am.Chem.Soc.,(1957), 79, 4839.

129. J.Feeney, J.Chem.Soc. (B), (1971),515.

130. Edward M. Engler and P.Laszlo, J.Am.Chem.Soc.,(1971), 93, 1317.

131. J. Homer and M.C.Cooke, J.Chem.Soc. (A),(1960),777.

132. J.V.Hatton and R.E.Richards, Mol. Phys. (1960),3, 253

133. J.E.Anderson, Tetrahedron Letters,(1965),4713

134. D.H.Williams and D.A.Wilson, J.Chem.Soc. (B), (1966),144

135. J.H.Bovie, J.Ronayne and D.H.Williams, J.Chem. Soc.(B),(1967)535.

136. Z.W.Wolkowsky,N.Thoai and J.Weimann,Tetrahechon.Lett.,(1970),93.

137. D.H.Williams and N.S.Bhacca,Tetrahedron,(1965),21, 2021.

138. J.D.Connolly and R.McCrindle, Chem.Ind.,(1965),379

139. A.A.Sandoval and M.W.Hanna,J.Phys.Chem.,(1966),70,1203.

140. T.Leddal,TetrahedronLetters, (1966),1653.

141. P.Laszlo and D.H.Williams, J.Am.Chem.Soc.,(1966),88, 2799.

142. C.E.Johnson and F.A.Bovey, J.Chem.Phys., (1958), 29, 1012.

143. B.P.Dailey,J.Chem.Phys., (1964), 41, 2304.

144. J.I.Musher,J.Chem.Phys.(1965),43,4018 and (1967),46,1219.

145. "PhysicalProperties of Organic Compounds",Adv. in Chemistry Series N. 15, Am.Chem.SoclPub., Washington (1955).

146. "Handbook of Chemistry and Physics",Chemical Rubber Co.,Ohio,(1964).

147. "Dictionary of Organic Compounds,Vol.5", Eyre and Spotliswoode, London, (1965).

148. J.Timmermans,"Physico-Chemical Constants of Pure Organic Compounds" Elsevier, Amsterdam, (1965).

149. "Physical Properties of Organic Compounds", Adv. in Chemistry Series N.22, Am.Chem.Soc.Pub., Washington, (1959).

150. W.L.Wilcox,J.H.Goldstein and J.W.Simmons, J.Chem.Phys.,(1955), 22, 516.

151. A.L.McClellan,"Table of Experimental Dipole Moments", Freeman, San Francisco,(1963).

152. "Iteratomic Distances Suppl.", Chem.Soc,Publ. No.18, London(1955).

153. "Table of Interatomic Distances and Configurations in Molecules and Ions", Chem.Soc.Pub. No.11, London, (1958).

154. J.E.Baldwin, J.Org.Chem., (1965), 30, 2423.

155. J.Ronayne, M.V.Sargent and D.H.Williams, J.Am.Chem.Soc., (1966), 88, 5288.

156. "Dictionary of Organic Compounds, Vol.1", Eyre and Spottiswoode, London (1965).

157. P.D.Foster, V.M.Rao and R.F.Curl, Jr., J.Chem.Phys.,(1965),43, 1064.

158. R.Mecke and K.Noak, Ber., (1960), 93, 210.

159. G.J.Karabatsos, D.J.Fenoglio and S.S.Lande, J.Am.Chem.Soc., (1969), 91. 3572.

160. W.F.Reynolds and D.J.Wood, Cand.J.Chem., (1969), 47, 1295.

161. M.T.Rogers, J.Am.Chem.Soc., (1947), 69, 2544.

162. I.D.Kuntz, Jr., M.D.Johnston,Jr.,J.Am.Chem.Soc.(1967),89,6008.

163. V.S.Watts and J.H.Goldstein, J.Chem.Phys.,(1965),42, 228.